

**AWARD NUMBER:** W81XWH-18-1-0113

**TITLE:** Modifying Heterocycles to Treat Gram + and Gram - Bacteria

**PRINCIPAL INVESTIGATOR:** Martin Conda-Sheridan

**CONTRACTING ORGANIZATION:** University of Nebraska Medical Center, Omaha, NE

**REPORT DATE:** February 2021

**TYPE OF REPORT:** Final

**PREPARED FOR:** U.S. Army Medical Research and Materiel Command  
Fort Detrick, Maryland 21702-5012

**DISTRIBUTION STATEMENT:** Approved for Public Release; Distribution Unlimited

The views, opinions and/or findings contained in this report are those of the author(s) and should not be construed as an official Department of the Army position, policy or decision unless so designated by other documentation.

# REPORT DOCUMENTATION PAGE

Form Approved  
OMB No. 0704-0188

Public reporting burden for this collection of information is estimated to average 1 hour per response, including the time for reviewing instructions, searching existing data sources, gathering and maintaining the data needed, and completing and reviewing this collection of information. Send comments regarding this burden estimate or any other aspect of this collection of information, including suggestions for reducing this burden to Department of Defense, Washington Headquarters Services, Directorate for Information Operations and Reports (0704-0188), 1215 Jefferson Davis Highway, Suite 1204, Arlington, VA 22202-4302. Respondents should be aware that notwithstanding any other provision of law, no person shall be subject to any penalty for failing to comply with a collection of information if it does not display a currently valid OMB control number. **PLEASE DO NOT RETURN YOUR FORM TO THE ABOVE ADDRESS.**

<b>1. REPORT DATE</b> February 2021			<b>2. REPORT TYPE</b> Final		<b>3. DATES COVERED</b> 01 May, 2018- 31 Oct 2020	
<b>4. TITLE AND SUBTITLE</b> Modifying Heterocycles to Treat Gram + and Gram - Bacteria					<b>5a. CONTRACT NUMBER</b> W81XWH-18-1-0113	
					<b>5b. GRANT NUMBER</b>	
					<b>5c. PROGRAM ELEMENT NUMBER</b>	
<b>6. AUTHOR(S)</b> Martin Conda Sheridan, PhD  E-Mail: martin.condasheridan@unmc.edu					<b>5d. PROJECT NUMBER</b>	
					<b>5e. TASK NUMBER</b>	
					<b>5f. WORK UNIT NUMBER</b>	
<b>7. PERFORMING ORGANIZATION NAME(S) AND ADDRESS(ES)</b>  University of Nebraska Medical Center 42nd and Emile, Omaha, NE 68198					<b>8. PERFORMING ORGANIZATION REPORT NUMBER</b>	
<b>9. SPONSORING / MONITORING AGENCY NAME(S) AND ADDRESS(ES)</b>  U.S. Army Medical Research and Development Command Fort Detrick, Maryland 21702-5012					<b>10. SPONSOR/MONITOR'S ACRONYM(S)</b>	
					<b>11. SPONSOR/MONITOR'S REPORT NUMBER(S)</b>	
<b>12. DISTRIBUTION / AVAILABILITY STATEMENT</b>  Approved for Public Release; Distribution Unlimited						
<b>13. SUPPLEMENTARY NOTES</b>						
<b>14. ABSTRACT</b> Bacterial infections are a serious threat to human health that are responsible for thousands of deaths in the United States. In order to confront this public health crisis, it is necessary to develop new interventions. A most promising treatment against pathogens will combine agents with distinct mechanism of action. This will lead to more potent therapies that can also overcome the development of bacterial resistance. Our goal for this project is to synthesize antimicrobial phenazines that can be used to modify membrane disruptors. Our hypothesis is the conjugation of the phenazines to amines, polyamines and peptides will provide systems with enhanced activity. The peptides will break the bacterial membrane allowing the penetration of the phenazine segment. We have been able to prepare and evaluate some intriguing phenazines and peptides that presented potent activity against a panel of gram positive and gram negative pathogens. We also identified some key structural features that we theorize give rise to the biological activity of the molecules.						
<b>15. SUBJECT TERMS</b> Phenazines, antibacterials, antimicrobial peptides, antibacterial hybrids, gram positive, gram negative, cylindrical proteases						
<b>16. SECURITY CLASSIFICATION OF:</b>				<b>17. LIMITATION OF ABSTRACT</b>	<b>18. NUMBER OF PAGES</b>	<b>19a. NAME OF RESPONSIBLE PERSON</b>
<b>a. REPORT</b>	<b>b. ABSTRACT</b>	<b>c. THIS PAGE</b>	<b>USAMRMC</b>			
Unclassified	Unclassified	Unclassified	Unclassified	60	<b>19b. TELEPHONE NUMBER (include area code)</b>	

## TABLE OF CONTENTS

	<u>Page</u>
1. Introduction	4
2. Keywords	4
3. Accomplishments	4
4. Impact	13
5. Changes/Problems	14
6. Products	15
7. Participants & Other Collaborating Organizations	16
8. Special Reporting Requirements	19
9. Appendices	19

**1. INTRODUCTION:** *Narrative that briefly (one paragraph) describes the subject, purpose and scope of the research.*

The Infectious Diseases Society of America has listed bacterial infections as “1 of the 3 greatest threats to human health.” The objective of this project is to synthesize phenazines, heterocyclic molecules with known antibacterial properties. Specifically, we plan to connect the prepared compounds to primary amines or peptides, both strategies that have been reported to enhance penetration inside bacteria. This will lead to novel hybrid systems with a dual mechanism of action: membrane disruption caused by the amines or peptides plus the killing effect of the phenazines (these molecules possess diverse mechanism of action including generation of free radicals, binding to essential proteins or DNA intercalation). We expect our compounds will become broad spectrum therapies capable of eliminating a series of dangerous pathogens including: *Staphylococcus aureus*, *Escherichia coli*, *Pseudomona aeruginosa*, *Klebsiella pneumoniae*, and *Acinetobacter baumannii*.

**2. KEYWORDS:**

Antimicrobial peptides; phenazines; cylindrical proteases; gram negative bacteria, bacteria membrane permeability; drug resistant bacteria

**3. ACCOMPLISHMENTS:**

**What were the major goals of the project?**

The major goals of the project are

- Synthesis, purification and characterization of phenazines linked to peptides and amines
  - This includes the synthesis of various phenazines and antimicrobial peptides to identify proper leads that can later be connected to each other
- The antimicrobial evaluation of the compounds
  - This includes testing the activity of phenazine-peptide complexes, phenazines, and antimicrobial peptides against a panel of bacteria
  - The ability of these hybrid systems to eradicate biofilms
- The evaluation of toxicity of the hybrids
  - This focuses in testing toxicity against human cells and a wax moth larva (simple in vivo model that does not require University approval)
- Note: based on the synthetic progress and preliminary results, we included another set of heterocycles (containing the pyridine core) to be tested and modified. Likewise, we decided to expand testing by including: chlamydia trachomatis, which is a gram negative bacteria, within the bacteria to be evaluated.

## What was accomplished under these goals?

As mentioned previously, we had three major, unexpected, setbacks: (1) personnel turnover due to better job offers, which affected continuity (described in the NCE letter). (2) Unpredicted, and unforeseen, synthetic challenges with side chain functionalization of the phenazines. As detailed in the previous reports, adding an amine side chain lead to an intramolecular rearrangement that yielded an inactive adduct. (3) The COVID-19 pandemic that resulted in the shutdown of the research enterprise (university wide policy) for ~4 months. Moreover, the research activities have not yet completely returned to the pre-pandemic levels. Students work at different times to minimize the number of people present in the lab. The PI has been working mainly from home since April 2020. The COVID also affected the testing of some of the molecules since some experiments were going to be performed at collaborators' lab.

However, we are very happy with the progress of the project and the achievements so far. We have published a paper that describes the synthesis and evaluation of antimicrobial peptides (Rodriguez de Almeida, N.; Catazaro, J.; Chhonker, Y.; Murry, D.; Powers, R.; **Conda-Sheridan, M.** Understanding Interactions of Citropin 1.1 Analogues with Model Membranes and Their Influence on Biological Activity. *Peptides* **2019**, 170119). We are currently working on two additional manuscripts that plan to submit by June 2021. Unfortunately, we have not been able to create the hybrid molecules. Below, we will describe the results we obtained so far. We will divide them in: (1) peptides, (2) phenazines, and (miscellaneous molecules).

### Section 1. Antimicrobial Peptides

We have synthesized various analogues of citropin 1.1 using solid phase peptide synthesis. They were prepared in a Rink Amide Am resin and Oxyma/DIC/DIPEA or HATU/DIPEA as coupling reagents (for special amino acids we used PYBOP/DIPEA. Deprotections were performed using 4-methyl-piperidine 20% in DMF.

The reactions of coupling and deprotection were performed in a Biotage microwave: 75 °C, 5 minutes reaction time, with 2 min of pre-stirring. If the coupling reactions were difficult, we performed them using a reaction time of 7 min with 3 min of pre-stirring. Figure 1 shows the structure of one of the new peptides. Table 1 shows the structures of the peptides we have prepared (the analogues that have already been published are excluded from the table).

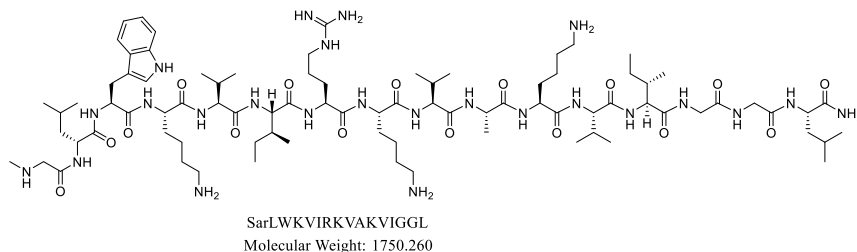


**Figure 1.** Structure of a potential antimicrobial peptide; AJP-1-102

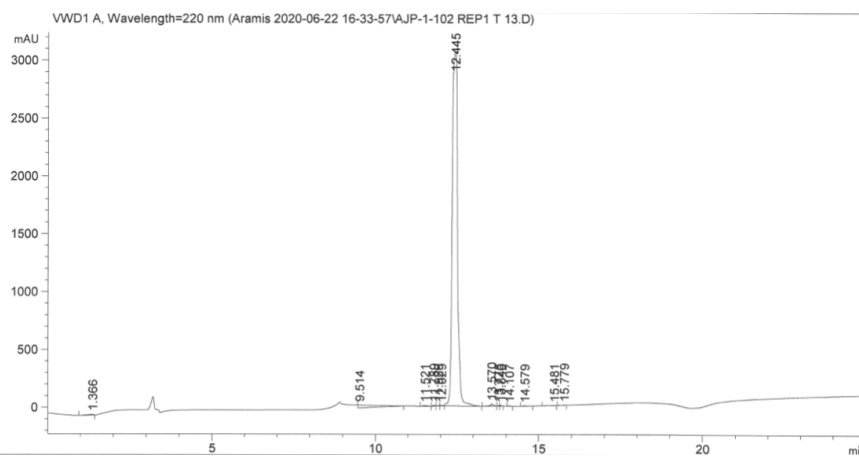
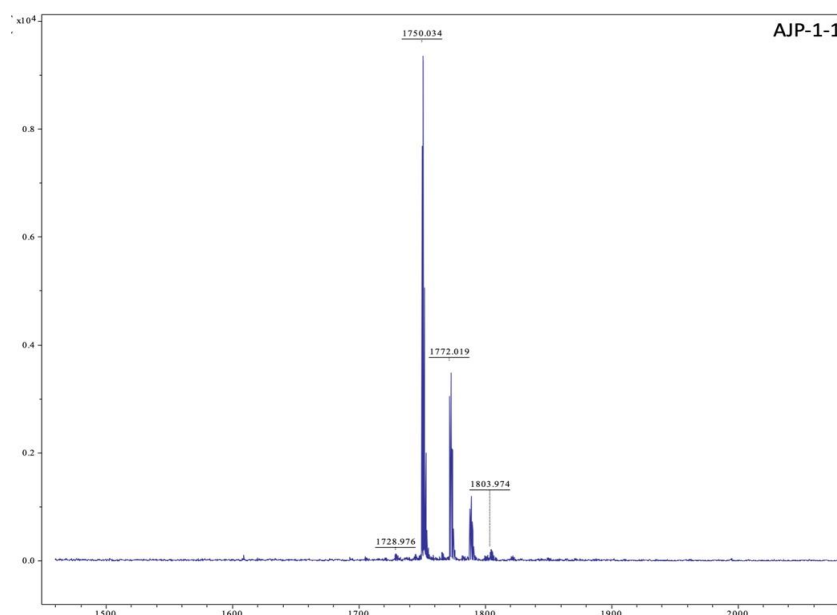
**Table 1.** Cit 1.1 and its analogues

Peptide sequence	Peptide code	MW	Purity
GLFDVIRKVASVIGGL-NH <sub>2</sub>	AMP-001	1615.00	96.60%
SarL(1-Nap)KVIRKVASVIGGL-NH <sub>2</sub>	AJP-1-1	1720.19	98.20%
SarL(1-Nap)DVIRKVASVIGGL-NH <sub>2</sub>	AJP-1-24	1707.10	95.08%
SarLWDVIRKV(Aib)SVIGGL-NH <sub>2</sub>	AJP-1-85	1710.10	98.88%
SarLWDVIRKV(d-Ala)SVIGGL-NH <sub>2</sub>	AJP-1-90	1696.08	95.11%
GLWKVIRKVASVIGGL-NH <sub>2</sub>	AJP-1-100	1695.14	96.76%
SarLWKVIRKVAKVIGGL-NH <sub>2</sub>	AJP-1-102	1750.26	96.54%
SarL(2-Nap)DVIRKVASVIGGL-NH <sub>2</sub>	AJP-1-116	1707.10	92.50%
SarL(Bta)DVIRKVASVIGGL-NH <sub>2</sub>	AJP-1-117	1713.12	96.80%
SarLWKVIRKVASVIGG(d-Leu)-NH <sub>2</sub>	AJP-2-12	1709.16	96.25%
SarLWKVIRKVASVI(Aib)GL-NH <sub>2</sub>	AJP-2-22	1737.22	98.53%
SarL(1-Nap)KVIRKVASVIGGL-NH <sub>2</sub>	AJP-2-26	1720.19	96.72%
SarLWKVIRKVASVIGL-NH <sub>2</sub>	AJP-2-27	1765.27	93.08%
SarLF(3,4-diF)KVIRKVAKVIGGL-NH <sub>2</sub>	AJP-2-56	1747.20	99.03%
SarLW(Orn)VIRKVAKVIGGL-NH <sub>2</sub>	AJP-2-57	1736.23	99.53%
SarL(Bip)DVIRKVASVIGGL-NH <sub>2</sub>	AJP-2-60	1733.14	96.31%
SarL(2-Nap)KVIRKVAKVIGGL-NH <sub>2</sub>	AJP-2-64	1761.28	98.28%
GLWKVIRVVASVIGGL-NH <sub>2</sub>	DAN-1-11	1666.09	96.92%
SarL(1-Nap)KVIRKVAKVIGGL-NH <sub>2</sub>	DAN-1-13	1761.28	99.13%
SarL(2-Nap)KVIRKVASVIGGL-NH <sub>2</sub>	HHX-2-28	1720.19	99.25%
GLWKVIRKVAKVIGGL-NH <sub>2</sub>	SYD-1-1	1736.23	98.09%
SarL(Bta)KVIRKVAKVIGG(d-Leu)-NH <sub>2</sub>	SYD-1-5	1767.30	95.59%

The "d" indicates the amino acid is the enantiomer of the natural one. AMP-001 = Citropin 1.1; Aib = Aminoisobutyric acid; Bta= Benzothiazole; 3,4-diF = phenylalanine with fluorine atoms at positions 3 and 4; Orn = Ornithine; Nap = Naphthalene substituent on the side chain

The synthesized peptides were purified using preparative liquid chromatography (using a Varian instrument form Agilent). The purity of the peptides was studied by high performance liquid chromatography (LC) using a water/Acetonitrile gradient run. The spectrum on the right shows AJP-1-102 (Figure 2), which is 96% pure.

Only peptides that presented over 95% purity were studied (this threshold is based on the Journal of Medicinal Chemistry guidelines for purity). The identity of all the AMPs was confirmed by mass spectrometry (usually MALDI). On the right, I show the MALDI trace of the AJP-1-102 peptide (Figure 3).

**Figure 2.** MALDI trace of an antimicrobial peptide (AJP-1-102).**Figure 3.** MALDI trace of an antimicrobial peptide (AJP-1-102).

In our previous report (Rodriguez de Almeida *et al. Peptides* **2019**, 170119) we have identified the presence of alpha helices as a key characteristic of the active peptides. We proceed to study this crucial feature using circular dichroism (CD). As can be seen all the peptides show  $\alpha$ -helical features with minima at 208 nm and 220 nm (in some cases the signature peaks are shifted to the blue or red light spectra). The small differences between the peptides suggest a degree of random coiling is present.

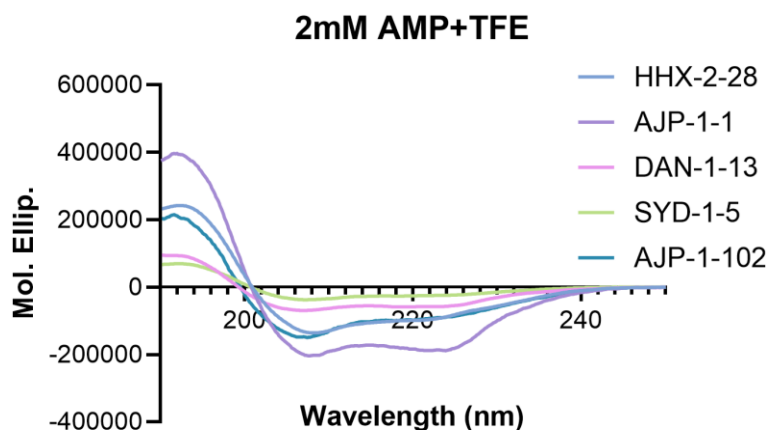


Figure 4. CD spectra of selected AMPs, samples in water-trifluoroethanol; 4:1

We then proceeded to test the various peptides using a disk assay to narrow down the number of peptides to be studied.

Table 2. Results of the disk test

AMPS	<i>S. aureus</i> ATCC	<i>S. aureus</i> HU25	<i>S. aureus</i> USA300	<i>P. aeruginosa</i> ATCC27853	<i>S. epidermidis</i> ATCC12228	<i>K. pneumonie</i> ATCC13883	<i>E. coli</i> ATCC25922	<i>E. cloacae</i> ATCC13047	<i>S. pseudintermedius</i>
DAN -1-7	>1024	>1024	>1024	>1024	>1024	>1024	>1024	>1024	>1024
DAN -1-11	>1024	>1024	>1024	>1024	>1024	>1024	>1024	>1024	>1024
DAN -1-12	>1024	>1024	>1024	>1024	>1024	>1024	>1024	>1024	>1024
DAN -1-13	512	512	512	512	512	512	512	512	512
DAN -1-	1024	>1024	1024	1024	1024	1024	1024	>1024	512
DAN -1-	1024	>1024	1024	512	1024	512	>1024	512	512
SYD-1-1	>1024	>1024	>1024	>1024	>1024	>1024	>1024	>1024	>1024
SYD -1-4	>1024	>1024	>1024	>1024	>1024	>1024	>1024	>1024	>1024
SYD -1-5	512	1024	512	>1024	512	512	1024	512	512
AJP -1-1	512	512	512	1024	512	512	512	512	512
HHX -2-28	512	512	512	512	512	1024	512	512	512

Values expressed in  $\mu\text{g/mL}$

Figure 5 shows a petri dish of *S. aureus* USA 300 that was treated with disks containing various of the studied peptides. Based on the disk method DAN-1-13 was the most promising lead of this series. The sequence of the peptide is Sar\_Leu\_1-Nap\_Lys\_Val\_Ile\_Arg\_Lys\_Val\_Alalys\_Val\_Ile\_Gly\_Gly\_Leu (1-Nap = Naphtyl side chain linked at carbon 1)

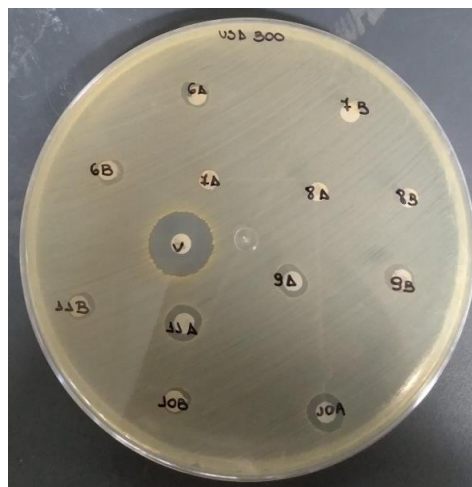


Figure 5. *Staphylococcus aureus* USA300 (MRSA strain). The AMPs: 4. DAN-1-13, 5. DAN-1-71A, 6. DAN-1-71B, 9. SYD-1-5, 10. AJP-1-1 and 11. HHX-2-28 showed activity against this strain. We used vancomycin “V” as a positive control.

The peptides that showed activity at 512 mg/mL were selected for further studies using the broth microdilution assay. **Table 3** shows the results for the most promising peptides (only values  $\leq 256$   $\mu\text{g/mL}$  are presented). The results are expressed as MIC (Minimal inhibitory concentration). Only selected bacteria are shown. The best lead, DAN-1-13 has a MIC value of 4  $\mu\text{g/mL}$  against *S. aureus* USA 300 (**Figure 6**). In this assay, the compound was more potent than the vancomycin control. The figure also shows data for DAN-1-71A, which has the following sequence: Sar\_Leu\_Trp\_Lys\_Val\_Ile\_Arg\_Lys\_Val\_Aib\_Lys\_Val\_Ile\_Gly\_Gly\_Leu (Aib= 2-Amino isobutyric acid, which is used to promote  $\alpha$ -helix formation).

**Table 3.** MIC values calculated by the Broth assay

AMPS	<i>S. aureus</i> ATCC	<i>S. aureus</i> HU25	USA300	<i>P. aeruginosa</i> ATCC27853	<i>S. epidermidis</i> ATCC12228
DAN -1-13	8 $\mu\text{g/mL}$	16 $\mu\text{g/mL}$	4 $\mu\text{g/mL}$	32 $\mu\text{g/mL}$	2 $\mu\text{g/mL}$
SYD -1-5	32 $\mu\text{g/mL}$	64 $\mu\text{g/mL}$	16 $\mu\text{g/mL}$	256 $\mu\text{g/mL}$	32 $\mu\text{g/mL}$
AJP -1-1	16 $\mu\text{g/mL}$	16 $\mu\text{g/mL}$	16 $\mu\text{g/mL}$	512 $\mu\text{g/mL}$	8 $\mu\text{g/mL}$
HHX-2-28	16 $\mu\text{g/mL}$	32 $\mu\text{g/mL}$	16 $\mu\text{g/mL}$	256 $\mu\text{g/mL}$	16 $\mu\text{g/mL}$
AJP-1-100			32 $\mu\text{g/mL}$	128 $\mu\text{g/mL}$	
AJP-1-102			16 $\mu\text{g/mL}$	64 $\mu\text{g/mL}$	
AJP-2-22			16 $\mu\text{g/mL}$	256 $\mu\text{g/mL}$	
AJP-2-26			32 $\mu\text{g/mL}$	512 $\mu\text{g/mL}$	
AJP-2-56			16 $\mu\text{g/mL}$	128 $\mu\text{g/mL}$	
AJP-2-60			32 $\mu\text{g/mL}$	256 $\mu\text{g/mL}$	
AJP-2-64			16 $\mu\text{g/mL}$	128 $\mu\text{g/mL}$	



**Figure 6.** Broth microdilution assay in triplicate. **Columns 1-3;** DAN-1-13 serial microdilution. **Columns 5-7;** DAN-1-71A serial microdilution. **Column 9.** Blank (culture medium only). **Column 11.** Negative control (medium and inoculum); in the last four wells, DMSO was applied to assess solvent-related toxicity. **Column 12.** Positive control: Vancomycin.

In order to validate the presented results, we determined the minimum bactericidal concentration (MBC) of the peptides. Briefly; we planted dilutions of the AMPs in a petri dish to observe growth of bacteria. **Figure 7** shows the MBC study of DAN-1-13. In **Table 4** we show the results of the molecules (only active AMPs and susceptible bacteria are shown). As can be appreciated some of the AMPs present promising activity against a panel of bacteria while others were active only against the USA300 *S. aureus* strain (a Methicillin-resistant *S. aureus* strain)

**Figure 7.** MBC of DAN-1-13 against USA300. One line of each triplicate was selected and applied on a Petri plate. From the left to the right, the first well “A” until “H”. The first well of positive control was applied in the last space.

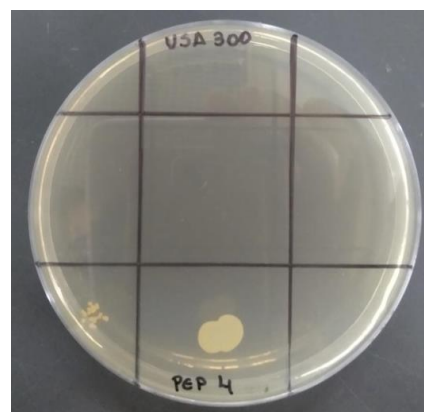


**Table 4.** Minimal Bactericidal Concentration of selected peptides

AMPS	<i>S. aureus</i> ATCC	<i>S. aureus</i> HU25	USA300	<i>S. epidermidis</i> ATCC12228	<i>S. schleiferi</i> subsp. schleiferi	<i>S. pseud</i> <i>intermedius</i>
DAN -1-13	32 $\mu\text{g/mL}$	32 $\mu\text{g/mL}$	8 $\mu\text{g/mL}$	2 $\mu\text{g/mL}$	8 $\mu\text{g/mL}$	16 $\mu\text{g/mL}$
SYD -1-5	64 $\mu\text{g/mL}$	128 $\mu\text{g/mL}$	16 $\mu\text{g/mL}$	32 $\mu\text{g/mL}$		
AJP -1-1	32 $\mu\text{g/mL}$	16 $\mu\text{g/mL}$	32 $\mu\text{g/mL}$	8 $\mu\text{g/mL}$	32 $\mu\text{g/mL}$	32 $\mu\text{g/mL}$
HHX-2-28	16 $\mu\text{g/mL}$	128 $\mu\text{g/mL}$	16 $\mu\text{g/mL}$	16 $\mu\text{g/mL}$	256 $\mu\text{g/mL}$	256 $\mu\text{g/mL}$
AJP-1-102			16 $\mu\text{g/mL}$			
AJP-2-12			64 $\mu\text{g/mL}$			
AJP-2-22			16 $\mu\text{g/mL}$			
AJP-2-64			16 $\mu\text{g/mL}$			



The formation of bacterial biofilms is a main reason for resistance, that also difficult the elimination of the pathogens. We also studied the ability of the peptides to eliminate biofilms or prevent their formation. We found three peptides that present promising activity. **Table 5** and **Figure 8** present some relevant data.

**Table 5.** MIC values for biofilm inhibition

AMPs	USA300	<i>S. pseudintermedius</i>
<b>DAN -1-13</b>	½ MIC (4 µg/mL)	½ MIC (8 µg/mL)
<b>AJP -1-1</b>	½ MIC (16 µg/mL)	¼ MIC (8 µg/mL)
<b>HHX -2-28</b>	½ MIC (16 µg/mL)	1/8 MIC (32 µg/mL)

\*No effect on inhibiting biofilm formation

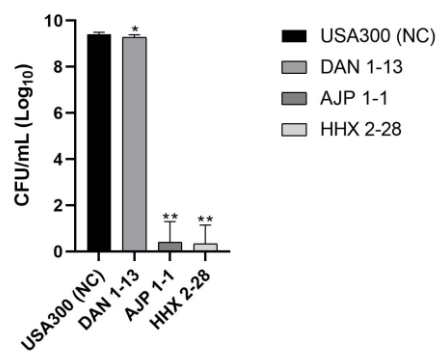


**Figure 8.** Viable USA300 biofilm cells with and without the influence of AMPs (CFU/mL, SEM of 6 replicates)

As published, the AMPs can disrupt the membrane of bacterial, causing their death. We studied the ability to the AMPs to disrupt the inner membrane of bacteria by monitoring the hydrolysis of O-Nitrophenyl-β-D-galactopyranoside (ONPG). If the inner barrier is permeated, galactosidases will escape or the ONPG will cross the barrier. In either case, the result is hydrolysis of the sugar and a change in absorbance. As shown in **Figure 9**, the AMPs can disrupt the inner membrane (the amount of hydrolysis correlated with the AMP concentration). The AMPs were more potent than the Polimyxin B control. We are currently testing the toxicity of the AMPs towards mammalian cells and worms. We also plan to study the ability of the molecules to disrupt bacterial membranes using transmission electron microscopy and atomic force microscopy. We expect to finish these experiments by June 2021. Thereafter, we plan to send the work for publication to a peer reviewed journal.

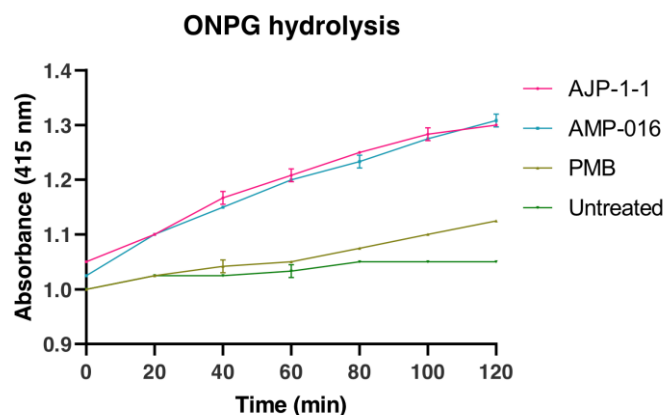
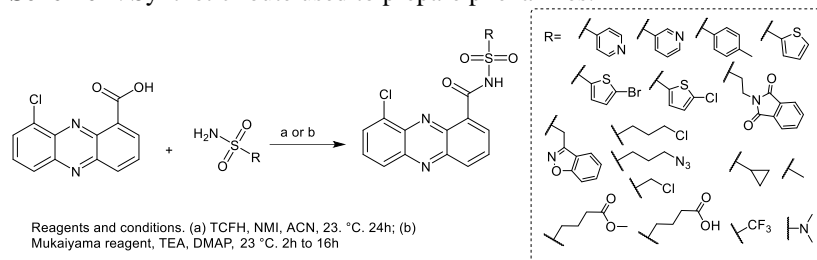


**Figure 9.** Inner membrane permeability caused by the AMPs at 2X MIC. AMP- is a control from our previous paper. Polymyxin B (PMB) was used as control.

## Section 2. Phenazines

The second set of molecules of interest are the phenazines. These heterocycles are known as antibacterial agents. Scheme 1 shows the synthetic route and the structure of some of the prepared phenazines. The precursor 9-chloro-1-phenazine carboxylic acid was reported previously by us (Udumula *et al.* Eur. J. Med. Chem. 2016, 128, 710–721). We used two synthetic routes to prepare the molecules as described below:

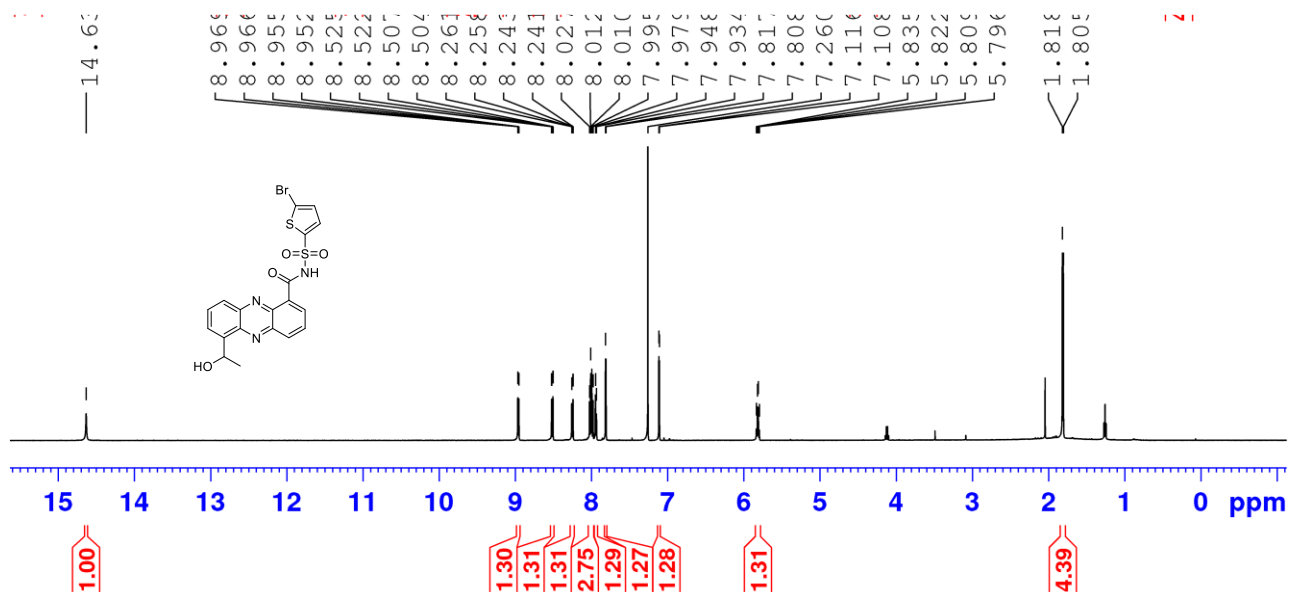
**Scheme 1.** Synthetic route used to prepare phenazines.



**Method A:** A phenazine derivative (0.018-0.20 mmol) and the appropriate sulfonamide derivative (1.2 eq) were dissolved in anhydrous acetonitrile (7 mL), then N-methylimidazole (NMI) (85  $\mu$ L, 0.025 mmol) and N,N,N',N'-Tetramethylchloroformamidinium Hexafluorophosphate (TCFH) (88 mg, 0.07 mmol) were added. The formed clear yellow solution was stirred at room temperature for 2 h. The formed bright yellow precipitate was filtered, washed with acetonitrile, and purified by column chromatography to afford the desired product.

**Method B:** A phenazine derivative (0.18 mmol), DMAP (10 mol%), and a sulfonamide derivative (0.2 mmol) in DCM (3 mL) were stirred for 10 minutes. Then, triethylamine (100  $\mu$ L, 0.8 mmol) was added dropwise, and the reaction mixture was stirred at room temperature for 16 h. After the reaction completion, the mixture was poured over 10 mL of DCM and washed with 2N HCl (5 mL x 3). The resulted organic layer was dried over sodium sulfate and purified using column chromatography.

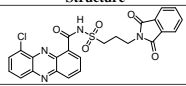
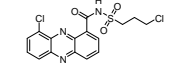
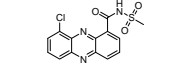
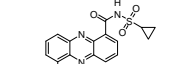
The identity and structure of the phenazines was studied by proton and carbon nuclear magnetic resonance ( $^1\text{H}$  and  $^{13}\text{C}$  NMR) and mass spectrometry. The purity of the compounds was assessed by HPLC. **Figure 5** shows the  $^1\text{H}$  NMR spectrum of one of the phenazine compounds.



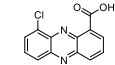
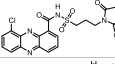
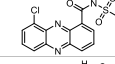
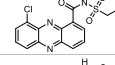
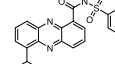
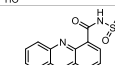
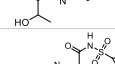
**Figure 9.** Structure of a novel phenazine and NMR spectrum confirming the identity of the molecule

We prepared 25 new phenazines that were evaluated against clinically-relevant bacterial strains such as: MRSA, *Staphylococcus epidermidis*, *Enterococcus faecalis*, and *Clostridium difficile*. The most relevant results are shown in **Tables 6** and **7**. The active phenazines did not show toxicity towards mammalian cells (HaCat, human keratinocytes, 100% survival at 128 mg/mL).

**Table 7.** MIC values of phenazines against *S. aureus* JE2

Structure	<i>S. aureus</i> JE2
	32 µg/mL
	16 µg/mL
	16 µg/mL
	32 µg/mL
Vancomycin	2 µg/mL

**Table 6.** MIC values (in µg/mL) of phenazines against the indicated pathogens

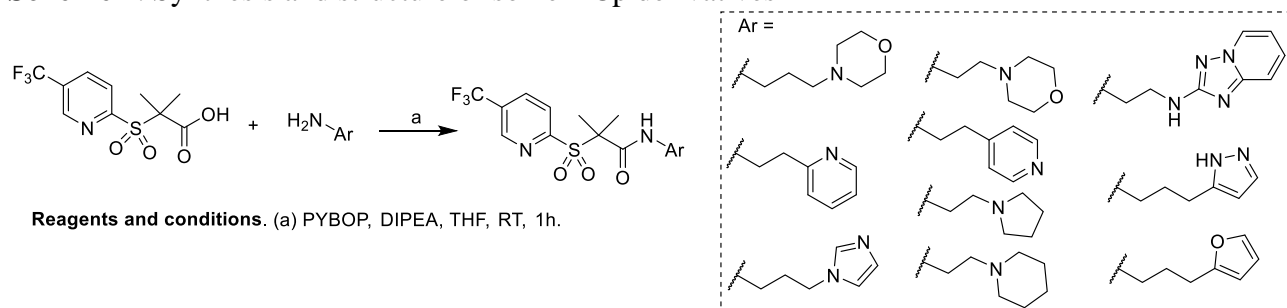
Structure	MRSA NRS 123	<i>Staphylococcus epidermidis</i> NRS 101	Methicillin-sensitive <i>S. aureus</i> ATCC 6538	MRSA USA300
	16	16	8	16
	16	32	8	64
	16	8	32	16
	8	8	8	8
	32	8	16	32
	32	8	16	32
	16	8	8	16
Vancomycin	4	4	1	1

However, we were not able to prepare the hybrids. We observed the phenazines underwent a rearrangement losing the sulfonamide group. We tried to add amines or acids using an alkyl sulfonamide but this was not possible either. At the moment we are trying to displace the chlorine atom with an azide. This will create adducts that can be linked to the peptides using click chemistry.

### Section 3. Miscellaneous Compounds

Given the difficulties with phenazine functionalization, we decided to explore an alternative heterocyclic core. The compounds, termed ACPs, activate cylindrical proteases, a promising new antibacterial target. We have prepared and characterized 25 new molecules as shown in **Scheme 2**.

**Scheme 2.** Synthesis and structure of some ACP derivatives



As is the case with all heterocycles, we characterized them by NMR (**Figure 10**) and MS.

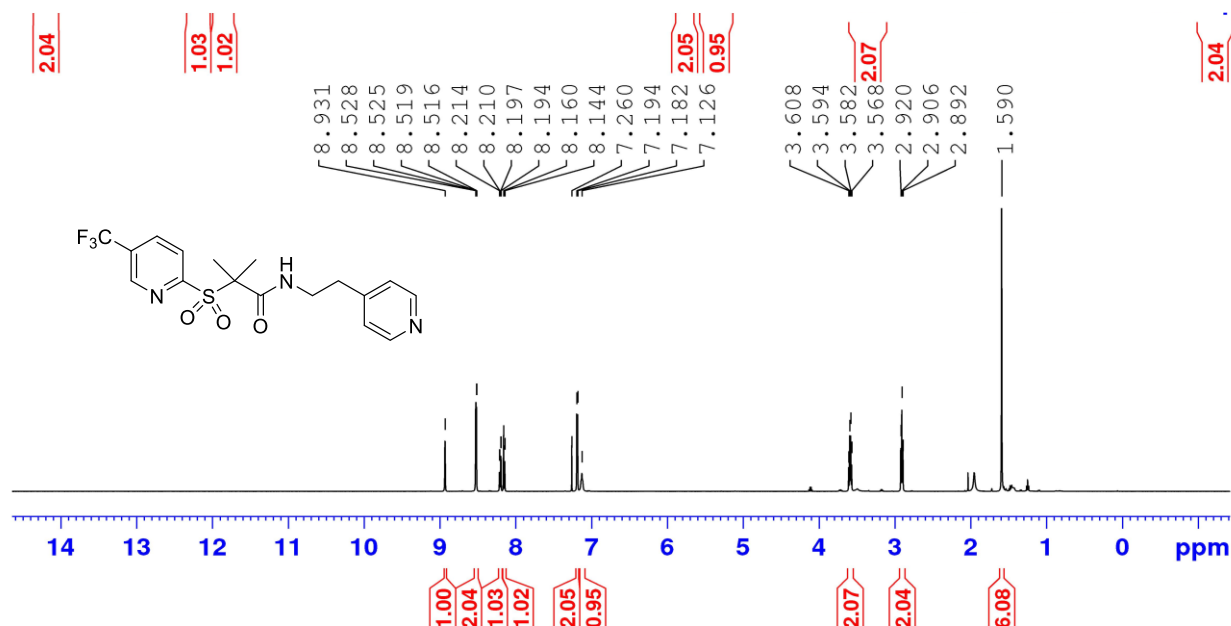


**Figure 10.** Structure of an ACP compound and NMR spectrum confirming its identity

In total we have prepared ~30 new molecules. We will test them and they try to further functionalize the most promising compounds in order to attach these molecules to the active AMPs to create the hybrid antibacterials.

### What opportunities for training and professional development has the project provided?

The people that benefited the most were the graduate students involved in the project. All of them were exposed to medicinal chemistry, peptide chemistry, computational chemistry, and microbiology. This will be essential to foster their careers as multidisciplinary scientists. Below I list the students that worked in the project and what they did and learned.:

**Mohamed Seleem**, PhD candidate. He was awarded the UNMC-Program of Excellence Assistantship. His proposal used the data generated in this project as preliminary results. The success rate of the UNMC fellowships is 31% (16 applicants from the department of pharmaceutical sciences, 5 awards). He is doing professional development courses as part of the award and has given a talk at the Midwest regional meeting of the American Chemical Society (October 2019). He learned computer aided drug design using the following programs: MOE, pymol, chimera, molinspiration, glide, and autodockVina.

**Luana the Campos** joined the project in September 2019. She learned techniques in organic synthesis and medicinal chemistry.

Other people that have been involved on the synthesis of peptides and molecules were Dr. **Audifas Matus Meza**, Mr. **Aramis Pereira**, Dr. **Nathalia Rodrigues de Almeida** (currently a faculty at the University of Nebraska at Omaha).

All of them have enhanced skills in peptide or organic chemistry and microbiology, either learning from me or collaborators across campus (Scot Ouellette and Kenneth Bayles labs at UNMC).

All the students attended several workshops from Agilent, Teledyne ([https://www.teledyneisco.com/en-us/chromatography/seminars-and-webinars?utm\\_source=Pardot&utm\\_medium=email&utm\\_campaign=C\\_2006\\_Peptide%20from%20Analytical%20Webinar](https://www.teledyneisco.com/en-us/chromatography/seminars-and-webinars?utm_source=Pardot&utm_medium=email&utm_campaign=C_2006_Peptide%20from%20Analytical%20Webinar)) and Chemical Computing group (<https://www.chemcomp.com/>). These workshops focused on chromatography techniques and *in silico* drug design, both essential skills for a medicinal chemist.

I have held personal and group meeting weekly (two group meetings, one focused in theoretical concepts, the other in research. Also, we have spent a large amount of time navigating funding agencies and their mechanisms, we discuss the funding calls, what is included in a proposal and general grantsmanship skills. We also discuss career options and useful strategies to achieve career goals (using books, papers, and my experience in detail).

Since I am in charge of the departmental seminar, I have arranged meetings between my group and the invited speakers. This practice enhances their network and provides them the opportunity of presenting their research (short presentations followed by Q&A). Having the chance to speak in a small room with some of the best scientists in the world has brought tremendous professional growth to my students. Finally, I arranged for **Luana Campos** to present a lecture focused on the synthesis of the molecules to students at the **Federal University of Itajuba**, in Brazil.

#### **How were the results disseminated to communities of interest?**

Besides peer-reviewed publications, the results were disseminated thru seminars and lectures. Since the beginning of the award, I have given 15 invited seminars in the United States and South America (Argentina, Brazil, and Chile). I have also been invited as guest lecturer twice: (1) Synthesis of Heterocycles, November 10-19, 2020 (10 hr, 5 lectures), **Federal University of Itajuba**, Minas Gerais, Brazil. (2) Heterocyclic Chemistry: Synthesis and Biological Applications. July 30-August 3, 2018 (20 hr, complete course). **Centro de Investigaciones en Bionanociencias** (CIBION), Buenos Aires, Argentina.

As mentioned, we are planning to publish the obtained results. Our expectation is to write 3 different papers.

#### **What do you plan to do during the next reporting period to accomplish the goals?**

Nothing to Report, the project has ended.

#### **4. IMPACT:**

##### **What was the impact on the development of the principal discipline(s) of the project?**

Our work in mainly medicinal chemistry instead of methodology developments; therefore, we use known methodologies rather than new reactions. We have prepared a library of two classes of compounds (phenazines and pyridines) using established protocols and also a series of AMPS. We have tested various molecules and need to study some that are left. Once this is done, we will be able to derive structure-activity relationships that can be used to further optimize the molecular structures in order to design new, more potent broad spectrum antibiotics.

Perhaps, the main promise of the project is the creation of hybrid systems with dual mechanism of action. We hope we will be able to introduce the modifications needed to achieve this.

### **What was the impact on other disciplines?**

Nothing at the moments. However, we have started mechanism of action studies to understand if the compounds kill bacteria using a traditional mechanism or if a new bacterial target has been identified. The miscellaneous compounds are potential activators of cylindrical proteases, which has been identified as a novel antimicrobial target Thus, there is potential to influence microbiology.

### **What was the impact on technology transfer?**

Nothing to Report

### **What was the impact on society beyond science and technology?**

This project is exploratory in nature and we do not expect short term outcomes at the public health level (drug approvals take years if not decades). However, the outreach activities have helped to conscientize students and parents of the power of medicinal chemistry in health and every day lives.

## **5. CHANGES/PROBLEMS:**

Other than the mentioned synthetic challenges, COVID-19 and personnel challenges, there is nothing to report. We have made several active phenazines that may be antibiotics on their own, without modifications by the AMPs. We also have various AMPs that present promising activity. As mentioned, we have included another set of heterocycles that seem to be more amenable for synthetic modifications than the phenazines. Given the new heterocycles also present antibacterial activity but possess limited penetration into bacteria, we believe they are within the scope of the grant (although the molecules were not originally described on the proposal).

### **Actual or anticipated problems or delays and actions or plans to resolve them**

We have fixed most synthetic problems. The issue with testing is related to COVID-19 but once things go back to normal, this issue will be promptly addressed.

### **Changes that had a significant impact on expenditures**

Although not of significant impact, personnel turnover coupled to the time to identify and hire replacements forced me to move budget from supplies to personnel and between technicians, postdocs, and students. However, as can be seen in the expenses, the changes were not substantial.

### **Significant changes in use or care of human subjects, vertebrate animals, biohazards, and/or select agents**

Not applicable.

## Significant changes in use or care of vertebrate animals

Not applicable

## Significant changes in use of biohazards and/or select agents

Not applicable.

## 6. PRODUCTS:

- **Publications, conference papers, and presentations**

*Report only the major publication(s) resulting from the work under this award.*

### **Journal publications.**

1. Seleem, M.; Rodrigues de Almeida, N.; Chhonker, Y. S.; Murry, D. J.; Guterres, Z.; Blocker, A. M.; Kuwabara, S.; Fisher, D. J.; Leal, E. S.; Martinefski, M. R.; Bollini, M.; Monge, M. E.; Ouellette, S.; Conda-Sheridan, M. Synthesis and Antichlamydial Activity of Potential Activators of Cylindrical Proteases. *J. Med. Chem.* 2020, 63, 4370-4387. Published, acknowledgement of federal support: yes
2. Rodriguez de Almeida, N.; Catazaro, J.; Chhonker, Y.; Murry, D.; Powers, R.; **Conda-Sheridan, M.** Understanding Interactions of Citropin 1.1 Analogues with Model Membranes and Their Influence on Biological Activity. *Peptides* **2019**, 170119. Published, acknowledgement of federal support: yes

### **Books or other non-periodical, one-time publications.**

Not applicable.

### **Other publications, conference papers and presentations.**

1. Heterocycles to treat Infectious Diseases: Old Chemistry, Old Infections, New Treatments. Federal University of Grande Dourados, Brazil, November 30, 2020 (Zoom). Host: Roberto Gomez/Vitor Rodrigues de Souza
2. Química, Ingeniería, y Ciencia de los Materiales; Intersección en la Nanotecnología (Seminar in Spanish). National University of General Sarmiento, Buenos Aires, Argentina, November 18, 2020 (Zoom). Host: Carlos Belmar Orellana
3. Peptide Amphiphiles; Structural Characteristics and Microbiology of a Promising Class of Biomaterials. University of Nebraska at Omaha, November 16, 2020 (Zoom). Host: Nathalia Rodrigues de Almeida
4. Peptide Amphiphiles; Structural Characteristics and Microbiology of a Promising Class of Biomaterials. INIFTA, University of La Plata, Buenos Aires, Argentina, July 20, 2020 (Zoom). Host: Agustin Picco
5. Peptide Amphiphiles, Microbiology and Structural Characteristics of a Promising Class of Biomaterials. Federal Fluminense University, Rio de Janeiro, Brazil, Oct. 25, 2019.
6. Design and Synthesis of Heterocycles as New Antibacterial Agents. Federal University of Itajuba, Minas Gerais, Brazil, Oct. 22, 2019. Nanostructures as Antibacterial Agents.
7. Peptide Amphiphiles, Microbiology and Structural Characteristics of a Promising Class of Biomaterials. Kansas State University, Oct. 15, 2019.
8. Role of Supramolecular Morphology in Biological Action. Georgia State University, April 23, 2019.

9. Nanostructures as Antibacterial Agents. Role of Supramolecular Morphology in Biological Action. University of Illinois at Chicago, April 3, 2019.

- **Website(s) or other Internet site(s)**

<https://www.condasheridanlab.com/> This is my laboratory website. It contains basic information regarding our research, news, publications, contact information, etc

- **Technologies or techniques**

Not applicable

- **Inventions, patent applications, and/or licenses**

Not applicable

- **Other Products**

Not applicable

## 7. PARTICIPANTS & OTHER COLLABORATING ORGANIZATIONS

### What individuals have worked on the project?

Note the % effort for every individual is for the totality of the grant period

<i>Name:</i>	Martin Conda-Sheridan
<i>Project Role:</i>	PI
<i>Researcher Identifier (e.g. ORCID ID):</i>	0000-0002-3568-2545
<i>Nearest person month worked:</i>	2.4 (7.9% effort)
<i>Contribution to Project:</i>	Dr. Conda-Sheridan supervised the project. He trained students and postdoctoral researchers on the synthetic aspect of the research, including purification and characterization of molecules. He reviewed the data.
<i>Funding Support:</i>	The remaining of my salary came from the national science foundation (NSF-Career), the American Chemical Society-PRF grant, a NIH-COBRE, and the UNMC-college of Pharmacy.

<i>Name:</i>	Mohamed Seleem
<i>Project Role:</i>	Graduate Student
<i>Researcher Identifier (e.g. ORCID ID):</i>	0000-0003-4379-5133
<i>Nearest person month worked:</i>	21.4 (71% effort)
<i>Contribution to Project:</i>	Mr. Seleem was involved on the synthesis, characterization, and purification of compounds. He also performed microbiological and cell studies. He is writing one of the manuscripts and will finish the required experiments.



<i>Funding Support:</i>	He was funded by this grant. Near the end of the funding period, he received a fellowship that supported him. He was still involved in the project.
-------------------------	---

<i>Name:</i>	Luana Campos
<i>Project Role:</i>	Graduate Student
<i>Researcher Identifier (e.g. ORCID ID):</i>	0000-0001-8527-688X
<i>Nearest person month worked:</i>	5.7 (19% effort)
<i>Contribution to Project:</i>	Ms. Campos performs the synthesis, characterization, and purification of compounds. She also does in silico studies.
<i>Funding Support:</i>	She was funded by this grant and a NIH-COBRE grant.

<i>Name:</i>	Aramis Pereira
<i>Project Role:</i>	Technician (accepted into graduate school, visa problems)
<i>Researcher Identifier (e.g. ORCID ID):</i>	N/A
<i>Nearest person month worked:</i>	2 (7% effort)
<i>Contribution to Project:</i>	Mr. Pereira works on the synthesis and identification of peptides.
<i>Funding Support:</i>	The remaining of his salary (mainly in the area of peptides) came from a NIH-COBRE, and the UNMC-college of Pharmacy.

<i>Name:</i>	Audifas Salvador Matus Meza
<i>Project Role:</i>	Postdoc
<i>Researcher Identifier (e.g. ORCID ID):</i>	
<i>Nearest person month worked:</i>	5 (16% effort)
<i>Contribution to Project:</i>	Dr. Matus Mesa trained students on the synthetic aspect of the research, including purification and characterization of molecules.
<i>Funding Support:</i>	The remaining of his salary (working in other small molecules antibacterials) came from the NIH-COBRE grant.

<i>Name:</i>	Nathali Rodrigues de Almeida
<i>Project Role:</i>	Postdoc
<i>Researcher Identifier (e.g. ORCID ID):</i>	0000-0002-9552-1233
<i>Nearest person month worked:</i>	4 (13% effort)
<i>Contribution to Project:</i>	Dr. Almeida trained students on microbiology.
<i>Funding Support:</i>	This grant and a NIH-COBRE grant.

<i>Name:</i>	Venkata Udumula
<i>Project Role:</i>	Postdoc
<i>Researcher Identifier (e.g. ORCID ID):</i>	
<i>Nearest person month worked:</i>	3 (10% effort)
<i>Contribution to Project:</i>	Synthesis of some heterocycles.
<i>Funding Support:</i>	This grant.

<i>Name:</i>	Krishnaiah Maddeboina
<i>Project Role:</i>	Postdoc
<i>Researcher Identifier (e.g. ORCID ID):</i>	
<i>Nearest person month worked:</i>	2.7 (9% effort)
<i>Contribution to Project:</i>	Synthesis of some heterocycles.
<i>Funding Support:</i>	This grant.

We have also established collaborations with Dr. Fabio Alves (University of Fluminense) and Dr. Mohamed Seleem (same name than my student) (Virginia Tech). They have shown interest in evaluation our compounds but due to the pandemic, things are in stand by at the moment.

**Has there been a change in the active other support of the PD/PI(s) or senior/key personnel since the last reporting period?**

**New grants:**  
 1R56AI146062-01A1 NIH-NIAID (Ouellette, PI) 10/01/2020-09/31/2021  
 ROLE OF THE CLP PROTEASE SYSTEMS IN THE GROWTH AND PATHOGENESIS OF CHLAMYDIA  
 The goal of this project is to understand how affecting the cylindrical protease machinery alters the growth of Chlamydia trachomatis  
 Role: Conda-Sheridan, I

1941731- National Science Foundation-CAREER 03/01/20-02/28/25  
 DESIGN AND UNDERSTANDING OF COMPLEX BIOMATERIALS  
 The goal of this CAREER proposal is to create nature-inspired self-assembling biomaterials with tunable properties that are stimuli sensitive and whose supramolecular architecture can be predicted with the aid of novel software tools.  
 Role: Conda-Sheridan, PI

**What other organizations were involved as partners?**

**Organization Name:** Fluminense Federal University

- **Location of Organization:** Rua Miguel de Frias 9; Icaraí; Niterói – RJ; Brazil; 24220-900
- **Partner's contribution to the project** They performed the biological evaluation of selected AMPs.
- **Financial support;** National Government (Brazil)

**Organization Name:** Community for Open Antimicrobial Drug Discovery (CO-ADD) -The University of Queensland

▪ **Location of Organization:** 306 Carmody Rd, The University of Queensland, St. Lucia, QLD, 4072, Australia

▪ **Partner's contribution to the project** They performed the biological evaluation of selected molecules against ESKAPE pathogens (E. coli, K. pneumoniae, A. baumannii, P. aeruginosa, S. aureus (MRSA)) and fungi C. neoformans and C. albicans.

▪ **Financial support;** Wellcome Trust

**Organization Name:** Virginia Polytechnic Institute and State University

▪ **Location of Organization:** 205 Duck Pond Drive; Blacksburg, VA 24061; United States

▪ **Partner's contribution to the project** They performed the biological evaluation of selected molecules against ESKAPE pathogens. We considered testing the compounds in two sites, plus our lab, will increase the robustness of our results and validate them.

▪ **Financial support;** NIH and Start-up from Virginia Tech.

## 8. SPECIAL REPORTING REQUIREMENTS

**COLLABORATIVE AWARDS:**

**QUAD CHARTS:**

## 9. APPENDICES:

**APPENDIX I**  
**Original STATEMENT OF WORK –**  
**Description of changes and status**

Site 1: University of Nebraska Medical Center  
S 42nd St & Emile St, Omaha, NE 68198  
PI: Martin Conda Sheridan

<b>Specific Aim 1</b>	<b>Timeline</b>	<b>Status</b>
<b>Synthesis of phenazines</b> (the peptides will be prepared by solid phase peptide synthesis, in all cases we add extra time for optimization and potential pitfalls).	Months	
Synthesis of the precursors (includes scaling-up) We may need to prepare additional molecules at a later time.	1, 13	Done
Attaching amine side chains.	2	See A
Attaching polyamines.	3	See A
Attachment of amphiphilic peptides.	4	See A
<b>Purification and characterization</b>		
Purify the amines by flash chromatography and recrystallization.	3-4	See A
Characterize the molecules using mass spectrometry, infrared spectroscopy, nuclear magnetic resonance, etc.	4-6	See A
<b>Specific Aim 2</b>	<b>Timeline</b>	<b>Site 1</b>
<b>Antibacterial activity</b>		
Assess minimum inhibitory concentration using broth microdilution method.	6-7	Done
Biofilm dispersion using a Cagliari Device.	8-9	See B
Mutant studies using the broth microdilution and the disk diffusion test.	9-10	See C
Permeability assessment across caco-2 cells.	10-11	See C
Metabolic stability in presence of human liver fraction S9.	12-13	See D
<b>Specific Aim 2</b>	<b>Timeline</b>	<b>Site 1</b>
<b>Toxicity assessment of the phenazines in vitro</b>		

Cell toxicity studies. We will assess toxicity against various mammalian cells using the MTT assay. All cells will be obtained from ATCC: HCT 116 (ATCC CCL-247); MCF7 (ATCC HTB-22); PC-3 (ATCC CRL-1435); Primary Dermal Fibroblast; Normal, Human, Adult (ATCC PCS-201-012).	14-15	Done
<b>In vivo studies</b>		
C. elegans, study effect of the peptides in this in vivo model.	16-17	See E
Wax moth larvae, study effect of the peptides in this in vivo model.	17-18	See E

- A. As stated in the report, the modification of the phenazines was an unexpected challenge. We have prepared various phenazines and peptides (and peptide amphiphiles) but no hybrids (at the moment). Consequently, these tasks has been partially completed, we have a wealth of information and results of the individual molecules but not the hydrid.
- B. We did not use a Calgary device but rather used 48-well plates instead. We are still evaluating antibiofilm activity (but should finish soon).
- C. We have not studied permeability but are currently performing mutant studies using a S. aureus transposon library. This will help us to understand which strains are sensitive to our compounds. We will later isolate resistant mutants.
- D. We have studied the stability of the individual molecules (some reported in the Peptides paper) but not the hybrids.
- E. We will finish this task using phenazines in the near future. It will add to our phenazine manuscript currenty in preparation

## APPENDIX II

**List of equipment purchased with award funds (please check the terms and agreement for applicability of this requirement or contact the contract/grants specialist below).**

Nothing to report

**List of residual inventory of unused supplies exceeding \$5,000 in value. (Please check the terms and agreement if for applicability of this requirement).**

Nothing to report

# Synthesis and Antichlamydial Activity of Molecules Based on Dysregulators of Cylindrical Proteases

Mohamed A. Seleem, Nathalia Rodrigues de Almeida, Yashpal Singh Chhonker, Daryl J. Murry, Zaira da Rosa Guterres, Amanda M. Blocker, Shiomi Kuwabara, Derek J. Fisher, Emilse S. Leal, Manuela R. Martinefski, Mariela Bollini, María Eugenia Monge, Scot P. Ouellette,\* and Martin Conda-Sheridan\*



Cite This: *J. Med. Chem.* 2020, 63, 4370–4387



Read Online

ACCESS |



Metrics & More

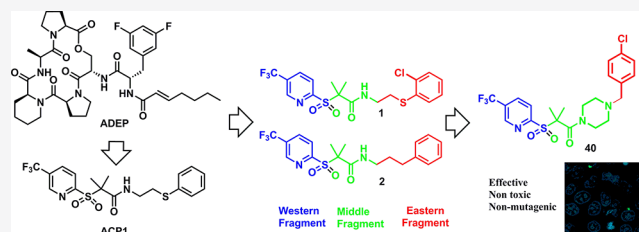


Article Recommendations



Supporting Information

**ABSTRACT:** *Chlamydia trachomatis* is the most common sexually transmitted bacterial disease globally and the leading cause of infertility and preventable infectious blindness (trachoma) in the world. Unfortunately, there is no FDA-approved treatment specific for chlamydial infections. We recently reported two sulfonylpyridines that halt the growth of the pathogen. Herein, we present a SAR of the sulfonylpyridine molecule by introducing substituents on the aromatic regions. Biological evaluation studies showed that several analogues can impair the growth of *C. trachomatis* without affecting host cell viability. The compounds did not kill other bacteria, indicating selectivity for *Chlamydia*. The compounds presented mild toxicity toward mammalian cell lines. The compounds were found to be nonmutagenic in a *Drosophila melanogaster* assay and exhibited a promising stability in both plasma and gastric fluid. The presented results indicate this scaffold is a promising starting point for the development of selective antichlamydial drugs.



## INTRODUCTION

*Chlamydia trachomatis* is a Gram-negative bacterium that infects 1.7 million people in the U.S. with an ~8.8% increase in infection rates since 2013.<sup>1,2</sup> It is the most commonly reported bacterial sexually transmitted infection (STI) worldwide according to recent surveillance by the Centers for Disease Control and Prevention.<sup>2,3</sup> *Chlamydia*, which primarily targets epithelial cells, is considered the leading cause of infertility and preventable infectious blindness (trachoma) in the world.<sup>4,5</sup> Perhaps the most serious issue with chlamydial infections, and a chief cause of its deleterious consequences, is the asymptomatic nature of the infection.<sup>6,7</sup> Untreated chlamydial infections can result in chronic sequelae, such as pelvic inflammatory disease, which can lead to ectopic pregnancy and tubal factor infertility.<sup>4</sup>

The chlamydial developmental cycle commences by attachment of an infective, nonreplicative elementary body (EB) to the plasma membrane of the host cell. Within the host cell, the EB remains within a host-derived vesicle, termed an inclusion. Later the EB differentiates into its replicative form, the reticulate body (RB), which begins the replication process.<sup>8,9</sup> After multiple rounds of polarized division<sup>10</sup> within the inclusion, RBs undergo a secondary differentiation to EBs, and the pathogen is released from the host cell starting another round of infection.<sup>9,11</sup>

Currently, there is no vaccine nor a selective drug approved by the FDA to treat *Chlamydia trachomatis*.<sup>12,13</sup> The first-line

antibiotics used for chlamydia infections (i.e., azithromycin (AZM) and doxycycline) are broad spectrum drugs that can affect regular functions of the commensal microbiota and encourage the development of bacterial resistance.<sup>14</sup> In addition, *C. trachomatis* recurrence after antibiotic treatment remains a considerable issue that may eventually lead to treatment failure and the chronic sequelae associated with this pathogen.<sup>15–17</sup> For example, repeated chlamydial infections at rates of ~25% for women and ~20% for men have been reported after AZM treatment.<sup>18</sup> Taking into consideration the steady increase in infection cases, the risk of contagion, and the rise of general bacterial resistance due to untargeted treatments, the development of a selective chlamydial drug is needed to meet the challenges posed by this STI.

Several approaches are being pursued to develop specific treatments against chlamydial infections. Noteworthy is the seminal work of Almqvist et al. that sought to inhibit chlamydial growth by blocking the glucose-6-phosphate pathway.<sup>19,20</sup> This group has developed a novel class of

Received: March 2, 2020

Published: March 31, 2020



thiazolino-2-pyridones that show remarkable inhibitory activity and low toxicity toward mammalian cells. Elofsson and co-workers also reported another intriguing approach focused on blocking the type II fatty acid synthesis pathway (FAS II).<sup>21</sup> The same group has prepared compounds with dual activity by combining key features from active compounds into hybrid systems.<sup>22</sup> These important works highlight the importance of designing compounds that affect nontraditional bacterial targets to eradicate this pathogen.

Another antimicrobial target that has gathered considerable attention recently are the cylindrical proteases.<sup>23,24</sup> It has been suggested that dysregulation of proteolytic enzymes is a novel approach to treat bacterial infections<sup>25–28</sup> because the indiscriminate degradation of proteins can damage the physiology, pathogenicity, and cellular processes of the organism.<sup>29,30</sup> Previously, Brötz-Oesterhelt et al. reported some cyclic acyldepsipeptides (ADEP) (Figure 1) activate

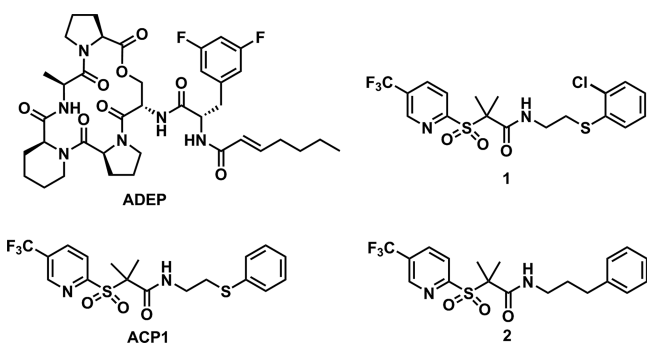


Figure 1. Structures of ADEP and ACP compounds.

ClpP, leading to the death of *Escherichia coli*.<sup>25</sup> Others expanded their findings showing that ClpP activation can kill other bacteria, including *Neisseria gonorrhoeae*, *Neisseria meningitidis*, *Haemophilus influenzae*, *Pseudomonas aeruginosa*, and *Staphylococcus aureus*, through various *in vitro* and *in vivo* assays.<sup>31–35</sup> Although promising, ADEPs possess some inherent limitations such as poor solubility, metabolic instability, fast clearance in animal studies, and challenging chemical synthesis.<sup>36–38</sup>

Building upon that precedent, Leung and co-workers combined computational chemistry and biochemical experiments to identify new scaffolds that can activate ClpP.<sup>35</sup> Two of the synthesized molecules, named ACP1a and b (1 and 2, Figure 1), showed moderate antibacterial activity against *N. meningitidis* (64  $\mu\text{g}/\text{mL}$  and 16  $\mu\text{g}/\text{mL}$ , respectively) and *H. influenzae* (32  $\mu\text{g}/\text{mL}$  and 8  $\mu\text{g}/\text{mL}$  respectively). Both molecules were 10–20-fold less potent than ADEP1. However, ACP1b was found to activate *E. coli* ClpP in an enzymatic assay, suggesting its potential as an antibiotic against this target.<sup>35</sup>

The biological functions of *Chlamydia* are also hypothesized to be regulated by cylindrical proteases, which degrade proteins and peptides to maintain homeostasis and perhaps to regulate differentiation of the developmental forms.<sup>39–41</sup> Recent work by us and others highlights the critical role of this degradation machinery in *Chlamydia*.<sup>41,42</sup> Four core Clp proteins have been identified in this organism: the caseinolytic proteases, ClpP1 and ClpP2, and two associated ATPase chaperones (AAA+) with diverse cellular activities,<sup>43</sup> ClpC and ClpX.<sup>27,44,45</sup> These chaperones bind to the axial faces of ClpP regulating its proteolytic activity. Using the work of Leung as a

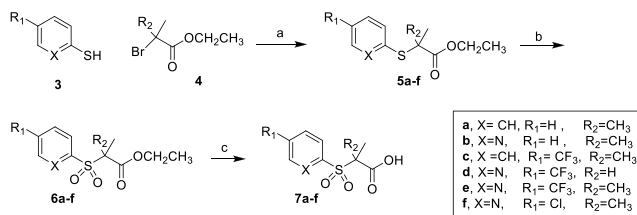
starting point, we synthesized molecules 1 and 2 and studied their ability to affect *C. trachomatis* as well as their effects on chlamydial growth and viability.<sup>41</sup> We found both compounds cause a drastic decrease in the formation of infectious EBs, although we could not definitively assign this effect to a disruption in ClpP activity in *Chlamydia*. Based on our early report, we decided to optimize compounds 1 and 2 to establish structure–activity relationships (SAR).

In the present work, we report the antichlamydial activity of new antichlamydial agents. One of the new molecules (compound 40) was found to affect both chlamydial inclusion numbers, size, and morphology in infected HEP-2 cells. In addition, we performed the preliminary mechanism of action studies to understand the eradication process. We also investigated the antimicrobial activity of the compounds against several Gram-positive and Gram-negative bacteria, as well as fungi, to establish their spectrum of activity. Finally, we assessed the toxicity of various compounds toward human cells, their mutagenicity in *Drosophila melanogaster*, and their stability in mouse plasma, simulated gastric fluid, and human liver microsomes. The results indicate these new compounds are selective for *Chlamydia trachomatis* and can be used as a starting point to develop new drugs selective toward this pathogen.

## RESULTS AND DISCUSSION

**Chemistry.** Our synthetic strategy was based on reacting a substituted sulfonyl aryl carboxylic acids with the desired amine.<sup>35,41</sup> The carboxylic acid derivatives (7a–7f, Scheme 1)

### Scheme 1. Synthesis of Key Carboxylic Acid Intermediates 7a–7f<sup>a</sup>

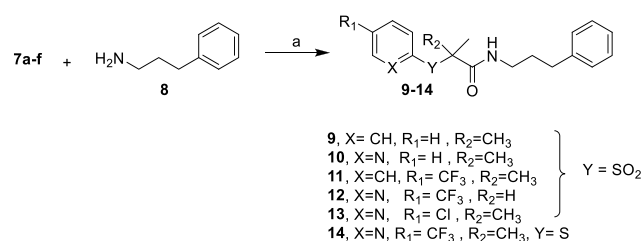


<sup>a</sup>Reagents and conditions: (a) KOH, EtOH, reflux, 18 h; (b) oxone, dioxane–water (5:1), 23 °C, 18 h; (c) LiOH·H<sub>2</sub>O, THF–water (4:1), 23 °C, 18 h.

were prepared by reacting 2-thioaryl derivatives (3) with an appropriate  $\alpha$ -halo ester derivative (4).<sup>35</sup> The obtained thioether derivatives 5a–5f were reacted, without further purification, with potassium peroxydisulfate (OXONE) in a dioxane–water mixture to provide the corresponding sulfone derivatives 6a–6f. Hydrolysis of the ester group under mild basic conditions provides the corresponding carboxylic acid derivatives 7a–7f. The monomethyl acid derivative 7d was alternatively prepared, in two steps, by the reaction of 5-(trifluoromethyl)pyridine-2-thiol with 2-bromopropanoic acid followed by oxidation (Scheme S1).<sup>46</sup>

The carboxylic acid derivatives 7a–7f were activated using PYBOP and DIPEA in tetrahydrofuran (THF) and then reacted with 3-phenylpropylamine to yield six derivatives, 9–14 (Scheme 2).<sup>41,47,48</sup> All the prepared molecules satisfy the Lipinski rule of five (Table S1).<sup>49</sup> PYBOP proved to be the best choice for this type of reaction while other coupling agents, such as HBTU and HATU (with or without Oxyma),

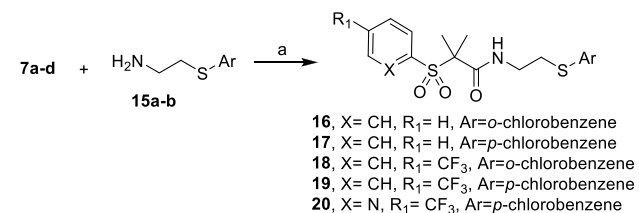


Scheme 2. Synthesis of ACP1 Analogues with the Modified Western Part<sup>a</sup>

<sup>a</sup>Reagents and conditions: (a) PYBOP, DIPEA, THF, RT, 1 h.

only gave trace amounts of the product. The selection of THF was also critical because using DMF resulted in a Smiles rearrangement reaction due to the presence of a sulfonyl moiety (Scheme S2).<sup>50</sup>

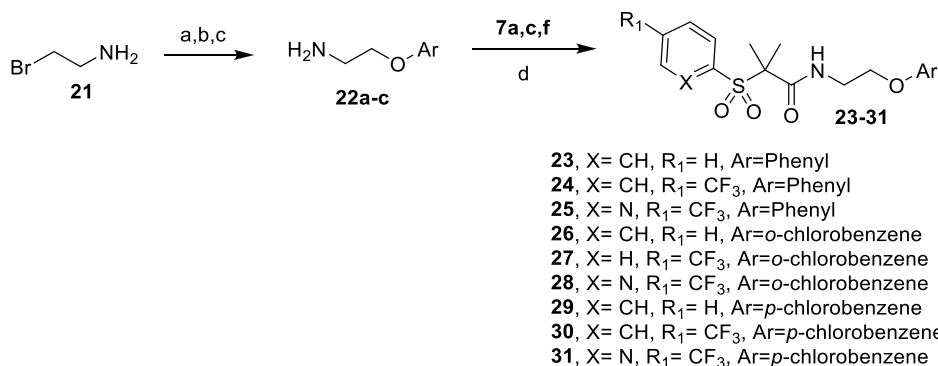
Then, five derivatives (16–20, Scheme 3) were synthesized to understand the importance of the thiol and chloro atoms on

Scheme 3. Synthesis of ACP1b Analogues by Modification in the Western Fragment<sup>a</sup>

<sup>a</sup>Reagents and conditions: (a) PYBOP, DIPEA, THF, 23 °C, 1 h.

the eastern part of the molecule. Accordingly, the amine precursors 15a,15b (a = 2-((2-chlorophenyl)thio)ethan-1-amine; b = 2-((4-chlorophenyl)thio)ethan-1-amine) were prepared as reported previously (Scheme S4)<sup>51,52</sup> and reacted with the carboxylic acids 7a–7d.

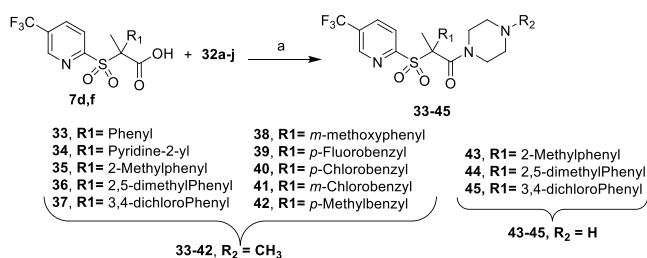
To investigate the importance of the thiol on the eastern part, we synthesized derivatives 23–31 (Scheme 4). First, we converted 2-bromoethylamine (21) into the functionalized 3-phenoxyethylamines 22a–22c (a = 2-phenoxyethan-1-amine; b = 2-(2-chlorophenoxy)ethan-1-amine; c = 2-(4-chlorophenoxy)ethan-1-amine). These molecules were

Scheme 4. ACP Derivatives with Oxygen in the Western Part<sup>a</sup>

<sup>a</sup>Reagents and conditions: (a) BOC<sub>2</sub>O, DCM, 23 °C, overnight; (b) *p*-chlorophenol, K<sub>2</sub>CO<sub>3</sub>, DMF; (c) TFA, H<sub>2</sub>O, dioxane, 23 °C, 18 h; (d) PYBOP, DIPEA, THF, 23 °C 1 h.

coupled to the carboxylic acid intermediates 7a, 7c, and 7f using the conditions described above.

To further develop SAR, we synthesized a set of compounds with restricted rotation by including piperazine linkers in the middle part (33–45). The carboxylic acid derivatives 7d,f were reacted with various piperazines (32a–32j) to evaluate the effect of this substitution on the eastern region of the molecules, as shown in Scheme 5. This rigid linker restricts the flexibility of the side chain and reduces the entropic penalty of binding of the compounds to their target.<sup>53,54</sup>

Scheme 5. Synthesis of ACP1 Analogues with a Rigid Linker<sup>a</sup>

<sup>a</sup>Reagents and conditions: appropriate piperazine derivative, PYBOP, DIPEA, THF, 23 °C, 1 h.

**Biological Evaluation. Antichlamydial Activity.** As mentioned, once EBs are internalized, they differentiate into RBs and remain within a membrane-bound vesicle called an inclusion. This protects the pathogen during its developmental cycle. Because the inclusions are linked to the growth and replication of the pathogen,<sup>55,56</sup> we determined antichlamydial activity by analyzing the number and size of the inclusions using an immunofluorescence assay (IFA).<sup>57,58</sup> Briefly, HEp-2 cells were infected with *C. trachomatis* serovar L2, and the synthesized molecules were added at 50 μg/mL, 8 h postinfection (hpi). After 16 h (total incubation of the cells for 24 h), the inclusions were analyzed and compared with the control, untreated cells. The morphology and viability of the cells were examined under phase contrast microscopy to ensure the eradication of the inclusions was not the result of a reduction in viable cells due to compound toxicity (Figure 3b and the Supporting Information). Table 1 shows the results of this prescreening assay.

**Table 1.** Initial Antichlamydial Activity Screening of ACP Derivatives vs *C. trachomatis* (Serovar LGV-L2)<sup>a</sup>

cmpd no.	inhibition activity	cmpd no.	inhibition activity
ACP1	–	28 <sup>59</sup>	+
1	++	29	–
2	–	30	–
9	–	31	–
10	–	33	–
11	++	34	–
12	–	35	+
13	+	36	++
14	toxic	37	++
16	–	38	+
17	–	39	–
18 <sup>59</sup>	++	40	++
19	++	41	++
20 <sup>59</sup>	–	42	+
23	–	43	–
24 <sup>59</sup>	++	44	–
25	++	45	–
26	–		
27	++		

<sup>a</sup>Compounds were tested at 50  $\mu\text{g}/\text{mL}$ . The compound's effectiveness is a measure of its ability to inhibit chlamydial inclusions and can be divided into three categories: [–] = not effective; [+] = intermediate effect; [++] = effective. One compound demonstrated clear toxicity to the host cells and is noted.

We found that analogues **9** and **10**, molecules lacking the trifluoromethyl group, were inactive, which highlighted the importance of electron withdrawing groups at position 4. Meanwhile, the presence of the trifluoromethyl-substituent (compound **11**) provided antichlamydial activity. Next, we replaced the trifluoromethyl group with a chlorine atom (**13**), obtaining an analogue with moderate activity. Two other derivatives containing an unsubstituted phenyl group (**16**, **17**) and a chlorine atom on the eastern part of the molecule did not exhibit activity. However, the addition of the trifluoromethyl group, while keeping with the same substitution pattern on the eastern part (**18**, **19**), yielded antichlamydial compounds.

The importance of the trifluoromethyl substituent was further highlighted in derivatives **23**–**29**, which also possess an aryl ether group. Surprisingly, three molecules contained a trifluoromethyl group and were still inactive against *Chlamydia*: compounds **20**, **30**, and **31**. Note that these inactive compounds possess a chlorine atom at the para position on the eastern portion of the molecules. Collectively, these data suggest a detrimental effect of substitution at the para position. To test the importance of the sulfonyl group, a thioether derivative **14** was synthesized by skipping the oxidation step in Scheme 2. The obtained derivative showed prominent host cell toxicity. Compound **12**, which has one methyl group instead of the *gem*-dimethyl group, was found to be inactive.

Next, we decided to replace the amide bond at the middle part of the core molecule with rigid cyclic amine (piperazine) groups to generate a series of derivatives without hydrogen bond donor groups (Table 1 and Table S1). Compounds **33** and **34**, possessing phenyl or pyridyl groups attached to the piperazine moiety, lacked antichlamydial activity. In contrast, replacement of the phenyl group with an *o*-tolyl (**35**), 2,5-

dimethyl phenyl (**36**), or 3,4-dichloro phenyl (**37**) enhanced antichlamydial activity. The inclusion of a methyl spacer between the piperazine and the eastern part, gave molecules **38** and **42**, which displayed moderate activity. The fluorinated analogue of **38**, molecule **39**, did not possess activity, but the chlorinated molecule (**40**) was active. Thus, the data suggest that a larger group with electron withdrawing properties is needed. Molecules **41** and **42** possess substituents at the meta position, and once again, the electron withdrawing group enhanced activity. Finally, three derivatives (**43**–**45**) with a monomethyl group in the middle part exhibited no antichlamydial activity.

After the initial assessment of antichlamydial activity, we determined the impact of the most active compounds *in vitro* by determining the number and morphology of infectious units (the EB) and compared their activity against two antibiotics: spectinomycin and penicillin, which are among the FDA approved antibiotics used to treat STDs.<sup>60,61</sup> We understand penicillin is not commonly used to treat *Chlamydia* since it blocks cell division and growth without eradicating the bacteria but we were looking for a comparison against a common drug.<sup>62</sup> HEP-2 cells were infected with *C. trachomatis* serovar L2, and then the selected molecules were added; 50  $\mu\text{g}/\text{mL}$  of our compounds, 128  $\mu\text{g}/\text{mL}$  of spectinomycin (2 $\times$  minimum inhibitory concentration. (MIC)),<sup>63</sup> and 5 units/mL of penicillin (3 $\times$  MIC)<sup>63</sup> 8 h after infection. To accurately determine the “infectious progeny” by quantifying the number of chlamydiae from treated cultures as well as controls, we used an inclusion forming units (IFU) assay as described elsewhere.<sup>62</sup> Briefly, after 24 h, the infected cells were scraped, collected in chlamydia transport medium, and used to reinfect a fresh HEP-2 cell monolayer. The chlamydial infectivity, reported as IFUs, was determined by counting the number of fluorescent inclusions after immunofluorescent staining, 24 h postsecondary infection (Figures 2 and 3a) from a minimum of 15 fields of view using an epifluorescence microscope. We also assessed the morphology, size, and appearance of the chlamydial inclusions after exposure to the tested compounds. Among the designated compounds, derivatives **11**, **24**, **25**, **35**, **37**, **40**, and **41** showed a remarkable impact on chlamydiae.

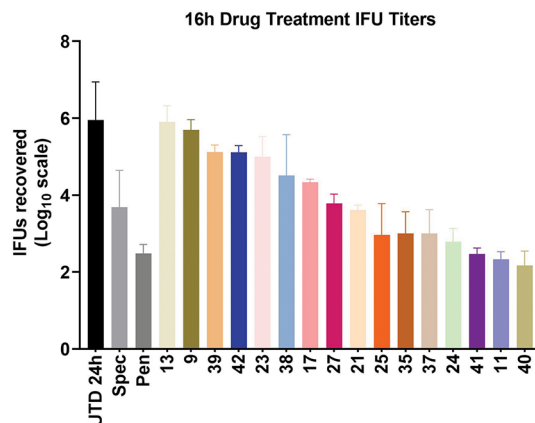


**Figure 2.** Quantification of chlamydial growth in the presence of selected ACP derivatives (numbered) and antibiotics spectinomycin (Spec) and penicillin (Pen) as compared to an untreated (UTD) control at 24 h postinfection. Results are reported as an average with standard deviation on a log<sub>10</sub> scale and represent a minimum of two biological replicates.

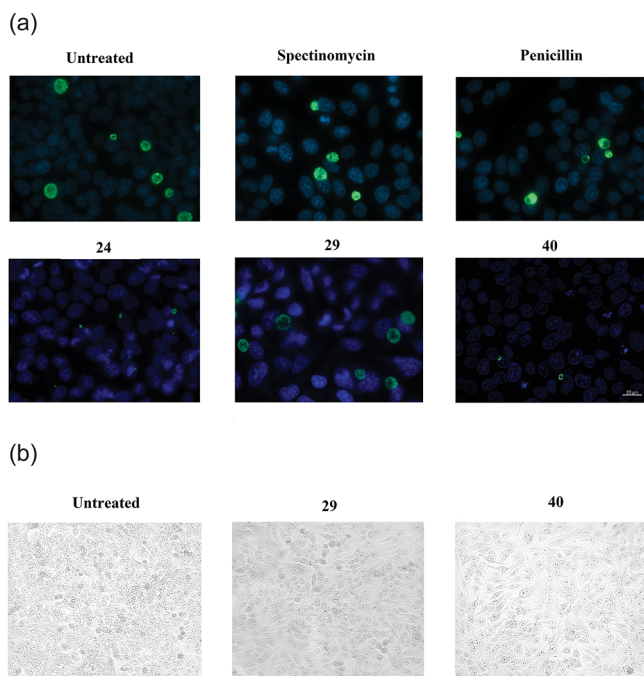


**Figure 3.** (a) Immunofluorescence images of the effects of selected compounds on chlamydial inclusion growth. In blue, HEP-2 cells nuclei; in green, chlamydial inclusions. Images were acquired at 24 h postinfection. (b) Cell morphology images using an EVOS FL auto cell imaging microscope.

Compound **40** showed superior activity than spectinomycin, which was used at a concentration roughly 2.5-fold higher (128  $\mu\text{g}/\text{mL}$ ) and on par with penicillin (5 U/mL to  $\sim 3 \mu\text{g}/\text{mL}$ ).<sup>64</sup> The immunofluorescent staining (Figure 3a) revealed the inclusions were relatively small and irregular in cells treated with our compounds when compared with the untreated sample and the reference molecules. The cell morphology investigation (Figure 3b) supported that the tested compounds did not show any toxicity during the assay. We reasoned the high activity of this derivative is due to the combination of amide bond restriction in the middle part, the electron withdrawing group in the eastern part, and the acceptable log *P* and HBD/HBA values (Table S1).

**Dose–Response Curve.** The dose–response effect was investigated for compound **40** on *Chlamydia* at six concentrations using the IFU assay described previously. As expected, compound **40** was found to exhibit inhibition activity in a dose-dependent manner with an  $\text{IC}_{50}$  (the concentration, which shows 50% inclusion inhibition) of 5.2  $\mu\text{g}/\text{mL}$  (Figure 4a). The dose–response curve revealed a high reduction of chlamydial progeny in a consistent way (Figure 4a). Besides affecting progeny yields, the immunofluorescence images showed an increase in the number and size of chlamydial inclusions as the concentration of the compound decreased (Figure 4). Compound **40** reduced the chlamydial infection at both 100 and 50  $\mu\text{g}/\text{mL}$  and still maintained good activity up to a concentration of 12.5  $\mu\text{g}/\text{mL}$ , with inclusion yields around 60% lower than the untreated cells. We did not observe cell toxicity at 100  $\mu\text{g}/\text{mL}$ , which supports the tolerability of **40**.

**Antichlamydial Effect of ACP Derivatives in Comparison with Two Marketed Drugs.** We further tested the activity of compound **40** at 50  $\mu\text{g}/\text{mL}$  and 5.20  $\mu\text{g}/\text{mL}$  ( $\text{IC}_{50}$  value) against our lead compound (ACP1b) at 50  $\mu\text{g}/\text{mL}$ , and two frontline antibiotics, azithromycin and doxycycline, at their

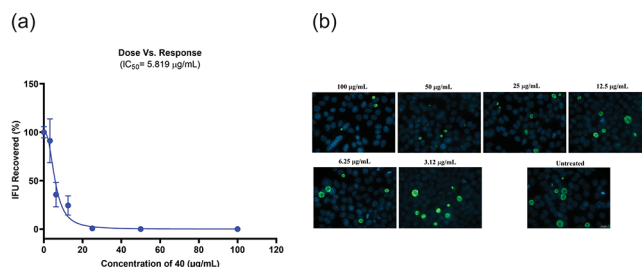


**Figure 4.** (a) Dose–response curve for the effect of **40** reported on a  $\log_{10}$  scale. (b) Immunofluorescence analysis of **40** inhibitory effect. In green, chlamydial inclusions; in blue, HEP-2 cell nuclei.

reported minimal chlamydicidal concentrations (MCCs), (4  $\mu\text{g}/\text{mL}$  and at 1  $\mu\text{g}/\text{mL}$ , respectively).<sup>65–68</sup> We confirmed our lead compound (ACP1b) and compound **40** showed good inhibitory activity against chlamydiae (Figure 5a). The four

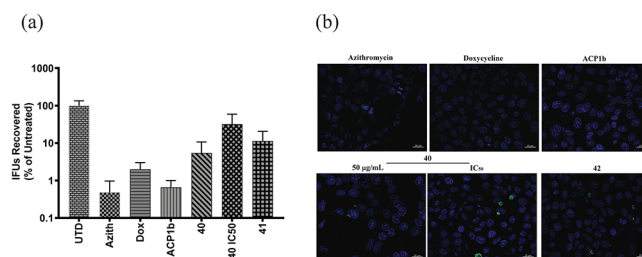


**Figure 5.** (a) Quantification of chlamydial growth in the presence of selected ACP derivatives (**40** and ACP1b) and antibiotics azithromycin (Azith) and doxycycline (Dox) as compared to an untreated (UTD) control at 24 h postinfection. (b) Immunofluorescence analysis of the tested compounds inhibitory effect; in green, chlamydial inclusions; in blue, HEP-2 cells nuclei.

tested compounds elicited a notable impact on the size as well as the number of the inclusions (Figure 5b). Despite the reported treatment efficacy of both drugs,<sup>69</sup> these antibiotics are associated with two major concerns. The first is treatment failure rate, which can reach 22% and lead to repeat infections, and existing complications associated with chlamydial infections.<sup>70</sup> The second concern involves bacterial resistance that can be triggered by these broad spectrum therapies (in both *Chlamydia* and other normal flora bacteria)<sup>71–74</sup> and can lead to chlamydial persistence.<sup>75–77</sup> Given these concerns and the promising activity of our compounds, we consider ACP a new scaffold with a unique mechanism of action that can serve as a starting point to generate new antichlamydial agents.

**Mechanism of Action.** Antibiotics can be bacteriostatic, stopping growth or reproduction by targeting essential functions such as cell wall growth, or bactericidal, which kills the bacteria.<sup>78</sup> To classify compound **40**, we treated HEP-2 cells at 8 hpi with 50  $\mu\text{g}/\text{mL}$  of the molecule, followed by incubation for an additional 16 h. Subsequently, the drug was washed out before the infected cells were further incubated for another 24 h. As seen in Figure 6a, compound **40** reduced the inclusion yield as expected, but 24 h after drug washout, the number of inclusions increased by  $\sim 1$  log in comparison with untreated cells, suggesting a bacteriostatic mechanism of action. Further, incubation of the infected cells with **40** for 48 h led to higher inclusion output suggesting a loss of the drug activity via metabolic degradation, development of resistance (unlikely on the time frame of the experiment), or an increase on the total number of inclusions at the end of the

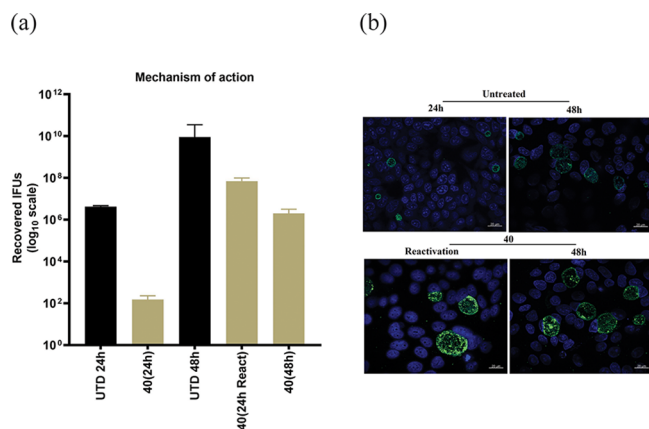


**Figure 6.** (a) Investigation of the bacteriostatic or bactericidal activity of **40** as measured by IFU output and reported on a log<sub>10</sub> scale. (b) Immunofluorescence analysis of **40** impact 24 h after its removal (reactivation) in comparison with untreated (UTD) samples at 24 h postinfection. In green, chlamydial inclusions; in blue, HEp-2 cell nuclei.

cycle, which cannot be eradicated by the drug or a combination of the three. Additional studies are needed to understand this result.

Although the EB numbers increased after drug removal or incubation for an additional 24 h, we noticed a reduction in the inclusion size and loss in inclusion morphology, reflecting a lack of development of the pathogen, which suggests the impact of our compounds on chlamydial growth (Figure 6b). Generally, the static effect of these compounds was consistent with a general mechanism depending on inhibition of protein turnover inside the chlamydial organisms. Bacteriostatic drugs can help in treatment of chlamydia infections since the progression of *Chlamydia* into a latent form and the clearance of bacteria are not only dependent on the antibiotic category but also on the capability of the host cells to eliminate the bacteria.<sup>79</sup>

**In Vitro Protease Activity.** The presented compounds are analogues to known ClpP activators.<sup>41,59</sup> Therefore, we tested the ability of selected compounds to stimulate ClpP-dependent protein degradation *in vitro* in the absence of a AAA+ chaperone. The protease activities of recombinant ClpP1 and ClpP2 from *C. trachomatis* L2, recombinant ClpP from *E. coli*, and recombinant ClpP from human and mouse cells (mitochondrially localized) were measured in the presence and absence of ACPs (Figure 7).<sup>41</sup> Briefly, 20 μM of FITC-labeled casein was incubated with 1 or 0.1 (**40** only) μM ClpP from *E. coli*, 1 μM mammalian ClpP, or 6 μM of *C. trachomatis* ClpP1 and ClpP2 at 32 °C for 3 h with or without compounds. Fluorescence owing to FITC-casein degradation was measured every 3 min. In parallel, degradation of unlabeled casein was also performed and measured by using SDS-PAGE followed by staining with Coomassie Brilliant Blue (Figure S4). Derivatives **11** and **40** enabled some species of ClpP to degrade casein in the absence of a chaperone while little or no degradation was observed for compounds **9**, **16**, or **17**. Importantly, **40** did not activate human or mouse ClpP, suggesting possible selectivity of the compounds for the bacterial ClpP at least in reference to the ClpP from *E. coli*. Surprisingly, we did not observe activation of chlamydial ClpP1, ClpP2, or the ClpP1/2 dimer (other than some residual decomposition triggered by **9** and **11**). We assessed the activity of the chlamydial ClpP1/P2

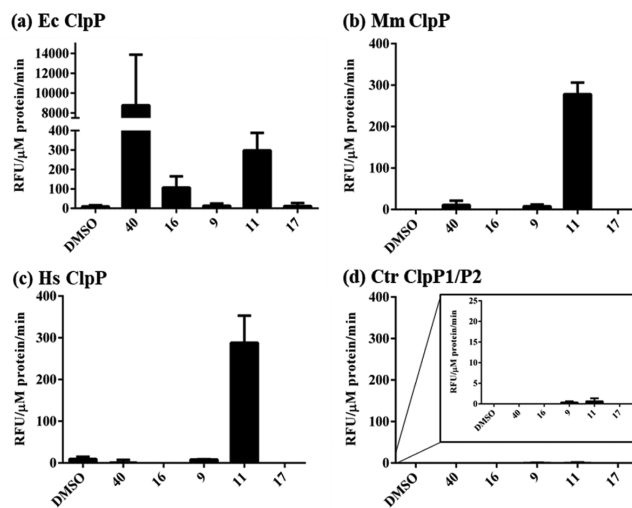


**Figure 7.** In vitro protease assay shows the degradation of casein (unlabeled) by three different recombinant ClpP preparations with or without the compounds as assessed by SDS-PAGE analysis. Ec = *Escherichia coli*, Ctr = *Chlamydia trachomatis*, Hs = *Homo sapiens*, Mm = *Mus musculus*. DMSO is a negative control. Note the mammalian ClpP orthologues migrate slightly lower than casein in the gels. The top band in all images is casein and the lower band is the respective ClpP. Molecular weight markers (in kDa) are present in lane 1 of each gel.

preparations using Native PAGE to confirm oligomerization (Figure S2) and digestion of the fluorescent peptide Suc-Luc-Tyr-AMC (Figure S3). This prompted us to consider the killing effect may be the result of ClpP inhibition. However, we did not observe inhibition of ClpP1/P2 activity using the Suc-Luc-Tyr-AMC fluorescent peptide assay. Also, under the conditions tested, we did not observe alterations in ClpP1/P2 activity in the presence of the compounds and the chaperones (data not shown). The results suggest that while *E. coli* ClpP is activated chlamydial ClpP function is not altered, suggesting the molecules may have a mechanism of action independent of this target.

**Other Antimicrobial Activity.** To evaluate the selectivity of our molecules, we tested their biological activity against other lab strains and ESKAPE microorganisms and selected fungal pathogens: *Staphylococcus aureus* JE 2, *S. aureus* ATCC 43300 MRSA; *E. coli* ATCC 25922; *E. coli* K12, *P. aeruginosa* ATCC 27853; *K. pneumoniae* ATCC 700603; *Acinetobacter baumannii* ATCC 19606; *Candida albicans* ATCC 90028; and *Cryptococcus neoformans* var. *grubii* H99 ATCC 20882. Notably, none of our compounds showed inhibitory activity against these species in a preliminary screening at 32 μg/mL (Table S2). To further investigate their selectivity, we subjected *S. aureus* JE2 and *E. coli* K12 to concentrations up to 256 μg/mL of compounds **11**, **21**, **25**, **28**, **35**, **37**, **40**, **42**, and once again, bacterial death was not observed. These results indicate that the compounds may be selective for *Chlamydia*. These data also suggest the molecules may not affect the normal gut flora, which in turn suggests the development of widespread resistance is unlikely. We think the lack of activity against other microorganisms is due to the unique cell wall structure of *C. trachomatis* when compared to other bacteria and the unique developmental cycle of *Chlamydia*, which may favor the selectivity of the compounds. In support of these points, **40** was a strong activator of the *E. coli* ClpP *in vitro* (Figure 6)

without showing antibacterial properties toward either tested *E. coli* strain.

**Cytotoxicity.** The previous assays not only indicated antichlamydial activity but also low toxicity toward the HEp-2 host cells (Figure 5b and Figure S1). To further examine the tolerability of the synthesized compounds, we evaluated their *in vitro* toxicity against epithelial cervix adenocarcinoma (HeLa 229) and human keratinocyte (HaCaT) cells. Molecules were evaluated at a concentration of 50  $\mu\text{g}/\text{mL}$ , i.e., the highest tested concentration used in antichlamydial assays, and results are summarized in Figure 8. The compounds were tolerated by

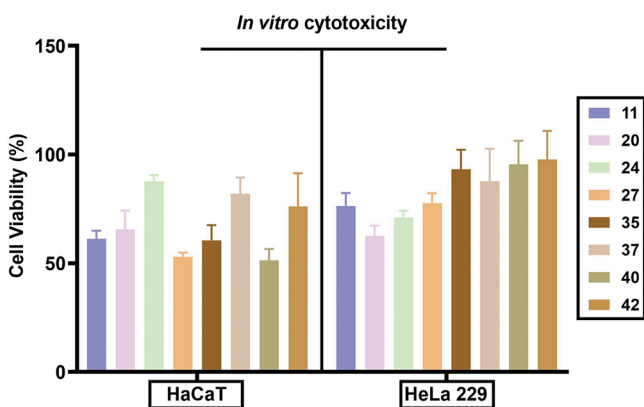


Figure 8. Toxicity analysis of the most active compounds against HeLa 229 and human keratinocytes.

HeLa 229 cells (only 20 and 24 presented viabilities less than 65%), while the normal HaCaT proved to be more sensitive to some of the molecules. For example, compound 40 was not toxic toward HeLa 229 cells but affected ~50% of the HaCaT cells. Compounds 24, 37, and 42 were more tolerated by the HaCaT cells. This result is not necessarily consistent with the *in vitro* casein degradation data. For example, 11 presented toxicity toward both cells and activated mammalian ClpP but 40 did not activate these ClpP orthologues. Future studies will be performed to assess if the observed degradation data is related to a limit of detection issue with the casein assay in combination with an increased need for ClpP/mitochondrial function in the HaCaT cells versus the HeLa cells or to other off-target mechanisms of action.

**Mutagenic Studies.** One major concern of potential antibiotics is their mutagenesis potential, which can damage the host cells and facilitate the adaptation of the bacteria to the antibiotic pressure and other types of stress. Accordingly, we evaluated whether the ACP derivatives were mutagenic toward eukaryotes using the Somatic Mutation and Recombination Tests (SMART) in wing-somatic cells of *Drosophila melanogaster*.<sup>80</sup> This *in vivo* assay simultaneously detects mutational and mitotic recombination events and quantifies the recombinogenic activity of chemicals and drugs. Some antimicrobial drugs have been reported to promote DNA damage because of oxidative stress in the mammalian genome,<sup>81–83</sup> leading to severe side effects such as bone marrow depression, aplastic anemia, and leukemia. We analyzed marked trans-heterozygous descendants (*mwh/flr3*) resulting from standard (ST) and high bioactivation (HB)

Table 2. Frequency of Mutant Spots in the Wings of Marked trans-Heterozygous Descendants (*mwh/flr3*) of *D. melanogaster* Using the Standard Cross (ST) and Marked Trans-Heterozygous Descendants (*mwh/flr3*) of *D. melanogaster* Using the High Bioactivation (HB) after Chronic Treatment of Larvae with 11, 40, and 41 Derivatives

cmpd ID	concn (mM)	no. of flies (N)	spots per fly (no. of spots) statistical diagnosis <sup>a</sup>				
			small single spots (1–2 cell) <sup>b</sup> <i>m</i> = 2	large single spots (>2 cell) <sup>b</sup> <i>m</i> = 2	twin spots <i>m</i> = 5	total spots <i>m</i> = 2	spots with <i>mwh clone</i> <sup>c</sup> ( <i>n</i> )
<i>mwh/flr3</i> of <i>D. melanogaster</i> —Standard Cross (ST)							
control		20	0.40 (8)	0.15 (3)	0.0 (0)	0.55 (11)	10
	0.25	20	0.25 (5) –	0.0 (0) –	0.0 (0) –	0.25 (5) –	5
11	0.50	20	0.20 (4) –	0.0 (0) –	0.0 (0) –	0.20 (4) –	4
	1.00	20	0.35 (7) –	0.05 (1) –	0.0 (0) –	0.40 (8) –	8
	0.25	20	0.20 (4) –	0.0 (0) –	0.0 (0) –	0.20 (4) –	4
40	0.50	20	0.15 (3) –	0.0 (0) –	0.0 (0) –	0.15 (3) –	3
	1.00	20	0.30 (6) –	0.05 (1) –	0.0 (0) –	0.35 (7) –	7
	0.25	20	0.10 (2) –	0.05 (1) –	0.0 (0) –	0.15 (3) –	3
41	0.50	20	0.15 (3) –	0.15 (3) –	0.05 (1) –	0.35 (7) –	7
	1.00	20	0.20 (4) –	0.05 (1) –	0.0 (0) –	0.25 (5) –	5
<i>mwh/flr3</i> of <i>D. melanogaster</i> —High Bioactivation (HB) Cross							
control		20	0.25 (5)	0.10 (2)	0.05 (1)	0.40 (8)	8
	0.25	20	0.15 (3) –	0.05 (1) –	0.05 (1) –	0.25 (5) –	5
11	0.50	20	0.10 (2) –	0.15 (3) –	0.0 (0) –	0.25 (5) –	5
	1.00	20	0.20 (4) –	0.05 (1) –	0.05 (1) –	0.30 (6) –	6
	0.25	20	0.45 (9) i	0.0 (0) –	0.0 (0) –	0.45 (9) –	9
40	0.50	20	0.25 (5) –	0.0 (0) –	0.10 (2) –	0.35 (7) –	7
	1.00	20	0.50 (10) i	0.05 (1) –	0.05 (1) –	0.60 (12) –	12
	0.25	20	0.40 (8) –	0.05 (1) –	0.0 (0) –	0.45 (9) –	9
41	0.50	20	0.40 (8) –	0.05 (1) –	0.05 (1) –	0.50 (10) –	10
	1.00	20	0.35 (7) –	0.10 (2) –	0.0 (0) –	0.45 (9) –	9

<sup>a</sup>Statistical diagnoses according to Frei and Würzler [1988]. *U* test, two-sided; probability levels: –, negative; +, positive; i, inconclusive; *P* < 0.05 vs untreated control. <sup>b</sup>Including *flr3* single spots. <sup>c</sup>Considering *mwh* clones from *mwh* single and twin spots.

crossings, which were chronically exposed to ACP derivatives at three different concentrations. The frequency of different mutant clones was scored and the total spots, which indicate the final genotoxicity of each compound at different concentrations, are shown in Table 2 and Table S3.

We found that flies treated with **11**, **20**, **24**, **26**, **40**, and **41** displayed frequencies of clone formation (per individual) for the ST and HB crosses ranging from 0.15 to 0.45 ( $P < 0.05$ ) and 0.20 to 0.60 ( $P < 0.05$ ), respectively, at 0.25, 0.5, and 1 mM. The flies treated with compound **26** at 1 mM showed a higher mutation frequency of 0.70 and 0.75 in descendants from both crossings, although these were not statistically significant. Overall, the results were negative, indicating that the compounds are nongenotoxic in somatic cells of *D. melanogaster* at the concentrations tested, even in HB cross, which has high metabolic bioactivation. However, **26** indicated that the mutant spot frequencies are directly dependent on the concentration, and it is possible that concentrations higher than 1 mM may present mutagenic potential. Compounds **11**, **20**, **24**, **26**, **40**, and **41** did not show toxicity against *D. melanogaster* at the tested concentrations, and it was observed that the survival rate in the treated groups did not differ statistically from the negative control ( $P < 0.05$ ).

**Stability Studies.** We investigated the *in vitro* metabolic stability of the compounds using liver microsomes and mouse plasma. The incubation with human liver microsomes (HLM) is considered a relevant pharmacokinetic indicator for a compound *in vivo*.<sup>84,85</sup> The metabolic half-life ( $t_{1/2}$ ) and the intrinsic clearance ( $CL_{int}$ ) of compounds **11**, **24**, **25**, **37**, and **40** are summarized in Table 3. The assay revealed that all

**Table 3.** *In Vitro* Experimental Values of  $T_{1/2}$ , Intrinsic Clearance, and Hepatic Clearance<sup>a</sup>

cmpd ID	$T_{1/2}$ (min)		CL(int) $\mu$ L/ (min*mg protein)		CL(int,H) mL/ (min*kg body wt)	
	mean	SD	mean	SD	mean	SD
<b>11</b>	6.13	0.16	113.09	3.02	890.58	23.77
<b>24</b>	2.98	0.17	233.77	13.74	1840.91	108.17
<b>25</b>	3.73	0.03	185.60	1.72	1461.60	13.51
<b>37</b>	6.25	0.16	111.96	2.85	873.80	22.45
<b>40</b>	<2.00	NA	NA		NA	

<sup>a</sup>NA: Not applicable

tested compounds underwent rapid modification with approximately 90% of the drug modified in 10 min as shown in Figure 9. All tested compounds were stable in the negative control experiment (without NADPH) up to 60 min. For compound **40** the main metabolite presented a M + 16 peak (Figure S5), which may correspond to the *N*-oxidated adduct. Fragmentation spectra of both neat and 10 min incubated samples indicated no chemical change in the eastern part (Figure S5). This compound persisted 60 min postincubation with HLM. The metabolic site and the complete chemical structure of this metabolite is still under investigation.

Then, we explored the stability of some representative compounds in mouse plasma and simulated gastric fluid (SGF, pH 1.2) by calculating the percentage of drug remaining after contact with both media. The tested compounds were incubated with diluted mouse plasma and SGF at 37 °C and the samples were analyzed by HPLC–MS. As shown in Figure 10, all the tested compounds exhibited a high stability profile and their concentrations remained constant for up to 120 min.

No modification or degradation was detected after the different incubation periods.

## CONCLUSION

Caseinolytic protease P (ClpP) activators have been shown to eradicate bacteria and prevent bacterial resistance. *C. trachomatis* is among the few bacterial species that possess two caseinolytic protease paralogues, ClpP1 and ClpP2.<sup>41</sup> The Clp protein machinery system is essential for the chlamydial developmental cycle, which includes differentiation between the EB and RB forms.<sup>86</sup> In this study, we synthesized compounds based on known ClpP activators to kill *C. trachomatis*. We found some interesting lead compounds that were able to eradicate the pathogen. The biological results allowed us to conduct initial SAR studies to identify key regions that promote biological action (Figure 11). Noteworthy is the fact that compounds did not present activity against other types of bacteria, suggesting a degree of selectivity for *Chlamydia*. While the active compounds were able to activate the *E. coli* ClpP, activation of chlamydial ClpP1/2 was not observed as determined by diverse assays. This suggests the compounds may impact *Chlamydia* by affecting a different target. *In vitro* metabolic stability assays revealed these ACP derivatives were enzymatically transformed by liver microsomes in the first 10 min of incubation. Conversely, the compounds demonstrated good stability in mouse plasma and simulated gastric fluid. Our results indicate the ACP derivatives represent a promising scaffold that can be further developed to obtain a specific treatment for *C. trachomatis* infection. Studies are currently underway to understand the target of the molecules.

## EXPERIMENTAL PROCEDURES

**Chemistry. General.** All reagents and solvents were used as received from commercial suppliers unless otherwise noted. All used solvents were dried and stored with activated molecular sieves to ensure dryness on the long run. All coupling reactions were carried out in dried glassware under N<sub>2</sub> atmosphere. Reaction progression was detected using thin layer chromatography (TLC), which was performed on Merck silica gel IB2-F plates (0.25 mm thickness), and the spots detected using a UV light source at 254 nm. <sup>1</sup>H and <sup>13</sup>CNMR spectra were run at 500 MHz in deuterated chloroform (CDCl<sub>3</sub>) or dimethyl sulfoxide (DMSO-*d*<sub>6</sub>) on a Bruker-500 NMR spectrometer. Chemical shifts are given in parts per million (ppm) on the delta ( $\delta$ ) scale. Chemical shifts were calibrated relative to those of the solvents. Flash chromatography was performed on the RF 200i Flash Chromatography System from Teledyne ISCO. Low-resolution mass spectra were obtained on an Agilent 6120 or 6150 mass spectrometer with an electrospray ionization (ESI) source. High-resolution mass spectra were run using a Q Exactive HF Hybrid Quadrupole Orbitrap mass spectrometer. The tested compounds possessed purities above 95%. The purity tests were performed on an Agilent 1200 HPLC system equipped with a multiple wavelength absorbance UV detector set for 254 nm and using 5 mM C-18 reversed-phase column with methanol and water as a mobile phase. All reported yields refer to isolated compounds. Marvin was used for characterizing of the physicochemical characters of the synthesized compounds, Marvin 20.4, ChemAxon (<https://www.chemaxon.com>).

**General Procedure for the Synthesis of Acid Derivatives 7a–7f. 2-(Arylthio)propanoate Derivatives 5a–5f.** To a stirred solution of an appropriated aryl thiol **3** (3.00 mmol) in ethanol (10 mL) were added potassium hydroxide pellets (0.25 g, 4.40 mmol) followed by ethyl  $\alpha$ -bromo ester **4** (3.00 mmol), and the reaction mixture was heated at reflux for 18 h. After completion of the reaction, the flask content was allowed to cool down to room temperature, and the formed inorganic salt was removed by filtration and washed with

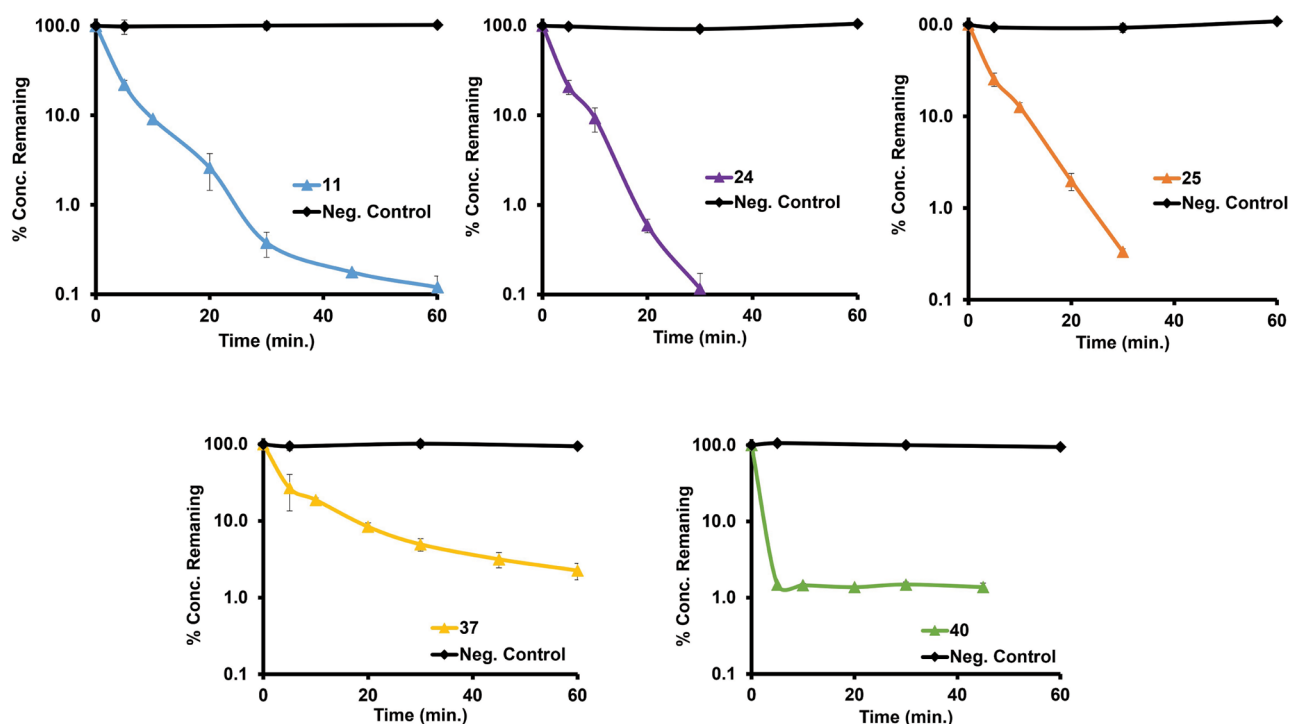


**Figure 9.** Time-dependent metabolic stability of the tested compounds in human liver microsomes fortified with NADPH and without NADPH (negative control). Metabolic elimination profiles (% turnover or amount remaining vs incubation time). Data shown as mean  $\pm$  SD ( $n = 3$ ).

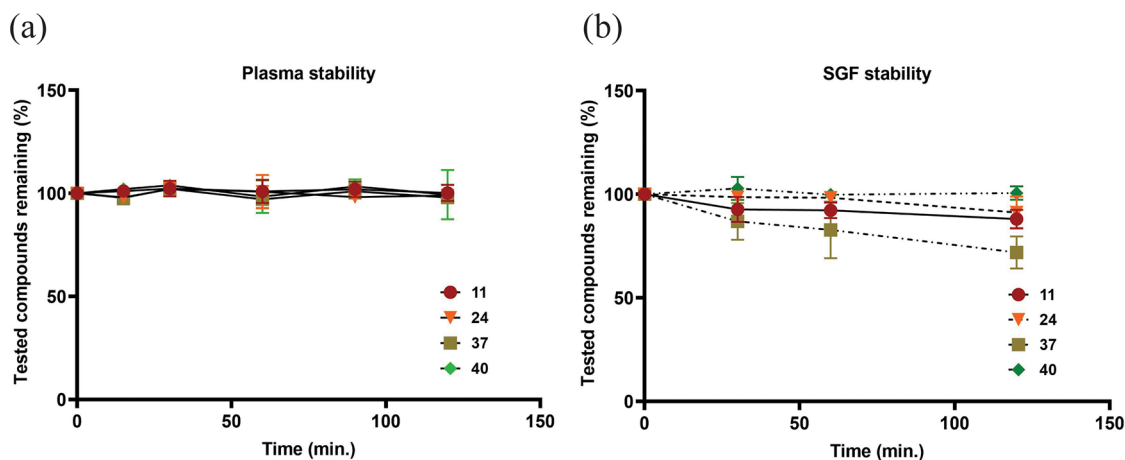


**Figure 10.** Stability profile in mouse plasma (a) and simulated gastric fluid (b). Relative concentration is represented as a function of incubation time between the tested compound and mouse plasma and simulated gastric fluid (SGF, pH 1.2). Error bars represent SD of three independent experiments.

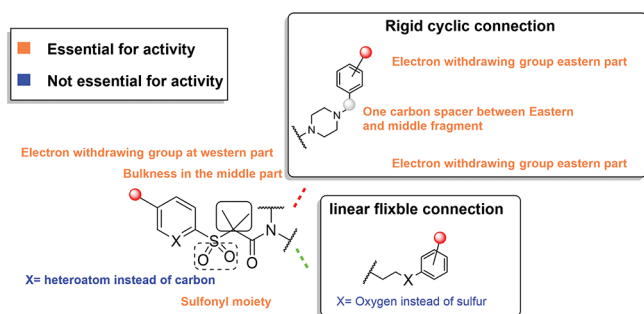


**Figure 11.** SAR graphical summary.

cold ethanol. The filtrate was evaporated under reduced pressure, and the oily residue was dissolved in DCM (20 mL) and washed with

deionized water ( $3 \times 10$  mL) and brine solution ( $1 \times 10$  mL), dried over anhydrous  $\text{Na}_2\text{SO}_4$ , filtered, and concentrated under reduced pressure to afford the desired product as yellow oil which was used in the next step without further purification.

**2-(Arylsulfonyl)propanoate Derivatives 6a–6f.** Potassium mono persulfate (OXONE) (2.2 equiv) was added in one portion to a solution of the 2-(arythio)propanoate derivatives 5a–5f (3.4 mmol) in dioxane–water 5:1 (25 mL). The formed white suspension was vigorously stirred at 23 °C for 18 h. The white solid was filtered off and washed with dioxane, and the combined filtrate was concentrated under reduced pressure to remove the organic layer. The resulting aqueous solution was extracted with DCM ( $3 \times 15$  mL). The combined organic solution was dried over  $\text{Na}_2\text{SO}_4$  and filtered, and the organic solvent was removed under reduced pressure to afford the desired product as white solids which were used directly in the next step without further purification.

**2-(Arylsulfonyl) Acid Derivatives 7a–7f.** 2-(Arylsulfonyl)propanoate derivative **6a–6f** (3.6 mmol) was dissolved in a mixture of THF–water (4:1, 20 mL), lithium hydroxide monohydrate (7.2 mmol) was milled and added portion wise over 30 min, and the reaction was stirred at room temperature for 18 h. The organic solvent was evaporated under reduced pressure, and the aqueous solution was washed with DCM (1 × 20 mL) to remove byproducts. Then, the aqueous layer was cooled in an ice bath and treated with 1 N HCl to pH 2. The formed precipitate was filtered off to afford the desired products. The physical characters and the spectral data of separated product are listed below.

**2-Methyl-2-(phenylsulfonyl)propanoic Acid (7a).** Starting with **6a** (925 mg), white solid (520 mg, 77%). <sup>1</sup>H NMR (500 MHz, CDCl<sub>3</sub>) δ 7.89 (d, *J* = 7.0 Hz, 2H), 7.71–7.68 (m, 2H), 7.70 (t, *J* = 7.5 Hz, 1H), 1.63 (s, 6H).

**2-Methyl-2-(pyridin-2-ylsulfonyl)propanoic Acid (7b).** Starting with **6b** (925 mg), white solid (280 mg, 41%). <sup>1</sup>H NMR (500 MHz, CDCl<sub>3</sub>) δ 8.77 (m, 1H), 8.14 (d, *J* = 8.0 Hz, 1H), 8.03 (t, *J* = 8.0 Hz, 1H), 7.63–7.61 (m, 1H), 1.70 (s, 6H).

**2-Methyl-2-((4-(trifluoromethyl)phenyl)sulfonyl)propanoic Acid (7c).** Starting with **6c** (1160 mg), white solid (840 mg, 82%). <sup>1</sup>H NMR (500 MHz, CDCl<sub>3</sub>) δ 8.04 (d, *J* = 8.5 Hz, 2H), 7.83 (d, *J* = 8.5 Hz, 2H), 1.66 (s, 6H); <sup>19</sup>F NMR δ –63.27 (s).

**2-((5-(Trifluoromethyl)pyridin-2-yl)sulfonyl)propanoic Acid (7d).** Starting with **6d** (1120 mg), white solid (750 mg, 85%). <sup>1</sup>H NMR (500 MHz, CDCl<sub>3</sub>) δ 9.01 (s, 1H), 8.253–8.250 (m, 1H), 4.75 (q, *J* = 7.5 Hz, 1H), 1.74 (d, *J* = 7.5 Hz, 3H). <sup>19</sup>F NMR δ –62.45 (s).

**2-Methyl-2-((5-(trifluoromethyl)pyridin-2-yl)sulfonyl)propanoic Acid (7e).** Starting with **6e** (1170 mg), white fluffy solid (890 mg, 83%). <sup>1</sup>H NMR (500 MHz, CDCl<sub>3</sub>) δ 9.02 (s, 1H), 8.27–8.22 (m, 2H), 1.76 (s, 6H). <sup>19</sup>F NMR δ –62.68 (s).

**2-((5-Chloropyridin-2-yl)sulfonyl)-2-methylpropanoic Acid (7f).** Starting with **6f** (1050 mg), white solid (700 mg, 79%). <sup>1</sup>H NMR (500 MHz, CDCl<sub>3</sub>) δ 8.73–8.72 (m, 1H), 8.07 (d, *J* = 8.5 Hz, 1H), 7.97–7.95 (m, 1H), 1.71 (s, 6H).

**General Procedures for Synthesis of 2-Methyl-N-(3-phenylpropyl)-2 (arylsulfonyl) Propanamide (9–14).** A solution of 2-methyl-2-(arylsulfonyl)propanoic acid **7a–7f** (0.16–0.17 mmol) in dry THF (10 mL) was treated with a solution of PyBOP (87 mg, 0.17 mmol) in THF (1 mL) followed by DIPEA (83 μL). Then, the reaction mixture was stirred at room temperature for 10 min. A solution of the 3-phenylpropan-1-amine (0.16 mmol) in THF (1 mL) was then added dropwise. The formed yellow solution was stirred at room temperature for 1 h. The solvent was removed under vacuum, and the crude product was absorbed onto silica gel and purified by flash column chromatography eluting with a 0–100% gradient of EtOAc in hexanes. The physical characters and the spectral data of the obtained products are listed below.

**2-Methyl-N-(3-Phenylpropyl)-2-(phenylsulfonyl)propanamide (9).** Starting with **7a** (37 mg), white solid (46 mg, 84%). <sup>1</sup>H NMR (500 MHz, CDCl<sub>3</sub>) δ 7.81 (d, *J* = 7.5 Hz, 2H), 7.65 (t, *J* = 7.5 Hz, 1H), 7.52 (t, *J* = 7.5 Hz, 2H), 7.31–7.26 (m, 2H), 7.21–7.18 (m, 3H), 7.05 (br s, 1H), 3.33 (q, *J* = 6.5 Hz, 2H), 2.70 (t, *J* = 6.5 Hz, 2H), 1.90 (q, *J* = 6.5 Hz, 2H), 1.54 (s, 6H). <sup>13</sup>C NMR (125 MHz, CDCl<sub>3</sub>) δ 167.44, 141.18, 135.10, 134.34, 130.04, 129.03, 128.54, 128.40, 126.10, 68.01, 39.90, 33.19, 30.79, 20.93. HPLC purity, 97.1%. HRMS (*m/z*): [M + H]<sup>+</sup> calcd for C<sub>19</sub>H<sub>24</sub>NO<sub>3</sub>S, 346.1399; found, 346.1470; exact mass (monoisotopic) from spectrum, 345.1397.

**2-Methyl-N-(3-Phenylpropyl)-2-(pyridin-2-ylsulfonyl)propanamide (10).** Starting with **7b** (37 mg), white solid (46 mg, 83%). <sup>1</sup>H NMR (500 MHz, CDCl<sub>3</sub>) δ 8.66–8.65 (m, 1H), 8.03 (d, *J* = 7.5 Hz, 1H), 7.92 (t, *J* = 7.5 Hz, 1H), 7.53–7.51 (m, 1H), 7.29–7.26 (m, 1H), 7.19–7.18 (m, 4H), 3.33 (q, *J* = 6.5 Hz, 2H), 2.70 (t, *J* = 6.5 Hz, 2H), 1.91 (q, *J* = 7.5 Hz, 2H), 1.60 (s, 6H). <sup>13</sup>C NMR (125 MHz, CDCl<sub>3</sub>) δ 167.76, 154.89, 150.25, 141.44, 137.94, 128.47, 128.42, 127.76, 125.99, 124.71, 67.40, 39.94, 33.13, 30.65, 20.73. HPLC purity, 98.9%. HRMS (*m/z*): [M + H]<sup>+</sup> calcd for C<sub>18</sub>H<sub>22</sub>N<sub>2</sub>O<sub>3</sub>S, 347.1351; found, 347.1423; exact mass (monoisotopic) from spectrum, 346.1350.

**2-Methyl-N-(3-Phenylpropyl)-2-((4-(trifluoromethyl)phenyl)sulfonyl)propanamide (11).** Starting with **7c** (48 mg), white solid (53 mg, 81%). <sup>1</sup>H NMR (500 MHz, CDCl<sub>3</sub>) δ 7.94 (d, *J* = 8 Hz, 2H), 7.78 (d, *J* = 8.5 Hz, 2H), 7.32–7.29 (m, 2H), 7.22–7.20 (m, 3H), 6.87 (br s, 1H), 3.33 (q, *J* = 6.5 Hz, 2H), 2.71 (t, *J* = 6.5 Hz, 2H), 1.93 (q, *J* = 6.5 Hz, 2H), 1.55 (s, 6H); <sup>13</sup>C NMR (125 MHz, CDCl<sub>3</sub>) δ 166.94, 141.03, 138.7, 136.06, 135.80, 130.68, 128.60, 128.37, 126.11 (q, *J* = 3.75 Hz), 126.19, 121.93, 68.32, 40.02, 33.19, 30.71, 20.67. HPLC purity, 97.4%. HRMS (*m/z*): [M + H]<sup>+</sup> calcd for C<sub>20</sub>H<sub>22</sub>F<sub>3</sub>NO<sub>3</sub>S, 414.1272; found, 414.1345, exact mass (monoisotopic) from spectrum, 413.1727.

**N-(3-Phenylpropyl)-2-((5-(trifluoromethyl)pyridin-2-yl)sulfonyl)propanamide (12).** Starting with **7d** (50 mg), white solid (48 mg, 68%). <sup>1</sup>H NMR (500 MHz, CDCl<sub>3</sub>) δ: 8.97 (s, 1 H), 8.19 (s, 2H), 7.30–7.26 (m, 2H), 7.21–7.16 (m, 3H), 6.58 (br s, 1H), 4.33 (q, *J* = 7.5 Hz, 1H), 3.32–3.28 (m, 2H), 2.66 (t, *J* = 7.5 Hz, 2H), 1.85 (p, *J* = 7.5 Hz, 2H), 1.55 (d, *J* = 7.0 Hz, 3H). <sup>13</sup>C NMR (125 MHz, CDCl<sub>3</sub>) δ 163.62, 158.79, 147.39, 147.36, 141.13, 135.81, 135.78, 130.22, 128.53, 128.35, 126.12, 123.22, 121.28, 62.55, 39.84, 33.02, 30.70, 11.47. HPLC purity, 98.3. ESIMS calcd for C<sub>18</sub>H<sub>19</sub>F<sub>3</sub>N<sub>2</sub>O<sub>3</sub>S: 401.42 [M + H]<sup>+</sup>; found, 401.01. HRMS (*m/z*): [M + H]<sup>+</sup> calcd for C<sub>18</sub>H<sub>19</sub>F<sub>3</sub>N<sub>2</sub>O<sub>3</sub>S, 401.1068; found, 401.1139; exact mass (monoisotopic) from spectrum, 400.1067.

**Alternative Method for the Synthesis of Molecule 12.** **N-(3-Phenylpropyl)-2-((5-(trifluoromethyl)pyridin-2-yl)thio)propanamide.** To a solution of 2-((5-(trifluoromethyl)pyridin-2-yl)thio)propanoic acid (0.05 g, 0.20 mmol) in dry THF (7 mL), PYBOP (0.08 g, 0.18 mmol) and DIPEA (70 μL, 0.5 mmol) were added and the mixture was stirred at room temperature for 15 min; phenyl propylamine (28 μL, 0.20 mmol) was added. The reaction mixture was stirred at room temperature for 1 h; thereafter, the organic solvent was evaporated under reduced pressure and the crude residue was purified by flash column chromatography to yield the desired product as yellow oil (55 mg, 75%). <sup>1</sup>H NMR (500 MHz, CDCl<sub>3</sub>) δ: 8.69 (s, 1 H), 7.73 (d, *J* = 8.5 Hz, 1H), 7.29 (d, *J* = 8.5 Hz, 1H), 7.28–7.24 (m, 2H), 7.19–7.16 (m, 1H), 7.08–7.06 (m, 2H), 4.47 (q, *J* = 7.5 Hz, 1H), 3.34–3.22 (m, 2H), 2.54 (t, *J* = 7.5 Hz, 2H), 1.82–1.76 (m, 2H), 1.60 (d, *J* = 7.5 Hz, 3H).

**N-(3-Phenylpropyl)-2-((5-(trifluoromethyl)pyridin-2-yl)sulfonyl)propanamide (12).** To a stirred solution of 3-phenylpropyl 2-((5-(trifluoromethyl)pyridin-2-yl)thio)propanoate (55 mg, 0.15 mmol) in dioxane/water (5:1, 3 mL) in a 10 mL scintillation vial, in one portion (160 mg, 0.3 mmol), potassium mono persulfate (OXON) was added. The obtained white suspension was stirred at room temperature for 16 h. After the reaction was completed as seen by TLC, the white solid was filtered off, and dioxane was removed under reduced pressure. Then, the aqueous solution was extracted with DCM (3 × 5 mL). The collected organic layers were dried over sodium sulfate, removed under reduced pressure, and purified with flash column chromatography to afford the desired oxidized derivative as white crystals (33 mg, 56%).

**2-((5-Chloropyridin-2-yl)sulfonyl)-2-methyl-N-(3-phenylpropyl)propanamide (13).** Starting with **6f** (42 mg), white solid (55 mg, 88%). <sup>1</sup>H NMR (500 MHz, CDCl<sub>3</sub>) δ 8.58 (s, 1H), 7.97 (d, *J* = 8.5 Hz, 1H), 7.88–7.86 (dd, *J* = 8.5 Hz, *J* = 1.5 Hz, 1H), 7.29–7.26 (m, 2H), 7.20–7.17 (m, 3H), 7.04 (br s, 1H), 3.30 (q, *J* = 6.5 Hz, 2H), 2.69 (t, *J* = 7.5 Hz, 2H), 1.90 (q, *J* = 7.5 Hz, 2H), 1.59 (6H, s). <sup>13</sup>C NMR (125 MHz, CDCl<sub>3</sub>) δ 167.46, 152.64, 149.31, 141.33, 137.51, 137.03, 128.52, 128.40, 126.06, 125.70, 67.65, 39.98, 33.12, 30.60, 20.62. HPLC purity, 98.5%. HRMS (*m/z*): [M + H]<sup>+</sup> calcd for C<sub>18</sub>H<sub>21</sub>ClN<sub>2</sub>O<sub>3</sub>S, 381.0961; found, 381.1033; exact mass (monoisotopic) from spectrum, 380.0960.

**2-Methyl-N-(3-phenylpropyl)-2-((5-(trifluoromethyl)pyridin-2-yl)thio)propanamide (14).** Starting with thioacid (50 mg), white solid (47 mg, 76%). <sup>1</sup>H NMR (500 MHz, CDCl<sub>3</sub>) δ 8.65 (s, 1H), 7.71 (d, *J* = 8.5 Hz, 1H), 7.34 (br s, 1H), 7.29 (d, *J* = 8.5 Hz, 1H), 7.24 (t, *J* = 7.5 Hz, 2H), 7.16 (t, *J* = 7.5 Hz, 1H), 7.06 (d, *J* = 7.5 Hz, 2H), 3.26 (q, *J* = 7.5 Hz, 2H), 2.54 (t, *J* = 6.5 Hz, 2H), 1.76 (q, *J* = 7.5 Hz, 2H), 1.68 (s, 6H). <sup>13</sup>C NMR (125 MHz, CDCl<sub>3</sub>) δ 173.85, 162.41, 146.06, 146.01, 141.36, 133.14, 133.11, 128.43, 128.24, 125.97, 124.59,



123.39, 123.12, 122.85, 52.77, 39.59, 33.13, 30.91, 26.61. HPLC purity, 98.9%. HRMS ( $m/z$ ):  $[M + H]^+$  calcd for  $C_{19}H_{21}F_3N_2OS$ , 383.1327; found, 383.1397; exact mass (monoisotopic) from spectrum, 382.1324. Note: For this derivative, we hydrolyzed 100 mg of **5e** using the same condition, followed by the reaction with phenyl propylamine.

**General Procedures for Synthesis of 2-((Chlorophenyl)thio)ethan-1-amine (15a, 15b).**<sup>51,52</sup> To a solution of sodium metal (97.0 mg, 4.22 mmol) in *i*-PrOH (15 mL), an appropriate chlorothiophenol derivative (475 mg, 3.30 mmol) was added, and the reaction mixture was stirred at room temperature for 30 min. Then, 2-oxazolidinone (100 mg, 1.14 mmol) was added and the reaction was heated at reflux for 6 h. After reaction completion, the organic solvent was evaporated under vacuum, and the crude product was purified using flash column chromatography (DCM–methanol 90:10) to afford the desired product as the following.

**2-((2-Chlorophenyl)thio)ethan-1-amine (15a).** Colorless oil with fruity odor (125 mg, 36%). <sup>1</sup>H NMR (500 MHz, CDCl<sub>3</sub>)  $\delta$ : 7.38–7.31 (dd,  $J = 7.0$  Hz, 1H 2H), 7.22–7.18 (m, 1H), 7.13–7.10 (m, 1H), 3.03 (t,  $J = 6.0$  Hz, 2H), 2.94 (t,  $J = 6.0$  Hz, 2H), 1.70 (s, 2H).

**2-((4-Chlorophenyl)thio)ethan-1-amine (15b).** Yellow oil with characteristic odor (305 mg, 88.6%). <sup>1</sup>H NMR (500 MHz, CDCl<sub>3</sub>)  $\delta$ : 7.28 (d,  $J = 8.5$  Hz, 2H), 7.229–7.23 (m, 4H), 2.90–2.89 (m, 2H), 1.54 (br s, 2H).

***N*-(2-((Chlorophenyl)thio)ethyl)-2-methyl-2-(arylsulfonyl)propanamide (16–20).** To a solution of the appropriate carboxylic acid derivative (**7a–7e**, 0.16–0.22 mmol) in dry THF (5 mL), PYBOP (1.05 equiv) and DIPEA (2.7 equiv) were added followed by stirring at room temperature for 10 min under nitrogen atmosphere. The reaction mixture was then charged with an appropriate chlorophenyl thioethan-1-amine derivative (**15a**, **15b** 0.16 mmol) and stirred for 1 h, after reaction completion, THF was evaporated under reduced pressure and the crude product was purified by flash column chromatography to yield the desired product.

***N*-(2-((2-Chlorophenyl)thio)ethyl)-2-methyl-2-(phenylsulfonyl)propanamide (16).** Starting with **7a** (50 mg) and **15a** (40 mg), white solid (70 mg, 82%). <sup>1</sup>H NMR (500 MHz, CDCl<sub>3</sub>)  $\delta$ : 7.84 (d,  $J = 8.0$  Hz, 2H), 7.64–7.52 (m, 1H), 7.50–7.44 (m, 2H), 7.44–7.37 (m, 3H include br s peak), 7.23–7.14 (m, 1H), 7.14–7.12 (m, 1H), 3.51 (q,  $J = 6.5$  Hz, 2H), 3.11 (t,  $J = 6.5$  Hz, 2H), 1.55 (s, 6H). <sup>13</sup>C NMR (125 MHz, CDCl<sub>3</sub>)  $\delta$  167.91, 135.00, 134.56, 134.41, 134.12, 130.12, 129.99, 129.85, 129.06, 127.43, 68.06, 39.19, 31.95, 20.85. HPLC purity, 95.3%. ESIMS calcd for  $C_{18}H_{20}ClNO_3S$ : 397.06; found mass  $[M + H]^+$ , 398.00. HRMS ( $m/z$ ):  $[M + H]^+$  calcd for  $C_{18}H_{20}ClNO_3S$ , 398.0573; found, 398.0647; exact mass (monoisotopic) from spectrum, 397.0574.

***N*-(2-((4-Chlorophenyl)thio)ethyl)-2-methyl-2-(phenylsulfonyl)propanamide (17).** Starting with **7a** (50 mg) and **15b** (40 mg), white solid (67 mg, 77%). ESIMS calcd for  $C_{18}H_{20}ClNO_3S$ , 397.06; found mass  $[M + H]^+$ : 398.00. <sup>1</sup>H NMR (500 MHz, CDCl<sub>3</sub>)  $\delta$ : 7.85 (d,  $J = 7.5$  Hz, 2H), 7.68 (t,  $J = 7.5$  Hz, 2H), 7.53 (t,  $J = 8.0$  Hz, 2H), 7.40 (br s, 1H), 7.36 (d,  $J = 9.0$  Hz, 2H), 7.29 (d,  $J = 8.5$  Hz, 2H), 3.49 (q,  $J = 6.5$  Hz, 2H), 3.09 (t,  $J = 6.5$  Hz, 2H), 1.56 (s, 6H). <sup>13</sup>C NMR (125 MHz, CDCl<sub>3</sub>)  $\delta$  167.85, 134.98, 134.43, 133.30, 132.77, 131.31, 130.08, 129.33, 129.07, 68.03, 39.26, 33.25, 20.87. HPLC purity, 98.7%. ESIMS calcd for  $C_{18}H_{20}ClNO_3S$ : 397.06; found mass  $[M + H]^+$ : 398.00. HRMS ( $m/z$ ):  $[M + H]^+$  calcd for  $C_{18}H_{20}ClNO_3S$ , 398.0573; found, 398.0647, exact mass (monoisotopic) from spectrum, 397.0575.

***N*-(2-((2-Chlorophenyl)thio)ethyl)-2-methyl-2-((4-(trifluoromethyl)phenyl)sulfonyl)propanamide (18).** Starting with **7c** (50 mg) and **15a** (33 mg), white solid (69 mg, 87%). <sup>1</sup>H NMR (500 MHz, CDCl<sub>3</sub>)  $\delta$ : 7.98 (d,  $J = 8.0$  Hz, 2H), 7.74 (d,  $J = 8.0$  Hz, 2H), 7.43–7.38 (m, 2H), 7.30 (br s, 1H), 7.26–7.22 (m, 1H), 7.18–7.14 (m, 1H), 3.51 (q,  $J = 6.5$  Hz, 2H), 3.12 (t,  $J = 6.5$  Hz, 2H), 1.57 (s, 6H). <sup>13</sup>C NMR (DMSO-*d*<sub>6</sub>)  $\delta$  167.46, 138.69, 134.85, 133.86, 130.78, 130.18, 130.09, 127.47, 126.15, 126.12, 68.35, 39.13, 32.27, 20.65. HPLC purity, 97%. HRMS ( $m/z$ ):  $[M + H]^+$  calcd for  $C_{19}H_{19}ClF_3NO_3S_2$ , 466.0447; found, 466.0522; exact mass (monoisotopic) from spectrum, 465.0449.

***N*-(2-((4-Chlorophenyl)thio)ethyl)-2-methyl-2-((4-(trifluoromethyl)phenyl)sulfonyl)propanamide (19).** Starting with **7c** (50 mg) and **15b** (33 mg), white crystals (65 mg, 82%). <sup>1</sup>H NMR (500 MHz, CDCl<sub>3</sub>)  $\delta$ : 7.96 (d,  $J = 8.0$  Hz, 2H), 7.77 (d,  $J = 8.0$  Hz, 2H), 7.34 (d,  $J = 8.5$  Hz, 2H), 7.28 (d,  $J = 8.5$  Hz, 2H), 7.24 (br s, 1H), 3.49 (q,  $J = 6.0$  Hz, 2H), 3.08 (t,  $J = 6.5$  Hz, 2H), 1.56 (s, 6H). <sup>19</sup>F NMR  $\delta$  –63.31 (s). <sup>13</sup>C NMR (125 MHz, CDCl<sub>3</sub>)  $\delta$  167.36, 138.64, 135.98 (q,  $J = 32.5$  Hz), 133.14, 132.92, 131.36, 130.74, 129.38, 126.15 (q,  $J = 3.75$  Hz), 124.08, 121.90, 68.32, 39.26, 33.33, 20.65. <sup>19</sup>F NMR  $\delta$  –63.31 (s). HPLC purity, 99.2%. ESIMS calcd for  $C_{19}H_{19}ClF_3NO_3S_2$ : 465.04; found mass  $[M + H]^+$ , 466.0. HRMS ( $m/z$ ):  $[M + H]^+$  calcd for  $C_{19}H_{19}ClF_3NO_3S_2$ , 466.0447; found, 466.0523, exact mass (monoisotopic) from spectrum, 465.0450.

***N*-(2-((4-Chlorophenyl)thio)ethyl)-2-methyl-2-(5-(trifluoromethyl)pyridin-2-yl)sulfonyl)propanamide (20).** Starting with **7e** (50 mg) and **15b** (31 mg), white solid (53 mg, 68%). <sup>1</sup>H NMR (500 MHz, CDCl<sub>3</sub>)  $\delta$ : 8.91 (s, 1H), 8.21–8.17 (m, 2H), 7.37 (br s, 1H), 7.33 (d,  $J = 8.5$  Hz, 2H), 7.26 (d,  $J = 8.5$  Hz, 2H), 3.48 (q,  $J = 6.5$  Hz, 2H), 3.09 (t,  $J = 6.5$  Hz, 2H), 1.62 (s, 6H). <sup>13</sup>C NMR (125 MHz, CDCl<sub>3</sub>)  $\delta$  167.09, 158.12, 147.16, 135.58, 133.44, 132.73, 131.25, 130.45, 130.18, 129.28, 124.47, 121.27, 67.59, 39.47, 33.09, 20.71. HPLC purity, 95%. ESIMS calcd for  $C_{19}H_{19}ClF_3NO_3S_2$ , 466.04; found mass  $[M + H]^+$ , 467.19. HRMS ( $m/z$ ):  $[M + H]^+$  calcd for  $C_{19}H_{19}ClF_3NO_3S_2$ , 467.0447; found, 467.1023.

**Synthesis of 2-(4-Chlorophenoxy)ethan-1-amine (22c).** Starting from 2-bromo ethan-1-amine **21** (500 mg, 2.45 mmol), the synthesis of **23c** was carried out over three successive steps.

**Step 1: Synthesis of tert-butyl (2-Bromoethyl)carbamate.** To a stirred solution of 2-bromo ethan-1-amine **21** (500 mg, 2.45 mmol) in DCM (15 mL) was added triethylamine (0.45 mL). The solution was cooled with an ice bath before a solution of di-*tert*-butyl dicarbonate (640 mg, 2.9 mmol) in DMC (5 mL) was added dropwise over 15 min. The mixture was stirred at 23 °C for 12 h. After reaction completion (as seen by TLC), the system was quenched with brine (15 mL), the organic layer washed with water (3 × 15 mL), dried over anhydrous Na<sub>2</sub>SO<sub>4</sub>, and evaporated under reduced pressure to afford the *N*-protected molecule as a yellowish oil (480 mg, 52%) <sup>1</sup>H NMR (500 MHz, CDCl<sub>3</sub>)  $\delta$ : 5.01 (br s, 1H), 3.50–3.41 (m, 2H), 3.42 (t,  $J = 5.5$  Hz, 2H), 1.41 (s, 12H).

**Step 2: Synthesis of tert-butyl (2-(4-Chlorophenoxy)ethyl)carbamate.** *p*-Chlorophenol (250 mg, 1.95 mmol) in DMF (1 mL) was added gradually to a stirred solution of *tert*-butyl (2-bromoethyl) carbamate (300 mg, 1.33 mmol) followed by oven-dried potassium carbonate (280 mg, 2.0 mmol) in DMF (3 mL). The mixture was stirred at 23 °C for 24 h before the flask content was poured over ice-cold ether (20 mL). The ether layer was washed with 2 M NaOH solution (15 mL), water (15 mL), and brine solution (15 mL). The ether layer was dried over Na<sub>2</sub>SO<sub>4</sub>, filtered, and evaporated under reduced pressure. The crude product was purified by flash column chromatography to afford the desired product as a colorless oil (155 mg, 43%). <sup>1</sup>H NMR (500 MHz, CDCl<sub>3</sub>)  $\delta$ : 7.44 (d,  $J = 12$  Hz, 2H), 6.79 (d,  $J = 12$  Hz, 2H), 5.02 (br s, 1H), 3.96 (t,  $J = 5$  Hz, 2H), 3.50–3.43 (m, 2H), 1.43 (s, 12H).

**2-(4-Chlorophenoxy)ethan-1-amine (22c).** To a stirred solution of the *tert*-butyl (2-(4-chlorophenoxy)ethyl)carbamate (155 mg, 0.5 mmol), trifluoroacetic acid (2.5 mL) in DMC (3 mL) was added dropwise over 30 min. The reaction mixture was stirred at 23 °C for 18 h. Then, the solvent was evaporated, and the crude product was dissolved in ethyl acetate (15 mL) and washed with 1 M NaOH aqueous solution (10 mL). The organic layer was dried over anhydrous Na<sub>2</sub>SO<sub>4</sub> and evaporated under reduced pressure to afford the desired product as white crystals (80 mg, 82%). <sup>1</sup>H NMR (500 MHz, CDCl<sub>3</sub>)  $\delta$ : 7.22 (d,  $J = 9$  Hz, 2H), 6.82 (d,  $J = 9$  Hz, 2H), 3.95 (t,  $J = 5$  Hz, 2H), 3.07 (t,  $J = 5$  Hz, 2H), 1.96 (br s, 2H).

**General Procedures for the Synthesis of 2-Methyl-*N*-(2-aryloxyethyl)-2-(arylsulfonyl)propanamide (23–31).** A solution of 2-methyl-2-(arylsulfonyl)propanoic acid **7a**, **7c**, **7f** (0.16–0.22 mmol) in dry THF (10 mL) in a 50 mL foil-wrapped rounded-bottom flask (to protect the amine derivatives from light as recommended) was treated with a solution of PyBOP (87 mg, 0.17

mmol) in THF (1 mL) followed by addition of DIPEA (83  $\mu$ L). The mixture was stirred at room temperature for 10 min. A solution of the appropriate phenoxyethan-1-amine derivative (0.16 mmol) in THF (1 mL) was added and the reaction mixture was allowed to stir at the same temperature for 1 h. The solvent was removed in vacuo, and the crude product was purified by flash column chromatography using ethyl acetate–hexanes (1:3) as the eluent. The physical characters and the spectral data of the separated products are listed below.

**2-Methyl-N-(2-phenoxyethyl)-2-(phenylsulfonyl) Propanamide (23).** Starting with 7a (50 mg, 0.22 mmol), white crystals (44 mg, 57%).  $^1\text{H NMR}$  (500 MHz,  $\text{CDCl}_3$ )  $\delta$ : 7.82 (d,  $J = 7.5$  Hz, 2H), 7.63 (br s, 1H), 7.55 (t,  $J = 7.5$  Hz, 1H), 7.34–7.32 (m, 2H), 7.29–7.27 (m, 2H), 6.97 (t,  $J = 7.5$  Hz, 1H), 6.97 (d,  $J = 7.5$  Hz, 1H), 4.06 (t,  $J = 5.0$  Hz, 2H), 3.70 (q,  $J = 5.5$  Hz, 2H), 1.60 (s, 6H).  $^{13}\text{C NMR}$  (500 MHz,  $\text{CDCl}_3$ )  $\delta$  168.09, 158.39, 135.09, 134.27, 130.06, 129.69, 129.00, 121.36, 114.56, 67.97, 65.98, 40.01, 20.71. HPLC purity, 100%. ESIMS calcd for  $\text{C}_{18}\text{H}_{21}\text{NO}_4\text{S}$ : 347.12, found mass  $[\text{M} + \text{H}]^+$ , 348.08;  $[\text{M} + \text{Na}]^+$ , 370.06. HRMS ( $m/z$ ):  $[\text{M} + \text{H}]^+$  calcd for  $\text{C}_{18}\text{H}_{21}\text{NO}_4\text{S}$ , 348.1191; found, 348.1263; exact mass (monoisotopic) from spectrum, 347.1190.

**2-Methyl-N-(2-phenoxyethyl)-2-(4-(trifluoromethyl)phenylsulfonyl) Propenamide (24).** Starting with 7c (50 mg, 0.16 mmol), white solid (38 mg, 54%).  $^1\text{H NMR}$  (500 MHz,  $\text{CDCl}_3$ )  $\delta$ : 7.94 (d,  $J = 8.0$  Hz, 2H), 7.52 (br s, 1H), 7.46 (d,  $J = 8.0$  Hz, 2H), 7.34 (t,  $J = 8.0$  Hz, 2H), 7.03 (t,  $J = 7.5$  Hz, 1H), 6.97 (d,  $J = 8.0$  Hz, 2H), 4.06 (t,  $J = 5.0$  Hz, 2H), 3.70 (q,  $J = 5.5$  Hz, 2H), 1.64 (s, 6H).  $^{13}\text{C NMR}$  (125 MHz,  $\text{CDCl}_3$ )  $\delta$  167.64, 158.26, 138.69, 135.91 (q,  $J = 32.5$  Hz), 130.68, 129.81, 126.10 (q,  $J = 3.75$  Hz), 124.47, 67.59, 39.47, 33.09, 20.71; HPLC purity, 100%. ESIMS calcd for  $\text{C}_{19}\text{H}_{20}\text{F}_3\text{NO}_4\text{S}$ : 415.11, found mass  $[\text{M} + \text{Na}]^+$ , 438.05; HRMS ( $m/z$ ):  $[\text{M} + \text{H}]^+$  calcd for  $\text{C}_{19}\text{H}_{20}\text{F}_3\text{NO}_4\text{S}$ , 416.1065; found, 416.1137, exact mass (monoisotopic) from spectrum, 415.1064.

**2-Methyl-N-(2-phenoxyethyl)-2-(5-(trifluoromethyl)pyridin-2-ylsulfonyl) Propenamide (25).** Starting with 7e (50 mg, 0.16 mmol), white solid (60 mg, 85%).  $^1\text{H NMR}$  (500 MHz,  $\text{CDCl}_3$ )  $\delta$ : 8.79 (s, 1H), 7.93 (d,  $J = 8.5$  Hz, 1H), 7.81 (d,  $J = 8.5$  Hz, 1H), 7.51 (br s, 1H), 7.30–7.27 (m, 2H), 7.00–6.97 (m, 1H), 6.88 (d,  $J = 8.0$  Hz, 2H), 4.01 (t,  $J = 5.0$  Hz, 2H), 3.69 (q,  $J = 5.5$  Hz, 2H), 1.70 (s, 6H).  $^{13}\text{C NMR}$  (125 MHz,  $\text{CDCl}_3$ )  $\delta$  167.84, 158.46, 158.19, 147.05, 147.02, 135.47, 147.02, 130.14 (q,  $J = 33.75$  Hz), 124.35, 121.33, 114.51, 67.83, 66.05, 39.98, 20.55. HPLC purity, 98.5%. ESIMS calcd for  $\text{C}_{18}\text{H}_{19}\text{F}_3\text{N}_2\text{O}_4\text{S}$ : 416.10, found mass  $[\text{M} + \text{H}]^+$ , 417.10;  $[\text{M} + \text{Na}]^+$ , 439.04. HRMS ( $m/z$ ):  $[\text{M} + \text{H}]^+$  calcd for  $\text{C}_{18}\text{H}_{19}\text{F}_3\text{N}_2\text{O}_4\text{S}$ , 417.1018; found, 417.1090; exact mass (monoisotopic) from spectrum, 416.1018.

**N-(2-(2-Chlorophenoxy)ethyl)-2-methyl-2-(Phenylsulfonyl) Propanamide (26).** Starting with 7a (50 mg, 0.22 mmol), white solid (40 mg, 48%).  $^1\text{H NMR}$  (500 MHz,  $\text{CDCl}_3$ )  $\delta$ : 7.85 (d,  $J = 7.5$  Hz, 2H), 7.60 (br s, 1H), 7.57 (t,  $J = 7.5$  Hz, 2H), 7.40 (d,  $J = 7.5$  Hz, 1H), 7.35 (m, 2H), 7.24 (m, 1H), 6.97–6.93 (m, 2H), 4.12 (t,  $J = 5.0$  Hz, 2H), 3.74 (q,  $J = 5.0$  Hz, 2H), 1.60 (s, 6H).  $^{13}\text{C NMR}$  (500 MHz,  $\text{CDCl}_3$ )  $\delta$  168.13, 153.95, 135.15, 134.26, 130.53, 130.14, 128.93, 127.85, 123.26, 122.14, 113.69, 68.02, 67.34, 39.88, 20.72. HPLC purity, 100%. ESIMS calcd for  $\text{C}_{18}\text{H}_{20}\text{ClNO}_4\text{S}$ : 381.08, found mass  $[\text{M} + \text{H}]^+$ , 382.05;  $[\text{M} + \text{Na}]^+$ , 404.03. HRMS ( $m/z$ ):  $[\text{M} + \text{H}]^+$  calcd for  $\text{C}_{18}\text{H}_{20}\text{ClNO}_4\text{S}$ , 382.0802; exact mass (monoisotopic) from spectrum, 381.0800.

**N-(2-(2-Chlorophenoxy)ethyl)-2-methyl-2-(4-(trifluoromethyl)phenylsulfonyl) Propanamide (27).** Starting with 7c (50 mg, 0.16 mmol), white solid (53 mg, 70%).  $^1\text{H NMR}$  (500 MHz,  $\text{CDCl}_3$ )  $\delta$ : 7.98 (d,  $J = 8.5$  Hz, 1H), 7.55 (d,  $J = 8.5$  Hz, 1H), 7.52 (br s, 1H), 7.42–7.40 (m, 1H), 7.27–7.23 (m, 1H), 6.99–6.96 (m, 1H), 6.94–6.92 (m, 1H), 4.12 (t,  $J = 5.0$  Hz, 2H), 3.73 (q,  $J = 5.0$  Hz, 2H), 1.62 (s, 6H).  $^{13}\text{C NMR}$  (500 MHz,  $\text{CDCl}_3$ )  $\delta$  167.69, 153.82, 138.81, 135.90 (q,  $J = 32.5$  Hz), 130.77, 130.59, 127.95, 125.97, 124.05, 123.17, 122.31, 113.66, 68.31, 67.24, 40.03, 20.52. HPLC purity, 97.4%. ESIMS calcd for  $\text{C}_{19}\text{H}_{19}\text{ClF}_3\text{NO}_4\text{S}$ : 449.07, found mass  $[\text{M} + \text{H}]^+$ , 450.01;  $[\text{M} + \text{Na}]^+$ , 472.00. HRMS ( $m/z$ ):  $[\text{M} + \text{H}]^+$  calcd for  $\text{C}_{19}\text{H}_{19}\text{ClF}_3\text{NO}_4\text{S}$ , 450.0675; found, 450.0751; exact mass (monoisotopic) from spectrum, 449.0678.

**N-(2-(2-Chlorophenoxy)ethyl)-2-methyl-2-((5-(trifluoromethyl)pyridin-2-ylsulfonyl) Propanamide (28).** Starting with 7e (50 mg, 0.16 mmol), white solid (64 mg, 84%).  $^1\text{H NMR}$  (500 MHz,  $\text{CDCl}_3$ )  $\delta$ : 8.75 (s, 1H), 8.11 (d,  $J = 8.5$  Hz, 1H), 7.81 (d,  $J = 8.5$  Hz, 1H), 7.51 (br s, 1H), 7.38–7.36 (m, 2H), 7.22 (t,  $J = 7.5$  Hz, 1H), 6.96–6.92 (m, 1H), 6.81 (d,  $J = 8.0$  Hz, 1H), 4.09 (t,  $J = 5.0$  Hz, 2H), 3.73 (q,  $J = 5.5$  Hz, 2H), 1.70 (s, 6H).  $^{13}\text{C NMR}$  ( $\text{DMSO}-d_6$ )  $\delta$  167.94, 158.44, 153.93, 146.97, 146.94, 135.41, 130.49, 129.91, 127.87, 124.40, 123.16, 122.17, 113.70, 67.95, 67.35, 39.86, 20.56. HPLC purity, 97.8%. ESIMS calcd for  $\text{C}_{18}\text{H}_{18}\text{ClF}_3\text{N}_2\text{O}_4\text{S}$ : 450.06, found mass  $[\text{M} + \text{H}]^+$ , 451.05. HRMS ( $m/z$ ):  $[\text{M} + \text{H}]^+$  calcd for  $\text{C}_{18}\text{H}_{18}\text{ClF}_3\text{N}_2\text{O}_4\text{S}$ , 451.0704; found, 450.0751; exact mass (monoisotopic) from spectrum, 450.0631.

**N-(2-(4-Chlorophenoxy)ethyl)-2-methyl-2-(phenylsulfonyl) Propanamide (29).** Starting with 7a (50 mg, 0.22 mmol), white solid (21 mg, 25%).  $^1\text{H NMR}$  (500 MHz,  $\text{CDCl}_3$ )  $\delta$ : 8.12 (d,  $J = 7.5$  Hz, 2H), 7.58 (t,  $J = 7.5$  Hz, 2H), 7.33 (d,  $J = 7.5$  Hz, 2H), 7.28–7.26 (m, 2H), 6.88 (d,  $J = 10.5$  Hz, 2H), 4.03 (t,  $J = 5.0$  Hz, 2H), 3.68 (q,  $J = 5.0$  Hz, 2H), 1.58 (s, 6H).  $^{13}\text{C NMR}$  (125 MHz,  $\text{CDCl}_3$ )  $\delta$  168.11, 157.01, 135.05, 134.36, 130.03, 129.57, 129.02, 126.30, 115.85, 67.97, 66.44, 39.87, 20.77. HPLC purity, 99.5%. ESIMS calcd for  $\text{C}_{18}\text{H}_{20}\text{ClNO}_4\text{S}$ : 381.08, found mass  $[\text{M} + \text{H}]^+$ , 382.20. HRMS ( $m/z$ ):  $[\text{M} + \text{H}]^+$  calcd for  $\text{C}_{18}\text{H}_{20}\text{ClNO}_4\text{S}$ , 382.0802; found, 382.0873; exact mass (monoisotopic) from spectrum, 381.0800.

**N-(2-(4-Chlorophenoxy)ethyl)-2-methyl-2-(4-(trifluoromethyl)phenylsulfonyl) Propanamide (30).** Starting with 7c (50 mg, 0.16 mmol), white solid (54 mg, 71%).  $^1\text{H NMR}$  (500 MHz,  $\text{CDCl}_3$ )  $\delta$ : 7.94 (d,  $J = 8.0$  Hz, 2H), 7.56 (d,  $J = 8.5$  Hz, 2H), 7.45 (br s, 1H), 7.29–7.26 (m, 2H), 6.90–6.87 (m, 2H), 4.03 (t,  $J = 5.0$  Hz, 2H), 3.68 (q,  $J = 5.5$  Hz, 2H), 1.60 (s, 6H).  $^{13}\text{C NMR}$  (125 MHz,  $\text{CDCl}_3$ )  $\delta$  167.60, 156.90, 138.69, 135.65 (q,  $J = 32.5$  Hz), 130.67, 129.64, 126.52, 126.11, 124.01, 115.84, 68.27, 66.37, 39.99, 20.58.  $^{19}\text{F NMR}$   $\delta$  –63.41 (s). HPLC purity, 98.7%. ESIMS calcd for  $\text{C}_{19}\text{H}_{19}\text{ClF}_3\text{NO}_4\text{S}$ : 449.07; found mass  $[\text{M} + \text{H}]^+$ , 450.03. HRMS ( $m/z$ ):  $[\text{M} + \text{H}]^+$  calcd for  $\text{C}_{19}\text{H}_{19}\text{ClF}_3\text{NO}_4\text{S}$ , 450.0675; found, 450.0750; exact mass (monoisotopic) from spectrum, 449.0677.

**N-(2-(4-Chlorophenoxy)ethyl)-2-methyl-2-((5-(trifluoromethyl)pyridin-2-ylsulfonyl) Propanamide (31).** Starting with 7e (50 mg, 0.16 mmol), white solid (43 mg, 57%).  $^1\text{H NMR}$  (500 MHz,  $\text{CDCl}_3$ )  $\delta$ : 8.76 (s, 1H), 8.13 (d,  $J = 8.5$  Hz, 1H), 7.98 (d,  $J = 8.0$  Hz, 1H), 7.49 (br s, 1H), 7.22 (d,  $J = 8.5$  Hz, 2H), 6.82 (d,  $J = 8.5$  Hz, 2H), 4.02 (t,  $J = 5.0$  Hz, 2H), 3.68 (q,  $J = 5.0$  Hz, 2H), 1.66 (s, 6H).  $^{13}\text{C NMR}$  (125 MHz,  $\text{CDCl}_3$ )  $\delta$  167.90, 158.22, 157.11, 147.04, 135.47, 129.87 (q,  $J = 33.75$  Hz), 129.46, 126.25, 124.25, 123.38, 115.85, 67.64, 66.51, 39.84, 20.54. HPLC purity, 97.8%. ESIMS calcd for  $\text{C}_{18}\text{H}_{18}\text{ClF}_3\text{N}_2\text{O}_4\text{S}$ : 450.06; found mass  $[\text{M} + \text{H}]^+$ , 451.01;  $[\text{M} + \text{Na}]^+$ , 473.01. HRMS ( $m/z$ ):  $[\text{M} + \text{H}]^+$  calcd for  $\text{C}_{18}\text{H}_{18}\text{ClF}_3\text{N}_2\text{O}_4\text{S}$ , 451.0628; found, 451.0703; exact mass (monoisotopic) from spectrum, 450.0630.

**General Procedure for Synthesis of 1-(4-Arylpiperazin-1-yl)-2-((5-(trifluoromethyl)pyridin-2-ylsulfonyl)alkyl)-1-one (33–45).** To a stirred solution of the appropriate carboxylic acid derivative (7d and 7e 50 mg, 0.16–0.17 mmol) in dry THF (10 mL), a solution of PyBOP (87 mg, 0.17 mmol) in THF (1 mL) followed by DIPEA (83  $\mu$ L) were added. Then, the mixture was stirred at room temperature for 10 min under nitrogen gas before a solution of the appropriate 4-aryl piperazine (0.16–0.17 mmol) in THF (1 mL) was added. The resulting yellow solution was allowed to stir at room temperature for 1 h. The solvent was removed under reduced pressure, and the crude product was absorbed onto silica gel and purified by flash column chromatography using ethyl acetate/hexanes as the eluent to afford the desired product as the following.

**2-Methyl-1-(4-phenylpiperazin-1-yl)-2-((5-(trifluoromethyl)pyridin-2-ylsulfonyl) Propan-1-one (33).** Starting with 7e (50 mg, 0.16 mmol) and 1-phenylpiperazine (25  $\mu$ L, 0.16 mmol), off-white solid (42 mg, 61%).  $^1\text{H NMR}$  (500 MHz,  $\text{CDCl}_3$ )  $\delta$ : 8.94 (s, 1 H), 8.23 (d,  $J = 8.5$  Hz, 1H), 8.19 (d,  $J = 12.0$  Hz, 1H), 7.29 (d,  $J = 7.5$  Hz, 2H), 6.95–6.92 (m, 3H), 3.91 (s, 4H), 3.26 (s, 4H), 1.87 (s, 6H).  $^{13}\text{C NMR}$  (125 MHz,  $\text{CDCl}_3$ )  $\delta$  166.62, 160.05, 146.83, 135.41, 135.40, 129.98, 129.71, 124.57, 123.75, 121.57, 120.68, 116.61, 71.54,

49.48, 45.75, 22.90. HPLC purity, 97.49%. ESIMS calcd for  $C_{20}H_{22}F_2N_2O_3S$ : 441.13; found mass  $[M + H]^+$ , 442.50. HRMS ( $m/z$ ):  $[M + H]^+$  calcd for  $C_{20}H_{22}F_2N_2O_3S$ , 442.1334; found, 442.1404; exact mass (monoisotopic) from spectrum, 441.1331.

**2-Methyl-1-(4-(pyridin-2-yl)piperazin-1-yl)-2-((5-(trifluoromethyl)pyridin-2-yl)sulfonyl) Propan-1-one (34).** Starting with **7e** (50 mg, 0.16 mmol) and 1-(pyridin-2-yl)piperazine (28  $\mu$ L, 0.16 mmol), off-white solid (57 mg, 81%).  $^1H$  NMR (500 MHz,  $CDCl_3$ )  $\delta$ : 8.94 (s, 1 H), 8.24–8.17 (m, 3H), 7.53 (d,  $J = 7.0$  Hz, 1H), 6.70–6.66 (m, 2H), 3.88 (s, 4H), 3.66–3.65 (m, 4H), 1.87 (s, 6H).  $^{13}C$  NMR (125 MHz,  $CDCl_3$ )  $\delta$  166.62, 159.93, 158.76, 147.62, 146.70, 137.98, 135.30, 129.71 (q,  $J = 33.75$  Hz), 124.45, 123.64, 114.00, 107.45, 71.44, 45.19, 22.73. HPLC purity, 97.69%. ESIMS calcd for  $C_{19}H_{21}F_3N_4O_3S$ : 442.13; found mass  $[M + H]^+$ , 443.39. HRMS ( $m/z$ ):  $[M + H]^+$  calcd for  $C_{19}H_{21}F_3N_4O_3S$ , 443.1286; found, 443.1357; exact mass (monoisotopic) from spectrum, 442.1284.

**2-Methyl-1-(4-(o-tolyl)piperazin-1-yl)-2-((5-(trifluoromethyl)pyridin-2-yl)sulfonyl) Propan-1-one (35).** Starting with **7e** (50 mg, 0.16 mmol) and 1-(o-tolyl)piperazine (30  $\mu$ L, 0.16 mmol), white solid (40 mg, 56%).  $^1H$  NMR (500 MHz,  $CDCl_3$ )  $\delta$ : 8.95 (s, 1 H), 8.26 (d,  $J = 8.0$  Hz, 1H), 8.19 (d,  $J = 7.5$  Hz, 1H), 7.20–7.15 (m, 2H), 7.03–6.99 (m, 2H), 3.87 (s, 4H), 2.95 (s, 3H), 2.32 (s, 3H), 1.90 (s, 6H).  $^{13}C$  NMR (125 MHz,  $CDCl_3$ )  $\delta$  166.75, 160.47, 150.60, 146.66, 135.26, 132.71, 131.25, 129.75, 129.48, 126.73, 124.40, 123.88, 119.16, 71.84, 51.77, 22.76, 17.83. HPLC purity, 97.9%. ESIMS calcd for  $C_{21}H_{24}F_3N_2O_3S$ : 455.16; found mass  $[M + H]^+$ , 456.53. HRMS ( $m/z$ ):  $[M + H]^+$  calcd for  $C_{21}H_{24}F_3N_2O_3S$ , 456.1490; found, 456.1561; exact mass (monoisotopic) from spectrum, 455.1489.

**1-(4-(2,5-Dimethylphenyl)piperazin-1-yl)-2-methyl-2-((5-(trifluoromethyl)pyridin-2-yl)sulfonyl) Propan-1-one (36).** Starting with **7e** (50 mg, 0.16 mmol) and 1-(2,5-dimethylphenyl) piperazine (32  $\mu$ L, 0.16 mmol), white solid (65 mg, 88%).  $^1H$  NMR (500 MHz,  $CDCl_3$ )  $\delta$ : 8.96 (s, 1 H), 8.26 (d,  $J = 8.5$  Hz, 1H), 8.20 (d,  $J = 8.0$  Hz, 1H), 7.08 (d,  $J = 7.5$  Hz, 1H), 6.82 (m, 2H), 3.86 (s, 4H), 2.95 (s, 4H), 2.30 (s, 3H), 2.27 (s, 3H), 1.90 (s, 6H).  $^{13}C$  NMR (125 MHz,  $CDCl_3$ )  $\delta$  166.73, 160.51, 150.43, 146.64, 136.33, 135.26, 131.05, 129.39, 124.49, 124.39, 123.70, 119.92, 71.87, 51.78, 22.76, 21.15, 17.41. HPLC purity, 98.9%. ESIMS calcd for  $C_{22}H_{26}F_3N_3O_3S$ : 469.16; found mass  $[M + H]^+$ , 470.24. HRMS ( $m/z$ ):  $[M + H]^+$  calcd for  $C_{22}H_{26}F_3N_3O_3S$ , 470.1647; found, 470.1719; exact mass (monoisotopic) from spectrum, 469.1647.

**1-(4-(3,4-Dichlorophenyl)piperazin-1-yl)-2-((5-(trifluoromethyl)pyridin-2-yl)sulfonyl) Propan-1-one (37).** Starting with **7e** (50 mg, 0.16 mmol) and 1-(3,4-dichlorophenyl) piperazine (39 mg, 0.16 mmol), white crystals (53 mg, 61.5%).  $^1H$  NMR (500 MHz,  $CDCl_3$ )  $\delta$ : 8.91 (s, 4 H), 8.21–8.19 (m, 2H), 7.30–7.28 (m,  $J = 9.0$  Hz, 1H), 6.96 (s, 1H), 6.76–6.73 (m, 1H), 3.99 (m, 4H), 3.25–3.23 (m, 4H), 1.83 (s, 6H).  $^{13}C$  NMR (125 MHz,  $CDCl_3$ )  $\delta$  166.38, 159.48, 150.12, 146.82, 135.34, 133.00, 130.63, 130.03, 129.76, 124.49, 123.10, 117.64, 115.65, 71.04, 48.78, 45.50, 22.90. HPLC purity, 98.1%. ESIMS calcd for  $C_{20}H_{20}Cl_2F_3N_3O_3S$ : 509.06; found mass  $[M + H]^+$ , 510.16. HRMS ( $m/z$ ):  $[M + H]^+$  calcd for  $C_{20}H_{20}Cl_2F_3N_3O_3S$ , 510.0555; found, 510.0636; exact mass (monoisotopic) from spectrum, 509.0564.

**1-(4-(3-Methoxyphenyl)piperazin-1-yl)-2-methyl-2-((5-(trifluoromethyl)pyridin-2-yl)sulfonyl) Propan-1-one (38).** Starting with **7e** (50 mg, 0.16 mmol) and 1-(*m*-methoxyphenyl) piperazine (30  $\mu$ L, 0.16 mmol), white solid (80 mg, 97.5%).  $^1H$  NMR (500 MHz,  $CDCl_3$ )  $\delta$ : 8.93 (s, 1 H), 8.22 (d,  $J = 8.0$  Hz, 1H), 8.17 (d,  $J = 8.5$  Hz, 1H), 7.18 (t,  $J = 8.5$  Hz, 1H), 6.54–6.52 (m, 1H), 6.46–6.45 (m, 2H), 3.88 (s, 4H), 3.78 (s, 3H), 3.25–3.24 (s, 4H), 1.86 (s, 6H).  $^{19}F$  NMR  $\delta$  –62.62 (s).  $^{13}C$  NMR (125 MHz,  $CDCl_3$ )  $\delta$  166.51, 160.69, 159.94, 152.09, 146.73, 146.70, 135.28, 135.25, 129.99, 124.44, 109.06, 105.22, 102.90, 71.42, 55.24, 49.20, 22.79. HPLC purity, 97.5%. ESIMS calcd for  $C_{21}H_{24}F_3N_3O_4S$ : 471.14; found mass  $[M + H]^+$ , 472.14. HRMS ( $m/z$ ):  $[M + H]^+$  calcd for  $C_{21}H_{24}F_3N_3O_4S$ , 472.1439; found, 472.1511; exact mass (monoisotopic) from spectrum, 471.1439.

**2-Methyl-1-(4-(4-fluorobenzyl)piperazin-1-yl)-2-((5-(trifluoromethyl)pyridin-2-yl)sulfonyl) Propan-1-one (39).** Starting

with **7e** (50 mg, 0.16 mmol) and 1-(4-fluorobenzyl)piperazine (33 mg, 0.16 mmol), white solid (42 mg, 53%).  $^1H$  NMR (500 MHz,  $CDCl_3$ )  $\delta$ : 8.91 (s, 1 H), 8.22 (d,  $J = 8.5$  Hz, 1H), 8.17 (d,  $J = 8.0$  Hz, 1H), 7.28–7.25 (m, 2H), 7.27 (t,  $J = 8.5$  Hz, 2H), 3.70 (s, 4H), 3.48 (s, 2H), 2.47 (s, 4H), 1.87 (s, 6H).  $^{13}C$  NMR (125 MHz,  $CDCl_3$ )  $\delta$  166.54, 161.18, 160.49, 146.58, 135.24, 133.12, 130.66, 130.59, 124.37, 115.29, 115.12, 71.83, 61.92, 52.74, 22.63.  $^{19}F$  NMR  $\delta$  –62.61, –70.08, –71.60. HPLC purity, 97.9%. ESIMS calcd for  $C_{21}H_{23}F_4N_2O_3S$ : 473.14; found mass  $[M + H]^+$ , 474.30. HRMS ( $m/z$ ):  $[M + H]^+$  calcd for  $C_{21}H_{23}F_4N_2O_3S$ , 474.1396; found, 474.1467; exact mass (monoisotopic) from spectrum, 473.1394.

**2-Methyl-1-(4-(4-Chlorobenzyl)piperazin-1-yl)-2-((5-(trifluoromethyl)pyridin-2-yl)sulfonyl) Propan-1-one (40).** Starting with **7e** (50 mg, 0.16 mmol) and 1-(4-chlorobenzyl)piperazine (30  $\mu$ L, 0.16 mmol), white solid (69 mg, 84.1%).  $^1H$  NMR (500 MHz,  $CDCl_3$ )  $\delta$ : 8.91 (s, 1 H), 8.22 (d,  $J = 8.0$  Hz, 1H), 8.18 (d,  $J = 8.0$  Hz, 1H), 7.31–7.28 (m, 4H), 3.73 (s, 4H), 3.52 (s, 2H), 2.51 (s, 3H), 2.170 (s, 2H), 1.83 (s, 6H).  $^{13}C$  NMR (125 MHz,  $CDCl_3$ )  $\delta$  166.54, 160.51, 146.57, 136.10, 135.26, 133.03, 130.36, 129.52 (q,  $J = 33.75$  Hz), 128.51, 124.37, 123.69, 121.51, 71.84, 61.94, 52.78, 45.62, 22.61. HPLC purity, 99.3%. ESIMS calcd for  $C_{21}H_{23}ClF_3N_3O_3S$ : 489.11; found mass  $[M + H]^+$ , 490.14. HRMS ( $m/z$ ):  $[M + H]^+$  calcd for  $C_{21}H_{23}ClF_3N_3O_3S$ , 490.1101; found, 490.1175; exact mass (monoisotopic) from spectrum, 489.1102.

**2-Methyl-1-(4-(3-chlorobenzyl)piperazin-1-yl)-2-((5-(trifluoromethyl)pyridin-2-yl)sulfonyl) Propan-1-one (41).** Starting with **7e** (50 mg, 0.16 mmol) and 1-(3-chlorobenzyl)piperazine (30  $\mu$ L, 0.16 mmol), white solid (72 mg, 88%).  $^1H$  NMR (500 MHz,  $CDCl_3$ )  $\delta$ : 8.91 (s, 1 H), 8.22 (d,  $J = 8.0$  Hz, 1H), 8.17 (d,  $J = 8.0$  Hz, 1H), 7.32 (s, 1H), 7.24–7.17 (m, 3H), 3.72–3.67 (m, 4H), 3.49 (s, 2H), 2.49–2.47 (m, 4H), 1.84 (s, 6H).  $^{13}C$  NMR (125 MHz,  $CDCl_3$ )  $\delta$  166.56, 160.50, 146.59, 144.60, 139.87, 135.21, 134.34, 129.63, 129.00, 127.54, 127.13, 124.36, 71.81, 62.11, 55.91, 52.83, 22.65. HPLC purity, 98.87%. ESIMS calcd for  $C_{21}H_{23}ClF_3N_3O_3S$ : 489.11; found mass  $[M + H]^+$ , 490.17. HRMS ( $m/z$ ):  $[M + H]^+$  calcd for  $C_{21}H_{23}ClF_3N_3O_3S$ , 490.1101; found, 490.1173; exact mass (monoisotopic) from spectrum, 489.1100.

**2-Methyl-1-(4-(4-methylbenzyl)piperazin-1-yl)-2-((5-(trifluoromethyl)pyridin-2-yl)sulfonyl) Propan-1-one (42).** Starting with **7e** (50 mg, 0.16 mmol) and 1-(4-methylbenzyl)piperazine (32 mg, 0.16 mmol), white solid (40 mg, 51%).  $^1H$  NMR (500 MHz,  $CDCl_3$ )  $\delta$ : 8.86 (s, 1 H), 8.22 (d,  $J = 8.5$  Hz, 1H), 8.17 (d,  $J = 8.0$  Hz, 1H), 7.22 (d,  $J = 7.5$  Hz, 1H), 7.14 (d,  $J = 7.5$  Hz, 1H), 3.73 (s, 4H), 3.55 (s, 2H), 2.53 (s, 4H), 2.34 (s, 3H), 1.84 (s, 6H).  $^{13}C$  NMR (125 MHz,  $CDCl_3$ )  $\delta$  166.59, 160.64, 146.53, 137.04, 135.22, 134.17, 129.18, 129.05, 124.37, 123.70, 121.53, 71.98, 62.47, 52.71, 45.70, 22.55, 21.11. HPLC purity, 95.9%. ESIMS calcd for  $C_{22}H_{26}F_3N_3O_3S$ : 469.16; found mass  $[M + H]^+$ , 470.58. HRMS ( $m/z$ ):  $[M + H]^+$  calcd for  $C_{22}H_{26}F_3N_3O_3S$ , 470.1647; found, 470.1722; exact mass (monoisotopic) from spectrum, 469.1649.

**1-(4-(o-Tolyl)piperazin-1-yl)-2-((5-(trifluoromethyl)pyridin-2-yl)sulfonyl)propan-1-one (43).** Starting with **7d** (50 mg, 0.17 mmol) and 1-(o-tolyl)piperazine (33  $\mu$ L, 0.17 mmol), yellowish-white solid (52 mg, 67%).  $^1H$  NMR (500 MHz,  $CDCl_3$ )  $\delta$ : 9.01 (s, 1 H), 8.24 (s, 2H), 7.19 (m, 2H), 7.01 (d,  $J = 7.5$  Hz, 2H), 4.97 (q,  $J = 7.0$  Hz, 1H), 3.96–3.71 (m, 4H), 3.15–2.93 (m, 4H), 2.36 (s, 3H), 1.62 (d,  $J = 7.0$  Hz, 3H).  $^{13}C$  NMR (125 MHz,  $CDCl_3$ )  $\delta$  163.32, 159.20, 150.53, 147.01, 135.72, 132.72, 131.24, 130.10 (q,  $J = 33.75$  Hz), 126.75, 123.94, 123.61, 121.43, 119.27, 58.80, 51.94, 51.53, 47.33, 43.23, 17.81, 13.37. HPLC purity, 98.3%. ESIMS calcd for  $C_{19}H_{22}F_3N_3O_3S$ : 441.13; found mass  $[M + H]^+$ , 442.01. HRMS ( $m/z$ ):  $[M + H]^+$  calcd for  $C_{19}H_{22}F_3N_3O_3S$ , 442.1334; found, 442.1406; exact mass (monoisotopic) from spectrum, 441.1334.

**1-(4-(2,5-Dimethylphenyl)piperazin-1-yl)-2-((5-(trifluoromethyl)pyridin-2-yl)sulfonyl) Propan-1-one (44).** Starting with **7d** (50 mg, 0.17 mmol) and 1-(2,5-dimethylphenyl)piperazine (35  $\mu$ L, 0.17 mmol), white solid (51 mg, 64%).  $^1H$  NMR (500 MHz,  $CDCl_3$ )  $\delta$ : 9.01 (s, 1 H), 8.23 (s, 2H), 7.19 (d,  $J = 7.5$  Hz, 1H), 7.06–7.03 (m, 2H), 4.97 (q,  $J = 7.0$  Hz, 1H), 3.96–3.68 (m, 4H), 3.13–2.90 (m, 4H), 2.30 (s, 6H), 1.62 (d,  $J = 7.0$  Hz, 3H).  $^{13}C$  NMR (125 MHz,

$\text{CDCl}_3$ )  $\delta$  163.28, 159.20, 150.38, 147.02, 136.36, 135.67, 131.04, 130.25, 129.98, 129.41, 124.59, 123.94, 120.04, 58.83, 51.93, 51.56, 47.36, 43.26, 21.13, 17.38, 13.36. HPLC purity, 99.7%. ESIMS calcd for  $\text{C}_{21}\text{H}_{24}\text{F}_3\text{N}_3\text{O}_3\text{S}$ : 455.15; found mass  $[\text{M} + \text{H}]^+$ , 456.17. HRMS ( $m/z$ ):  $[\text{M} + \text{H}]^+$  calcd for  $\text{C}_{21}\text{H}_{24}\text{F}_3\text{N}_3\text{O}_3\text{S}$ , 456.1490; found, 456.1560; exact mass (monoisotopic) from spectrum, 455.1487.

1-(4-(3,4-Dichlorophenyl)piperazin-1-yl)-2-((5-(trifluoromethyl)pyridin-2-yl)sulfonyl) Propan-1-one (**45**). Starting with **7d** (50 mg, 0.17 mmol) and 1-(3,4-dichlorophenyl)piperazine (40 mg, 0.17 mmol), shiny white crystals (31 mg, 58%).  $^1\text{H}$  NMR (500 MHz,  $\text{CDCl}_3$ )  $\delta$ : 9.00 (s, 1 H), 8.42–8.20 (m, 2H), 7.30 (d,  $J = 9.0$  Hz, 1H), 6.97 (s, 1H), 6.75 (dd,  $J = 6.0$  Hz, 1H), 4.97 (q,  $J = 7.0$  Hz, 1H), 4.03–3.11 (m, 8H), 1.58 (d,  $J = 8.0$  Hz, 3H).  $^{13}\text{C}$  NMR (125 MHz,  $\text{CDCl}_3$ )  $\delta$  162.96, 158.88, 150.05, 147.12, 135.78, 133.00, 130.66, 123.86, 123.54, 123.31, 121.36, 117.94, 115.92, 58.44, 49.06, 48.78, 46.33, 42.37, 13.38. HPLC purity (methanol–water, 1:1), 95.4%. ESIMS  $[\text{M} + \text{H}]^+$  calcd for  $\text{C}_{19}\text{H}_{18}\text{Cl}_2\text{F}_3\text{N}_3\text{O}_3\text{S}$ : 497.04; found mass  $[\text{M} + \text{H}]^+$ , 497.15. HRMS ( $m/z$ ):  $[\text{M} + \text{H}]^+$  calcd for  $\text{C}_{21}\text{H}_{24}\text{F}_3\text{N}_3\text{O}_3\text{S}$ , 496.0398; found, 496.0474; exact mass (monoisotopic) from spectrum, 495.0401.

**Biology. Cell Culture, Chlamydia trachomatis Propagation, and IFU Assay.** The human epithelial cell line HEp-2 was routinely propagated in Dulbecco's modified Eagle medium (DMEM; Gibco) supplemented with 2% L-glutamine and 10% fetal bovine serum (FBS) at 37 °C with 5%  $\text{CO}_2$ . All infected and uninfected cell cultures were incubated at these conditions. Compounds stocks of the synthesized compounds were prepared in sterile dimethyl sulfoxide (50 mg/mL) and frozen at –20 °C in 5  $\mu\text{L}$  aliquots.<sup>41</sup>

To quantify the effect of the most active compounds on *C. trachomatis*, HEp-2 cells were first seeded in a 24-well plate. Cells were infected with *C. trachomatis* L2 at a multiplicity of infection of 1, and the tested compounds were added in triplicate 8 h postinfection (hpi). At 24 hpi, cell lysates, which contain *C. trachomatis* elementary bodies, were collected from infected HEp-2 cell cultures in sucrose storage medium. The resulting mixture was frozen at –80 °C and used to infect a fresh HEp2 cell monolayer in a series of 10-fold dilutions. After a further 24 hpi, the recoverable EBs from the initial infection were stained using primary goat anti-MOMP antibody and a secondary donkey antigoat antibody labeled with Alexa488. The fluorescent inclusions were counted from 15 fields of view (FOV) at 20 $\times$  magnification. IFUs were calculated as the average count of inclusions in each FOV corrected for the dilution factor.<sup>41,87</sup> In the mechanism of action assays, we followed the same protocol described in the IFU assay. For (24 h reactivation) samples, the DMEM medium was removed after 24 hpi and the wells were washed three times with Hanks' balanced salt solution and fresh medium without compounds was added (0.5 mL/well).

**Casein Degradation Assay.** All recombinant, C-terminal 6X His-tagged ClpP proteins were expressed using *E. coli* and purified as previously described using a *clpAPX*-null *E. coli* strain kindly provided by Dr. Peter Sass.<sup>41,42</sup> The *clpP* human (NM\_006012.4) and mouse (NM\_017393.2) mRNA sequences were used to obtain the ClpP-encoding ORF minus the mitochondrial localization signal. Genes were then codon optimized for *E. coli* expression and synthesized by Integrated DNA Technologies. The mouse and human *clpP* paralogues were cloned into the pLATE31 vector (Thermo Scientific) as previously performed for the bacterial ClpPs. Examples of purified protein samples are shown in Figure S2. FITC-casein (Sigma-Aldrich, C0528) was treated with Zeba 7K cutoff spin columns (Thermo Scientific) to remove free FITC. Assays were carried out in buffer PZ (25 mM HEPES [pH 7.6], 200 mM KCl, 5 mM  $\text{MgCl}_2$ , 1 mM DTT, and 10% v/v of glycerol) using 100  $\mu\text{L}$  reactions and 20  $\mu\text{M}$  FITC-casein. 1  $\mu\text{M}$  or 0.1  $\mu\text{M}$  (for **40**) of ClpP from *E. coli*, 1  $\mu\text{M}$  mouse or human ClpP, or 6  $\mu\text{M}$  of ClpP1 and ClpP2 were preincubated with either 25  $\mu\text{g}/\mu\text{L}$  compounds or DMSO solvent at 32 °C for 30 min before adding FITC-casein. Reactions were monitored for 3 h with readings every 3 min on a Tecan m Plex plate reader using an excitation wavelength of  $\lambda_{\text{ex}} = 490$  nm and an emission wavelength  $\lambda_{\text{em}} = 525$  nm. Reactions were run at least three times using at least two independent protein purification preparations.

**Antibacterial Assay against Additional Strains.** *S. aureus* USA 300 JE2 and *E. coli* K12 were provided by the Dr. Bayles' research lab at the Department of Pathology and Microbiology of the University of Nebraska Medical Center (UNMC). The MICs of the synthesized compounds were tested in triplicate samples, using the broth microdilution method as previously reported.<sup>88</sup> The bacterial cultures were made in Muller Hinton Broth (MHB) using the direct colony suspension method at  $1.5 \times 10^8$  CFU/mL, followed by dilution to  $\sim 10^5$  CFU/mL. The stock solutions of the tested compounds were prepared in sterile DMSO at 1 mg/mL concentration. Then, serial dilutions of the tested compounds were made in MHB in Cellstar 96-well microtiter plates using vancomycin as a positive control, and blank media as a negative control. 10  $\mu\text{L}$  of bacterial culture was added per well followed by incubating the plates for 16 h at the optimum temperature. The MIC was categorized as the concentration at which no visible growth of bacteria was observed at 600 nm in a particular well using an AccuScan, MultiScan FC. The average of triplicate MIC determinations is reported (for further details please see the Supporting Information).

**Cytotoxicity Assay (CCK-8).** The immortal keratinocyte cell line (HaCaT) and HeLa 229 were cultured in DMEM media containing 10% FBS and 1% penicillin/streptomycin solution at 37 °C with 5%  $\text{CO}_2$ . The cells were seeded separately at a density of 5000 cells per well in 96-well plates. On the next day, cells were treated with 50  $\mu\text{g}/\text{mL}$  of the tested drugs in triplicate, and as controls we used DMSO at a concentration equivalent to the one used in drug-treated cells. Then, the plates were incubated for an additional 24 h before the addition of 10  $\mu\text{L}$  of the assay reagent Cell Counting Kit-8 (CCK-8) (DOJINDO laboratories) followed by incubation of the plates for 2 h. Corrected absorbance readings were determined with a 450 nm filter using a multiscan FC microplate photometer (Thermo Fisher Scientific).

**Mutagenic Studies: SMART.** We assessed the mutagenicity of the compounds by Somatic Mutation and Recombination Test (SMART) using wing-somatic cells of *Drosophila melanogaster*.<sup>89,90</sup> The following 3 crosses of mutant flies were set up: (1) Standard cross (ST): *flare-3 (flr<sup>3</sup>)* virgin females, with genetic constituent *flr<sup>3</sup>/In(3LR)TM3, ri p<sup>15</sup>sep I(3)89Aa bx<sup>34e</sup> Bd<sup>S</sup>* crossed with *multiple wing hairs (mwh)* males, with genetic constituent *y; mwh jv* and (2) High bioactivation (HB) cross: *ORR; flare (ORR; flr3)* virgin female, with genetic constituent *ORR; flr<sup>3</sup>/In (3LR) TM3, ri pp sep I(3)89 Aa bx 34e Bd<sup>S</sup>* crossed with *mwh* males. The *ORR;flr3* strain carries the chromosomes 1 and 2 from a DDT-resistant Oregon R (R) line, which contain genes responsible for the high level of metabolizing enzymes of the cytochrome P450, P(CYP)6 A2 type.<sup>89</sup>

Eggs were collected from flies of the two different crosses in culture flasks containing a solid agar–agar base (5% w/v), covered by a layer of live baker's yeast supplemented with sugar for 8 h. Third instar larvae (72  $\pm$  4 h) were washed out of the culture bottles with tap water and collected with a fine meshed strainer. Larvae groups were transferred to glass vials containing hydrated alternative medium (instant mashed potato flakes Yoki) and exposed to compounds **11**, **20**, **24**, **26**, **40**, and **41** at 0.25, 0.5, and 1.0 mM final concentrations. Solvent (Milli-Q water, 1% of Tween-80, and 3% ethanol) was used as a negative control.

The hatched flies of the marker heterozygote (*mwh + /+ flr3*) and the balancer heterozygote (*mwh + /+ TM3, Bds*) genotypes were collected and fixed in 70% ethanol. Wings were removed, mounted on slides containing Faure's solution (30 g of gum Arabic, 50 g of chloral hydrate, 20 mL of glycerol, and 50 mL of water), and analyzed under an optical microscope (400 $\times$ ) for the occurrence of different types of mutant spots.<sup>91</sup>

The statistical analysis was performed as described by Frei and Würzler,<sup>90</sup> using the chi-squared test. Results were considered statistically significant when  $p < 0.05$ . The frequencies of each spot (single small, single large, or twin) and the total frequency of spots per fly, for each treatment, were compared in pairs (i.e., negative control versus compound-treated).

**Metabolic Stability.** The *in vitro* metabolism stability experiment was done using human liver microsomes (XenoTech, LLC, Lenexa, KS) for phase I metabolism. The results were expressed as the

percentage of drug remaining (solution were 1  $\mu\text{M}$  in 0.1% methanol), and the studies were performed in triplicate as described previously.<sup>92</sup> For the microsomal stability test, we used a solution of phosphate buffer (100 mM, pH 7.4), microsomal protein (1.0 mg/mL), magnesium chloride (10 mM), and NADPH (2 mM) at a final volume of 1.0 mL. This mixture was preincubated at 37 °C for 10 min in a water bath maintained at 60 rpm. The reaction was initialized by adding the selected compounds (1  $\mu\text{g}/\text{mL}$ ). Aliquots (100  $\mu\text{L}$ ) were collected at 0, 5, 15, 20, 30, 45, and 60 min. The reaction was quenched by adding MeOH (300  $\mu\text{L}$ ) containing IS (100 ng/mL). The aliquot and quenching reaction were contained in a 1.5 mL Eppendorf tube. The incubation without the addition of NADPH was used as a negative control. Testosterone was incubated similarly as positive control substrates. Then, 5  $\mu\text{L}$  samples of the supernatants were analyzed by LC–MS/MS.

**LC–MS/MS Assay.** (A) A Shimadzu LC–MS/MS system (LC–MS/MS 8060, Shimadzu, Japan) was utilized for analysis. The LC system consisted of two LC-30 AD pumps and a CTO-30AS column oven plus an autosampler (SIL-30AC), which was used to inject 10  $\mu\text{L}$  aliquots of the processed samples. The MS/MS system operated at unit resolution in the multiple reaction monitoring (MRM) mode. The following precursor ion > product ion combinations were used: 489.95 > 280.15, 510.05 > 280.05, 417.10 > 280.10, 416.15 > 98.10, and 414.10 > 176.25  $m/z$  for **40**, **37**, **25**, **24**, and **11**, respectively. The compound dependent mass spectrometer parameters, such as temperature, voltage, gas pressure, etc., were optimized by auto method optimization via precursor ion search for each analyte and the internal standard (IS) using a 0.5  $\mu\text{g}/\text{mL}$  solution in methanol.

(B) Chromatographic separation was achieved on an ACE Excel C<sub>18</sub> column (1.7  $\mu\text{m}$ , 100 mm  $\times$  2.1 mm, from Advance Chromatography Technologies Ltd., U.K.) with a Phenomenex C<sub>18</sub> guard column (Phenomenex, Torrance, CA). The mobile phase consisted of formic acid in water (0.1%, solvent A) and methanol (MeOH) (solvent B) using a total flow rate of 0.25 mL/min. The chromatographic separation was achieved using a 5.0 min gradient elution. The initial mobile phase composition was 35% B, increasing to 90% B over 4 min, and finally brought back to the initial conditions of 35% B in 0.10 min, followed by 1 min re-equilibration. The injection volume (5  $\mu\text{L}$ ) was consistent for all samples.

**Mouse Plasma Stability.** The tested compounds were dissolved in DMSO to yield 2.5 mM solutions. Mouse plasma was diluted to 80% with PBS and heated at 37 °C before the assay. The tested compounds were incubated with the preheated plasma solution (final concentration: 50  $\mu\text{M}$ ) in a shaking water bath at 37 °C at six different time points: 0, 15, 30, 60, 90, and 120 min. Experiments were independently conducted in triplicate. At the end of the incubation time, 50  $\mu\text{L}$  of sample was collected and mixed with 200  $\mu\text{L}$  of cold acetonitrile to stop the reaction. Solutions were vortex-mixed and then centrifuged at 4 °C and 14 000 rpm for 15 min. Supernatants were diluted in methanol–water (50:50 v/v) and analyzed by HPLC–PDA–ESI–SQ–MS. Peak areas of test compounds were computed for each incubation time and relative levels to time zero are reported. Enalapril was used as a positive control during incubation.

**SGF Stability.** The tested compounds were dissolved in DMSO to yield 1 mM. Compounds were incubated with SGF solution (final concentration, 50 mM) in a shaking water bath at 37 °C for four different time points: 0, 30, 60, and 120 min. Experiments were independently conducted in triplicate. At the end of the incubation, 125  $\mu\text{L}$  of sample solution was taken and 375  $\mu\text{L}$  of acetonitrile was added to stop the reaction. The solutions were vortex-mixed and centrifuged at 25 °C and 15 000 rpm for 15 min. The supernatant was diluted in methanol–water (50:50 v/v) and analyzed by HPLC–MS. The percentage of compound remaining at the individual time points relative to the 0 min sample is reported based on the peak area of the test compound.

The HPLC–PDA–ESI–SQ–MS analysis was performed using a Waters Alliance e2695 system with a Phenomenex Kinetex XB-C18 (4.6 mm  $\times$  150 mm, 5  $\mu\text{m}$  particle size) column, coupled to a Waters 2998 photodetector array and a Waters SQD2 single quadrupole mass

spectrometer with an ESI source. Gradient elution was utilized in the chromatographic separation method using 0.1% formic acid in water (mobile phase A) and methanol (mobile phase B), with the following program: 0–9 min 75% B; 9–10 min 75–95% B; 10 min 95% B. The flow rate was constant at 0.4 mL min<sup>-1</sup>. After each sample injection, the gradient was returned to its initial condition in 16 min. The injection volume was 5  $\mu\text{L}$ , and the column temperature was 40 °C. The mass spectrometer was operated in positive ion mode with a probe capillary voltage of 3.0 kV. The sampling cone voltage was set to 45.0 V. The source and desolvation gas temperatures were set at 150 and 350 °C, respectively. The nitrogen gas desolvation flow rate was 600 L h<sup>-1</sup>, and the cone gas flow rate was 10 L h<sup>-1</sup>. The mass spectrometer was calibrated across the range of  $m/z$  20–2023 with a sodium and cesium iodide solution. Data were acquired in scan mode with a scan duration of 0.2 s; in SIR mode for each test compound based on the  $m/z$  value for  $[\text{M} + \text{H}]^+$  adduct ions and with unit resolution. Data acquisition and processing were conducted using MassLynx, version 4.1 (Waters Corp.).

## ■ ASSOCIATED CONTENT

### Supporting Information

The Supporting Information is available free of charge at <https://pubs.acs.org/doi/10.1021/acs.jmedchem.0c00371>.

Additional synthetic pathways; chlamydial immunofluorescence images; HPLC traces, MS and NMR spectra; and purified protein examples (PDF)

Additional ClpP activity data (oligomerization, casein degradation, peptide degradation) (CSV)

## ■ AUTHOR INFORMATION

### Corresponding Authors

**Scot P. Ouellette** – Department of Pathology and Microbiology, College of Medicine, University of Nebraska Medical Center, Omaha, Nebraska 68198, United States; Phone: 402-559-0763; Email: [scot.ouellette@unmc.edu](mailto:scot.ouellette@unmc.edu)

**Martin Conda-Sheridan** – Department of Pharmaceutical Sciences, College of Pharmacy, University of Nebraska Medical Center, Omaha, Nebraska 68198, United States; [orcid.org/0000-0002-3568-2545](https://orcid.org/0000-0002-3568-2545); Phone: 402-559-9361; Email: [martin.condasherida@unmc.edu](mailto:martin.condasherida@unmc.edu)

### Authors

**Mohamed A. Seleem** – Department of Pharmaceutical Sciences, College of Pharmacy, University of Nebraska Medical Center, Omaha, Nebraska 68198, United States; [orcid.org/0000-0003-4379-5133](https://orcid.org/0000-0003-4379-5133)

**Nathalia Rodrigues de Almeida** – Department of Chemistry, College of Arts and Sciences, University of Nebraska at Omaha, Omaha, Nebraska 68182, United States; [orcid.org/0000-0002-9552-1233](https://orcid.org/0000-0002-9552-1233)

**Yashpal Singh Chhonker** – Clinical Pharmacology Laboratory, Department of Pharmacy Practice and Science, College of Pharmacy, University of Nebraska Medical Center, Omaha, Nebraska 68198, United States; [orcid.org/0000-0001-6455-5388](https://orcid.org/0000-0001-6455-5388)

**Daryl J. Murry** – Clinical Pharmacology Laboratory, Department of Pharmacy Practice and Science, College of Pharmacy, University of Nebraska Medical Center, Omaha, Nebraska 68198, United States; [orcid.org/0000-0002-4169-5027](https://orcid.org/0000-0002-4169-5027)

**Zaira da Rosa Guterres** – Laboratory of Cytogenetics and Mutagenesis, State University of Mato Grosso do Sul, Mundo Novo, Matto Grasso do Sul, Brazil

**Amanda M. Blocker** – School of Biological Sciences, Southern Illinois University Carbondale, Carbondale, Illinois 62901, United States

**Shiomi Kuwabara** – School of Biological Sciences, Southern Illinois University Carbondale, Carbondale, Illinois 62901, United States

**Derek J. Fisher** – School of Biological Sciences, Southern Illinois University Carbondale, Carbondale, Illinois 62901, United States; [orcid.org/0000-0002-1663-8389](https://orcid.org/0000-0002-1663-8389)

**Emilse S. Leal** – Centro de Investigaciones en BioNanociencias (CIBION), Consejo Nacional de Investigaciones Científicas y Técnicas (CONICET), 2390 Ciudad de Buenos Aires, Argentina

**Manuela R. Martinefski** – Centro de Investigaciones en BioNanociencias (CIBION), Consejo Nacional de Investigaciones Científicas y Técnicas (CONICET), 2390 Ciudad de Buenos Aires, Argentina; [orcid.org/0000-0002-4501-3783](https://orcid.org/0000-0002-4501-3783)

**Mariela Bollini** – Centro de Investigaciones en BioNanociencias (CIBION), Consejo Nacional de Investigaciones Científicas y Técnicas (CONICET), 2390 Ciudad de Buenos Aires, Argentina; [orcid.org/0000-0002-8718-6236](https://orcid.org/0000-0002-8718-6236)

**María Eugenia Monge** – Centro de Investigaciones en BioNanociencias (CIBION), Consejo Nacional de Investigaciones Científicas y Técnicas (CONICET), 2390 Ciudad de Buenos Aires, Argentina; [orcid.org/0000-0001-6517-5301](https://orcid.org/0000-0001-6517-5301)

Complete contact information is available at:  
<https://pubs.acs.org/10.1021/acs.jmedchem.0c00371>

## Notes

The authors declare no competing financial interest.

## ACKNOWLEDGMENTS

This work was supported by the National Institute of Health-NIGMS, Nebraska Center for Molecular Target Discovery and Development (Grant 1P20GM121316-01A1; PI, Robert Lewis; Project Leader, Martin Conda-Sheridan), the Department of Defense-Peer Reviewed Medical Research Program 2017 (Grant W81XWH-18-1-0113, Martin Conda-Sheridan), and the National Science Foundation (CAREER Award 1810599 to Scot P. Ouellette). María Eugenia Monge and Mariela Bollini are research staff members from CONICET (Consejo Nacional de Investigaciones Científicas y Técnicas), Argentina.

## ABBREVIATIONS USED

EB, elementary body; RB, reticulate body; STI, sexually transmitted infection; STDs, sexually transmitted diseases; ACP, activators of cylindrical protease; PyBOP, benzotriazole-1-yl-oxy-tris-pyrrolidino-phosphonium hexafluorophosphate; HBTU, *N,N,N',N'*-tetramethyl-O-(1H-benzotriazol-1-yl)-uronium hexafluorophosphate; HATU, 1-[bis-(dimethylamino)methylene]-1H-1,2,3-triazolo[4,5-b]pyridinium 3-oxid hexafluorophosphate; DIPEA, *N,N* diisopropylethylamine; IFA, immunofluorescence assay; IFU, inclusion forming unit; Hep-2, human epithelial type 2; HBD, hydrogen bond donor; HBA, hydrogen bond acceptor; SDS, sodium dodecyl sulfate; Suc-Luc-Tyr-AMC, succinic acid-leucin-tyrosin-7-amino-4-methyl-2H-chromen-2-one; TLC, thin layer chromatography; brs, broad signal; DMEM, Dulbecco's modified eagle medium

## REFERENCES

- (1) Centers for Disease Control. *New CDC Analysis Shows Steep and SPrevention. New CDC Analysis Shows Steep and Sustained Increases in STDs in Recent Years*. 2017, <https://www.cdc.gov/media/releases/2018/p0828-increases-in-stds.html> (accessed 2018-08-28).
- (2) Braxton, J.; Davis, D. W.; Emerson, B.; Flagg, E. W.; Grey, J.; Grier, L.; Harvey, A.; Kidd, S.; Kim, J.; Kreisel, K. *Sexually Transmitted Disease Surveillance 2017*. 2018, <https://www.cdc.gov/nchhstp/newsroom/2018/2017-STD-surveillance-report.html> (accessed 2018-09-25).
- (3) Manavi, K. A Review on Infection with *Chlamydia Trachomatis*. *Best Pract. Res. Cl. OB* **2006**, *20*, 941–951.
- (4) Hafner, L. M.; Pelzer, E. S. Tubal Damage, Infertility and Tubal Ectopic Pregnancy: *Chlamydia Trachomatis* and Other Microbial Aetiologies. In *Ectopic Pregnancy-Modern Diagnosis and Management*; IntechOpen, 2011; pp 13–44, DOI: 10.5772/21555.
- (5) Darville, T.; Hiltke, T. J. Pathogenesis of Genital Tract Disease due to *Chlamydia Trachomatis*. *J. Infect. Dis.* **2010**, *201*, S114–S125.
- (6) Workowski, K. A.; Berman, S. M. Centers for Disease Control and Prevention Sexually Transmitted Disease Treatment Guidelines. *Clin. Infect. Dis.* **2011**, *53*, S59–S63.
- (7) Dalaker, K.; Gjønnæss, H.; Kvile, G.; Urnes, A.; Anestad, G.; Bergan, T. *Chlamydia Trachomatis* as a Cause of Acute Perihepatitis Associated with Pelvic Inflammatory Disease. *Sex. Transm. Infect.* **1981**, *57*, 41–43.
- (8) Hatch, T. P.; Allan, I. t.; Pearce, J. Structural and Polypeptide Differences Between Envelopes of Infective and Reproductive Life Cycle Forms of *Chlamydia* spp. *J. Bacteriol.* **1984**, *157*, 13–20.
- (9) Abdelrahman, Y. M.; Belland, R. J. The Chlamydial Developmental Cycle. *FEMS Microbiol. Rev.* **2005**, *29*, 949–959.
- (10) Abdelrahman, Y.; Ouellette, S. P.; Belland, R. J.; Cox, J. V. Polarized Cell Division of *Chlamydia Trachomatis*. *PLoS Pathog.* **2016**, *12*, No. e1005822.
- (11) Moore, E. R.; Ouellette, S. P. Reconceptualizing the Chlamydial Inclusion as a Pathogen-Specified Parasitic Organelle: an Expanded Role for Inc Proteins. *Front. Cell. Infect. Microbiol.* **2014**, *4*, 157.
- (12) Schutteet, K.; De Clercq, E.; Vanrompay, D. *Chlamydia Trachomatis* Vaccine Research Through the Years. *Infect. Dis. Obstet. Gynecol.* **2011**, *2011*, 963513.
- (13) de la Maza, L. M.; Zhong, G.; Brunham, R. C. Update on *Chlamydia Trachomatis* Vaccinology. *Clin. Vaccine Immunol.* **2017**, *24*, e00543-16.
- (14) Langdon, A.; Crook, N.; Dantas, G. The Effects of Antibiotics on the Microbiome Throughout Development and Alternative Approaches for Therapeutic Modulation. *Genome Med.* **2016**, *8*, 39.
- (15) Kjaer, H.; Dimcevski, G.; Hoff, G.; Olesen, F.; Østergaard, L. Recurrence of Urogenital *Chlamydia Trachomatis* Infection Evaluated by Mailed Samples Obtained at Home: 24 weeks' Prospective Follow up Study. *Sex. Transm. Infect.* **2000**, *76*, 169–172.
- (16) Horner, P. J. Azithromycin Antimicrobial Resistance and Genital *Chlamydia Trachomatis* Infection: Duration of Therapy May be the Key to Improving Efficacy. *Sex. Transm. Infect.* **2012**, *88*, 154–156.
- (17) Horner, P.; Saunders, J. Should Azithromycin 1 g be Abandoned as a Treatment For Bacterial STIs? The Case for and Against. *Sex. Transm. Infect.* **2017**, *93*, 85–87.
- (18) Kong, F. Y.; Hocking, J. S. Treatment Challenges for Urogenital and Anorectal *Chlamydia Trachomatis*. *BMC Infect. Dis.* **2015**, *15*, 293.
- (19) Good, J. A.; Kulén, M.; Silver, J.; Krishnan, K. S.; Bahnan, W.; Nunez-Otero, C.; Nilsson, I.; Wede, E.; de Groot, E.; Gylfe, Å; Bergström, S.; Almqvist, F. Thiazolino 2-Pyridone Amide Isosteres as Inhibitors of *Chlamydia Trachomatis* Infectivity. *J. Med. Chem.* **2017**, *60*, 9393–9399.
- (20) Good, J. A.; Silver, J.; Nunez-Otero, C.; Bahnan, W.; Krishnan, K. S.; Salin, O.; Engström, P.; Svensson, R.; Artursson, P.; Gylfe, Å; Bergström, S.; Almqvist, F. Thiazolino 2-Pyridone Amide Inhibitors of *Chlamydia Trachomatis* Infectivity. *J. Med. Chem.* **2016**, *59*, 2094–2108.

- (21) Mojica, S. A.; Salin, O.; Bastidas, R. J.; Sunduru, N.; Hedenstrom, M.; Andersson, C. D.; Nunez-Otero, C.; Engstrom, P.; Valdivia, R. H.; Elofsson, M.; Gylfe, A. N-Acylated Derivatives of Sulfamethoxazole Block Chlamydia Fatty Acid Synthesis and Interact with FabF. *Antimicrob. Agents Chemother.* **2017**, *61*, No. e00716-17.
- (22) Sunduru, N.; Salin, O.; Gylfe, Å.; Elofsson, M. Design, Synthesis and Evaluation of Novel Polypharmacological Antichlamydial Agents. *Eur. J. Med. Chem.* **2015**, *101*, 595–603.
- (23) Moreno-Cinos, C.; Goossens, K.; Salado, I. G.; Van Der Veken, P.; De Winter, H.; Augustyns, K. ClpP Protease, a Promising Antimicrobial Target. *Int. J. Mol. Sci.* **2019**, *20*, 2232.
- (24) Culp, E.; Wright, G. D. Bacterial Proteases, Untapped Antimicrobial Drug Targets. *J. Antibiot.* **2017**, *70*, 366.
- (25) Brotz-Oesterhelt, H.; Beyer, D.; Kroll, H.-P.; Endermann, R.; Ladel, C.; Schroeder, W.; Hinzen, B.; Raddatz, S.; Paulsen, H.; Henninger, K.; Bandow, J. E.; Sahl, H.-G.; Labischinski, H. Dysregulation of Bacterial Proteolytic Machinery by a New Class of Antibiotics. *Nat. Med.* **2005**, *11*, 1082–1087.
- (26) Frees, D.; Brøndsted, L.; Ingmer, H. Bacterial Proteases and Virulence. In *Regulated Proteolysis in Microorganisms*; Subcellular Biochemistry, Vol. 66; Springer: Dordrecht, The Netherlands, 2013; pp 161–192, DOI: 10.1007/978-94-007-5940-4.
- (27) McGillivray, S. M.; Tran, D. N.; Ramadoss, N. S.; Alumasa, J. N.; Okumura, C. Y.; Sakoulas, G.; Vaughn, M. M.; Zhang, D. X.; Keiler, K. C.; Nizet, V. Pharmacological Inhibition of the ClpXP Protease Increases Bacterial Susceptibility to Host Cathelicidin Antimicrobial Peptides and Cell Envelope-Active Antibiotics. *Antimicrob. Agents Chemother.* **2012**, *56*, 1854–1861.
- (28) Gur, E.; Biran, D.; Ron, E. Z. Regulated Proteolysis in Gram-Negative Bacteria—How and When? *Nat. Rev. Microbiol.* **2011**, *9*, 839–848.
- (29) Sauer, R. T.; Baker, T. A. AAA+ Proteases: ATP-Fueled Machines of Protein Destruction. *Annu. Rev. Biochem.* **2011**, *80*, 587–612.
- (30) Konovalova, A.; Søgaard-Andersen, L.; Kroos, L. Regulated Proteolysis in Bacterial Development. *FEMS Microbiol. Rev.* **2014**, *38*, 493–522.
- (31) Lavey, N. P.; Coker, J. A.; Ruben, E. A.; Duerfeldt, A. S. Sclerotiamide: The First Non-Peptide-Based Natural Product Activator of Bacterial Caseinolytic Protease P. *J. Nat. Prod.* **2016**, *79*, 1193–1197.
- (32) Kirstein, J.; Hoffmann, A.; Lilie, H.; Schmidt, R.; Rübsamen-Waigmann, H.; Brötz-Oesterhelt, H.; Mogk, A.; Turgay, K. The Antibiotic ADEP Reprogrammes ClpP, Switching it From a Regulated to an Uncontrolled Protease. *EMBO Mol. Med.* **2009**, *1*, 37–49.
- (33) Socha, A. M.; Tan, N. Y.; LaPlante, K. L.; Sello, J. K. Diversity-Oriented Synthesis of Cyclic Acyldepsipeptides Leads to the Discovery of a Potent Antibacterial Agent. *Bioorg. Med. Chem.* **2010**, *18*, 7193–7202.
- (34) Carney, D. W.; Schmitz, K. R.; Truong, J. V.; Sauer, R. T.; Sello, J. K. Restriction of the Conformational Dynamics of the Cyclic Acyldepsipeptide Antibiotics Improves Their Antibacterial Activity. *J. Am. Chem. Soc.* **2014**, *136*, 1922–1929.
- (35) Leung, E.; Datti, A.; Cossette, M.; Goodreid, J.; McCaw, S. E.; Mah, M.; Nakhamchik, A.; Ogata, K.; El Bakkouri, M.; Cheng, Y.-Q.; Wodak, S. J.; Eger, B. T.; Pai, E. F.; Liu, J.; Gray-Owen, S.; Batey, R. A.; Houry, W. A. Activators of Cylindrical Proteases as Antimicrobials: Identification and Development of Small Molecule Activators of ClpP Protease. *Chem. Biol.* **2011**, *18*, 1167–1178.
- (36) Hinzen, B.; Raddatz, S.; Paulsen, H.; Lampe, T.; Schumacher, A.; Habich, D.; Hellwig, V.; Benet-Buchholz, J.; Endermann, R.; Labischinski, H.; Brotz-Oesterhelt, H. Medicinal Chemistry Optimization of Acyldepsipeptides of the Enopeptin Class Antibiotics. *ChemMedChem* **2006**, *1*, 689–693.
- (37) Famulla, K.; Sass, P.; Malik, I.; Akopian, T.; Kandror, O.; Alber, M.; Hinzen, B.; Ruebsamen-Schaeff, H.; Kalscheuer, R.; Goldberg, A. L.; Brötz-Oesterhelt, H. Acyldepsipeptide Antibiotics Kill Mycobacteria by Preventing the Physiological Functions of the ClpP1P2 Protease. *Mol. Microbiol.* **2016**, *101*, 194–209.
- (38) Arvanitis, M.; Li, G.; Li, D.-D.; Cotnoir, D.; Ganley-Leal, L.; Carney, D. W.; Sello, J. K.; Mylonakis, E. A Conformationally Constrained Cyclic Acyldepsipeptide is Highly Effective in Mice Infected with Methicillin-Susceptible and -Resistant *Staphylococcus aureus*. *PLoS One* **2016**, *11*, No. e0153912.
- (39) Yu, A. Y. H.; Houry, W. A. ClpP: A Distinctive Family of Cylindrical Energy-Dependent Serine Proteases. *FEBS Lett.* **2007**, *581*, 3749–3757.
- (40) Rodgers, A. K.; Wang, J.; Zhang, Y.; Holden, A.; Berryhill, B.; Budrys, N. M.; Schenken, R. S.; Zhong, G. Association of Tubal Factor Infertility with Elevated Antibodies to *Chlamydia Trachomatis* Caseinolytic Protease P. *Am. J. Obstet. Gynecol.* **2010**, *203*, 494.e7.
- (41) Wood, N. A.; Chung, K. Y.; Blocker, A. M.; Rodrigues de Almeida, N.; Conda-Sheridan, M.; Fisher, D. J.; Ouellette, S. P. Initial Characterization of the Two ClpP Paralogs of *Chlamydia Trachomatis* Suggests Unique Functionality for Each. *J. Bacteriol.* **2019**, *201*, No. e00635-18.
- (42) Pan, S.; Malik, I. T.; Thomy, D.; Henrichfreise, B.; Sass, P. The Functional ClpXP Protease of *Chlamydia Trachomatis* Requires Distinct ClpP Genes From Separate Genetic Loci. *Sci. Rep.* **2019**, *9*, 1–14.
- (43) Neuwald, A. F.; Aravind, L.; Spouge, J. L.; Koonin, E. V. AAA+: A Class of Chaperone-like ATPases Associated with the Assembly, Operation, and Disassembly of Protein Complexes. *Genome Res.* **1999**, *9*, 27–43.
- (44) Krüger, E.; Zühlke, D.; Witt, E.; Ludwig, H.; Hecker, M. Clp-Mediated Proteolysis in Gram-positive Bacteria is Autoregulated by the Stability of a Repressor. *EMBO J.* **2001**, *20*, 852–863.
- (45) Baker, T. A.; Sauer, R. T. ClpXP, an ATP-Powered Unfolding and Protein-Degradation Machine. *Biochim. Biophys. Acta, Mol. Cell Res.* **2012**, *1823*, 15–28.
- (46) Kanishchev, O. S.; Dolbier, W. R., Jr Ni/Ir-Catalyzed Photoredox Decarboxylative Coupling of S-Substituted Thiolactone Acids with Heteroaryl Bromides: Short Synthesis of Sulfoxalor and Its SF5 Analog. *Chem. - Eur. J.* **2017**, *23*, 7677–7681.
- (47) Valeur, E.; Bradley, M. Amide Bond Formation: Beyond the Myth of Coupling Reagents. *Chem. Soc. Rev.* **2009**, *38*, 606–631.
- (48) Coste, J.; Le-Nguyen, D.; Castro, B. PyBOP®: A new Peptide Coupling Reagent Devoid of Toxic by-Product. *Tetrahedron Lett.* **1990**, *31*, 205–208.
- (49) Lipinski, C. A.; Lombardo, F.; Dominy, B. W.; Feeney, P. J. Experimental and Computational Approaches to Estimate Solubility and Permeability in Drug Discovery and Development Settings. *Adv. Drug Delivery Rev.* **1997**, *23*, 3–25.
- (50) Snape, T. J. A Truce on the Smiles Rearrangement: Revisiting an Old Reaction—the Truce—Smiles Rearrangement. *Chem. Soc. Rev.* **2008**, *37*, 2452–2458.
- (51) Ishibashi, H.; Uegaki, M.; Sakai, M.; Takeda, Y. Base-Promoted Aminoethylation of Thiols with 2-Oxazolidinones: A Simple Synthesis of 2-Aminoethyl Sulfides. *Tetrahedron* **2001**, *57*, 2115–2120.
- (52) Ishibashi, H.; Uegaki, M.; Sakai, M. A Simple Synthesis of  $\beta$ -amino Sulfides. *Synlett* **1997**, *1997*, 915–916.
- (53) Chang, C.-e. A.; Chen, W.; Gilson, M. K. Ligand Configurational Entropy and Protein Binding. *Proc. Natl. Acad. Sci. U. S. A.* **2007**, *104*, 1534–1539.
- (54) Fang, Z.; Song, Y. n.; Zhan, P.; Zhang, Q.; Liu, X. Conformational Restriction: An Effective Tactic in Follow-on-Based Drug Discovery. *Future Med. Chem.* **2014**, *6*, 885–901.
- (55) Fields, K. A.; Hackstadt, T. The Chlamydial Inclusion: Escape from the Endocytic Pathway. *Annu. Rev. Cell Dev. Biol.* **2002**, *18*, 221–245.
- (56) Volceanov, L.; Herbst, K.; Biniossek, M.; Schilling, O.; Haller, D.; Nölke, T.; Subbarayal, P.; Rudel, T.; Zieger, B.; Häcker, G. Septins Arrange F-Actin-Containing Fibers on the *Chlamydia Trachomatis* Inclusion and Are Required for Normal Release of the Inclusion by Extrusion. *mBio* **2014**, *5*, 1802–1814.
- (57) Hakala, E.; Hanski, L.; Uvell, H.; Yrjönen, T.; Vuorela, H.; Elofsson, M.; Vuorela, P. M. Dibenzocyclooctadiene Lignans from *Schisandra* spp. Selectively Inhibit the Growth of the Intracellular

Bacteria *Chlamydia Pneumoniae* and *Chlamydia Trachomatis*. *J. Antibiot.* **2015**, *68*, 609.

(58) Marwaha, S.; Uvell, H.; Salin, O.; Lindgren, A. E.; Silver, J.; Elofsson, M.; Gylfe, Å. N-Acylated Derivatives of Sulfamethoxazole and Sulfafurazole Inhibit Intracellular Growth of *Chlamydia Trachomatis*. *Antimicrob. Agents Chemother.* **2014**, *58*, 2968–2971.

(59) Batey, R.; Cossette, M.; Datti, A.; Eger, B. T.; Fai, E. F.; Goodreid, J.; Gray-Owen, S. D.; Houry, W. A.; Leung, E.; Liu, J.; Nhieu, A. J. Activators of Cylindrical Proteases. WO 2012079164A1, 2011.

(60) Shang, S.; Xia, L.; Zhong, M.; Zhang, J.; Zhao, J.; Gong, X.; Mabe, D.; Wang, Q. In Vitro Effects of Spectinomycin and Ceftriaxone Alone or in Combination with Other Antibiotics Against *Chlamydia Trachomatis*. *Antimicrob. Agents Chemother.* **2005**, *49*, 1584–1586.

(61) Wyrick, P. B. *Chlamydia Trachomatis* Persistence In Vitro: An Overview. *J. Infect. Dis.* **2010**, *201*, S88–S95.

(62) Ouellette, S. P.; Karimova, G.; Subtil, A.; Ladant, D. Chlamydia Co-opts the Rod Shape-Determining Proteins MreB and Pbp2 for Cell Division. *Mol. Microbiol.* **2012**, *85*, 164–78.

(63) Ridgway, G.; Owen, J.; Oriol, J. The Antimicrobial Susceptibility of *Chlamydia Trachomatis* in Cell Culture. *Sex. Transm. Infect.* **1978**, *54*, 103–106.

(64) Keat, A. C.; Maini, R. N.; Nkwazi, G. C.; Pegrum, G. D.; Ridgway, G. L.; Scott, J. T. Role of *Chlamydia Trachomatis* and HLA-B27 in Sexually Acquired Reactive Arthritis. *Br. Med. J.* **1978**, *1*, 605–7.

(65) Suchland, R.; Geisler, W.; Stamm, W. E. Methodologies and Cell Lines Used for Antimicrobial Susceptibility Testing of *Chlamydia* spp. *Antimicrob. Agents Chemother.* **2003**, *47*, 636–642.

(66) Somani, J.; Bhullar, V. B.; Workowski, K. A.; Farshy, C. E.; Black, C. M. Multiple Drug-Resistant *Chlamydia Trachomatis* Associated with Clinical Treatment Failure. *J. Infect. Dis.* **2000**, *181*, 1421–1427.

(67) Foschi, C.; Salvo, M.; Cevenini, R.; Marangoni, A. *Chlamydia Trachomatis* Antimicrobial Susceptibility in Colorectal and Endocervical Cells. *J. Antimicrob. Chemother.* **2018**, *73*, 409–413.

(68) Smelov, V.; Perekalina, T.; Gorelov, A.; Smelova, N.; Artemenko, N.; Norman, L. In Vitro Activity of Fluoroquinolones, Azithromycin and Doxycycline against *Chlamydia Trachomatis* Cultured from Men with Chronic Lower Urinary Tract Symptoms. *Eur. Urol.* **2004**, *46*, 647–650.

(69) Lau, C.-Y.; Qureshi, A. K. Azithromycin Versus Doxycycline for Genital Chlamydial Infections: a Meta-Analysis of Randomized Clinical Trials. *Sex. Transm. Dis.* **2002**, *29*, 497–502.

(70) Kong, F. Y. S.; Hocking, J. S. Treatment Challenges for Urogenital and Anorectal *Chlamydia Trachomatis*. *BMC Infect. Dis.* **2015**, *15*, 293.

(71) Unemo, M.; Del Rio, C.; Shafer, W. M. Antimicrobial Resistance Expressed by *Neisseria gonorrhoeae*: A Major Global Public Health Problem in the 21st Century. *Microbiol. Spectrum* **2016**, *4*, 4.

(72) Holmes, N. E.; Charles, P. G. P. Safety and Efficacy Review of Doxycycline. *Clin. Med.: Ther.* **2009**, DOI: 10.4137/CMT.S2035.

(73) Peyriere, H.; Makinson, A.; Marchandin, H.; Reynes, J. Doxycycline in the Management of Sexually Transmitted Infections. *J. Antimicrob. Chemother.* **2017**, *73*, 553–563.

(74) Whittles, L. K.; White, P. J.; Paul, J.; Didelot, X. Epidemiological Trends of Antibiotic Resistant Gonorrhoea in the United Kingdom. *Antibiotics* **2018**, *7*, 60.

(75) Wang, S. A.; Papp, J. R.; Stamm, W. E.; Peeling, R. W.; Martin, D. H.; Holmes, K. K. Evaluation of Antimicrobial Resistance and Treatment Failures for *Chlamydia Trachomatis*: A Meeting Report. *J. Infect. Dis.* **2005**, *191*, 917–923.

(76) Páez-Carro, C.; Alzate, J. P.; González, L. M.; Rubio-Romero, J. A.; Lethaby, A.; Gaitán, H. G. Antibiotics for Treating Urogenital *Chlamydia Trachomatis* Infection in Men and Non-Pregnant Women. *Cochrane Database Syst. Rev.* **2019**, *1*.

(77) Sandoz, K. M.; Rockey, D. D. Antibiotic Resistance in Chlamydiae. *Future Microbiol.* **2010**, *5*, 1427–1442.

(78) Wilson, G.; Miles, A.; Knox, R.; Parker, M.; Macrae, A.; Meynell, G.; Meynell, E. *Topley and Wilson's Principles of Bacteriology and Immunity*, 5th ed., Vol. 2; Williams & Wilkins Company: Baltimore, MD, 1964.

(79) Redgrove, K. A.; McLaughlin, E. A. The Role of the Immune Response in *Chlamydia Trachomatis* Infection of the Male Genital Tract: A Double-Edged Sword. *Front. Immunol.* **2014**, *5*, 534.

(80) Graf, U.; Würzler, F.; Katz, A.; Frei, H.; Juon, H.; Hall, C.; Kale, P. Somatic Mutation and Recombination Test in *Drosophila melanogaster*. *Environ. Mutagen.* **1984**, *6*, 153–188.

(81) Thomé, S.; Bizarro, C. R.; Lehmann, M.; Abreu, B. R. R. d.; Andrade, H. H. R. d.; Cunha, K. S.; Dihl, R. R. Recombinogenic and Mutagenic Activities of Fluoroquinolones in *Drosophila melanogaster*. *Mutat. Res., Genet. Toxicol. Environ. Mutagen.* **2012**, *742*, 43–47.

(82) Kalghatgi, S.; Spina, C. S.; Costello, J. C.; Liesa, M.; Morones-Ramirez, J. R.; Slomovic, S.; Molina, A.; Shirihai, O. S.; Collins, J. J. Bactericidal Antibiotics Induce Mitochondrial Dysfunction and Oxidative Damage in Mammalian Cells. *Sci. Transl. Med.* **2013**, *5*, 192ra85–192ra85.

(83) Ohnishi, S.; Murata, M.; Ida, N.; Oikawa, S.; Kawanishi, S. Oxidative DNA Damage Induced by Metabolites of Chloramphenicol, an Antibiotic Drug. *Free Radical Res.* **2015**, *49*, 1165–1172.

(84) Houston, J. B.; Galetin, A. Methods for Predicting in Vivo Pharmacokinetics Using Data From in Vitro Assays. *Curr. Drug Metab.* **2008**, *9*, 940–951.

(85) Pang, K. S.; Rowland, M. Hepatic Clearance of Drugs. I. Theoretical Considerations of a “Well-Stirred” Model and a “Parallel Tube” Model. Influence of Hepatic Blood Flow, Plasma and Blood Cell Binding, and the Hepatocellular Enzymatic Activity on Hepatic Drug Clearance. *J. Pharmacokin. Biopharm.* **1977**, *5*, 625–653.

(86) Beatty, W. L.; Byrne, G. I.; Morrison, R. P. Morphologic and Antigenic Characterization of Interferon Gamma-Mediated Persistent *Chlamydia Trachomatis* Infection In Vitro. *Proc. Natl. Acad. Sci. U. S. A.* **1993**, *90*, 3998–4002.

(87) Marwaha, S.; Uvell, H.; Salin, O.; Lindgren, A. E.; Silver, J.; Elofsson, M.; Gylfe, Å. N-acylated Derivatives of Sulfamethoxazole and Sulfafurazole Inhibit Intracellular Growth of *Chlamydia Trachomatis*. *Antimicrob. Agents Chemother.* **2014**, *58*, 2968–2971.

(88) Rodrigues de Almeida, N.; Han, Y.; Perez, J.; Kirkpatrick, S.; Wang, Y.; Sheridan, M. C. Design, Synthesis, and Nanostructure-Dependent Antibacterial Activity of Cationic Peptide Amphiphiles. *ACS Appl. Mater. Interfaces* **2019**, *11*, 2790–2801.

(89) Graf, U.; van Schaik, N. Improved High Bioactivation Cross for the Wing Somatic Mutation and Recombination Test in *Drosophila melanogaster*. *Mutat. Res./Environ. Muta.* **1992**, *271*, 59–67.

(90) Frei, H.; Würzler, F. E. Statistical Methods to Decide Whether Mutagenicity Test Data from *Drosophila* Assays Indicate a Positive, Negative, or Inconclusive Result. *Mutat. Res./Environ. Muta.* **1988**, *203*, 297–308.

(91) de Rezende, A. A. A.; Graf, U.; Guterres, Z. d. R.; Kerr, W. E.; Spanó, M. A. Protective Effects of Proanthocyanidins of Grape (*Vitis Vinifera* L.) Seeds on DNA Damage Induced by Doxorubicin in Somatic Cells of *Drosophila melanogaster*. *Food Chem. Toxicol.* **2009**, *47*, 1466–1472.

(92) Chhonker, Y. S.; Chandasana, H.; Mukkavilli, R.; Prasad, Y. D.; Laxman, T. S.; Vangala, S.; Bhatta, R. S. Assessment of In Vitro Metabolic Stability, Plasma protein Binding, and Pharmacokinetics of E- and Z-Guggulsterone in Rat. *Drug Test. Anal.* **2016**, *8*, 966–975.





## Understanding interactions of Citropin 1.1 analogues with model membranes and their influence on biological activity

Nathalia Rodrigues de Almeida<sup>a,1</sup>, Jonathan Catazaro<sup>b,1</sup>, Maddeboina Krishnaiah<sup>c</sup>, Yashpal Singh Chhonker<sup>d</sup>, Daryl J. Murry<sup>d</sup>, Robert Powers<sup>b,e,\*</sup>, Martin Conda-Sheridan<sup>a,\*\*</sup>

<sup>a</sup> Department of Pharmaceutical Sciences, University of Nebraska Medical Center – Omaha, NE, 68198-6125, USA

<sup>b</sup> Department of Chemistry, University of Nebraska – Lincoln, NE, 68588-0304, USA

<sup>c</sup> Department of Pediatrics Computational Chemistry, University of Nebraska Medical Center – Omaha, NE, 68198-2168, USA

<sup>d</sup> Clinical Pharmacology Laboratory, Department of Pharmacy Practice, University of Nebraska Medical Center – Omaha, NE, 68198-6145, USA

<sup>e</sup> Nebraska Center for Integrated Biomolecular Communication, Lincoln, NE, 68588-0304, USA

### ARTICLE INFO

#### Keywords:

Antimicrobial peptides  
NMR structural biology  
Peptide structures  
Membrane disruption  
Helical peptides  
Serum stability

### ABSTRACT

The rapid emergence of resistant bacterial strains has made the search for new antibacterial agents an endeavor of paramount importance. Cationic antimicrobial peptides (AMPs) have the ability to kill resistant pathogens while diminishing the development of resistance. Citropin 1.1 (Cit 1.1) is an AMP effective against a broad range of pathogens. 20 analogues of Cit 1.1 were prepared to understand how sequence variations lead to changes in structure and biological activity. Various analogues exhibited an increased antimicrobial activity relative to Cit 1.1. The two most promising, AMP-016 (W3F) and AMP-017 (W3F, D4R, K7R) presented a 2- to 8-fold increase in activity against MRSA (both = 4 µg/mL). AMP-017 was active against *E. coli* (4 µg/mL), *K. pneumoniae* (8 µg/mL), and *A. baumannii* (2 µg/mL). NMR studies indicated that Cit 1.1 and its analogues form a head-to-tail helical dimer in a membrane environment, which differs from a prior study by Sikorska et al. Active peptides displayed a greater tendency to form  $\alpha$ -helices and to dimerize when in contact with a negatively-charged membrane. Antimicrobial activity was observed to correlate to the overall stability of the  $\alpha$ -helix and to a positively charged N-terminus. Biologically active AMPs were shown by SEM and flow cytometry to disrupt membranes in both Gram-positive and Gram-negative bacteria through a proposed carpet mechanism. Notably, active peptides exhibited typical serum stabilities and a good selectivity for bacterial cells over mammalian cells, which supports the potential use of Cit 1.1 analogues as a novel broad-spectrum antibiotic for drug-resistant bacterial infections.

### 1. Introduction

The emergence of drug resistant bacteria has made the development of novel antibacterial agents a pressing issue [1]. In fact, most experts consider bacterial infections one of the greatest threats to human health, which may result in more than 10 million deaths worldwide by 2050 [2]. Bacterial resistance to common antibiotics occurs through a variety of mechanisms [3]. For example, the Gram-positive pathogen

methicillin resistant *Staphylococcus aureus* (MRSA) copes with antibiotic agents by increasing its membrane thickness or altering penicillin binding proteins (PBP) [4]. Gram-negative bacteria such as *Enterobacter* spp., *Escherichia coli*, *Klebsiella pneumoniae*, and *Pseudomonas aeruginosa* present resistance by virtue of a double membrane, by the development of efflux pumps, by the production of degrading enzymes, by gene transfer or by altering drug binding targets [5,6]. Antimicrobial peptides (AMPs) are an interesting option for combating resistant bacteria

**Abbreviations:** ALLOC, allyloxycarbonyl; AMP(s), antimicrobial peptide(s); CFU, colony forming unit; Cit 1.1, Citropin 1.1; CLint, *in vitro* intrinsic clearance; Dab, 2,4-diaminobutyric acid; DFQ-COSY, double quantum filtered COSY; Dpr, 2,3-diaminopropionic acid; Fmoc, fluorenylmethyloxycarbonyl; Gd-DTPA, gadolinium-diethylenetriamine pentaacetic acid; HMDS, hexamethyldisilazane; IC<sub>50</sub>, half maximal inhibitory concentration; MIC, minimum inhibitory concentration; Orn, ornithine; PMDS, polydimethylsiloxane; PSVS, protein structure validation software; Sar, sarcosine; SEM, scanning electron microscopy; TMSP, trimethylsilylpropanoic acid; TOCSY, T-Total Correlated Spectroscopy

\* Corresponding author at: Department of Chemistry, University of Nebraska – Lincoln, NE, 68588-0304, USA.

\*\* Corresponding author. Department of Pharmaceutical Sciences, University of Nebraska Medical Center – Omaha, NE, 68198-6125, USA.

E-mail addresses: [rpowers3@unl.edu](mailto:rpowers3@unl.edu) (R. Powers), [martin.condasheridan@unmc.edu](mailto:martin.condasheridan@unmc.edu) (M. Conda-Sheridan).

<sup>1</sup> Equal contribution.

<https://doi.org/10.1016/j.peptides.2019.170119>

Received 15 May 2019; Received in revised form 9 July 2019; Accepted 13 July 2019

Available online 20 July 2019

0196-9781/ © 2019 Elsevier Inc. All rights reserved.

to conventional small molecule antibiotics [7]. AMPs are capable of killing a wide range of microorganisms by membrane pore formation, or membrane disruption. In addition, AMPs can present antibacterial activity by inhibiting protein synthesis, enzymatic activity, or cell wall synthesis [8–10]. The most attractive feature of AMPs is the observation that bacteria are less likely to develop resistance to AMPs when compared to non-peptide antibiotics [11]. This stems from the fact that the fundamental structure of the membrane is not easily altered by mutations. In order to develop AMPs as antimicrobial agents it is essential to determine its mechanism of action and the structural features that give rise to their activities. This understanding is key to improving and evolving their efficacy.

Citropin 1.1 (**Cit 1.1/AMP-001**) is an AMP derived from the skin of an Australian tree frog of the *Litora* genus. **Cit 1.1** has shown intriguing activity against Gram-positive and Gram-negative species including: *Staphylococcus aureus*, *Staphylococcus epidermis*, *Enterococcus faecalis*, *Escherichia coli*, and *Klebsiella pneumonia* [12]. Conversely, studies evaluated the antifungal activity of **Cit 1.1** against *Candida* species using direct bioautography [13] and against *Candida albicans*, *Candida tropicalis* and *Candida krusei* isolated from patients with oral cavity and respiratory tract infections [14]. They found that the peptide was weekly active and less potent than amphotericin B and nystatin against clinical strains [13,14]. To our knowledge, **Cit 1.1** has not been further tested against any other fungal strains besides *Candida* spp., suggesting the antifungal potential of this peptide and its analogues can be further explored.

Previous structure-activity relationship (SAR) reports indicated that truncation of **Cit 1.1** sequence, such as deletion of Gly1, Leu2, or Phe3, completely ablated the peptide's activity. On the other hand, deletion of Gly14, Gly15, or Leu16 had no impact on **Cit 1.1** activity [15]. Tyler and co-workers suggested that the  $\alpha$ -helical conformation of **Cit 1.1** was critical to antimicrobial activity [16]. In fact, replacement of the L-amino acids with their D-isomers yielded an AMP with similar biological activity [16]. Later studies showed that if an isoAsp bond is formed between Leu5 and the carboxylic acid side chain of Asp4 biological activity is abolished while the serum stability is greatly enhanced [17]. This conformational change does not affect the total charge of **Cit 1.1** and only marginally changes the isoelectric point and hydrophobicity; however, an isoAsp bond significantly alters its secondary structure hinting to the importance of the peptide's conformation [17]. It has been additionally proposed that two  $\alpha$ -helices are formed upon contact of **Cit 1.1** with bacterial membranes [15]. Accordingly, an  $\alpha$ -helical structure for **Cit 1.1** appears to play an important role in the peptide's antimicrobial activity. It is important to note that these prior studies relied on the introduction of relatively large structural changes to investigate a relationship between amino acid composition and peptide conformation on biological activity.

In this report, we sought to develop new **Cit 1.1** analogues enhanced antimicrobial action against various pathogens. Further, we expanded upon the previous structural investigations by further characterizing the conformation and interactions of **Cit 1.1** and its analogues in a membrane mimetic environment. The membrane-bound solution structures of the **Cit 1.1** peptides were determined using nuclear magnetic resonance (NMR) spectroscopy. The mode of membrane disruption was visualized using transmission and scanning electron microscopy techniques (TEM and SEM), flow cytometry and confocal microscopy. The toxicity of the most potent AMP was studied *in vitro* against mammalian and human red blood cells. Poor serum stability of peptide-based antimicrobials is another factor limiting the use of AMPs and, therefore, we have also studied the serum stability of **Cit 1.1** and its analogues. The experimental data has enabled us to define a mechanism of action for **Cit 1.1**, to describe the structural arrangement of the peptide when in contact with membranes, and to understand the impact of subtle molecular and conformational changes on peptide activity.

**Table 1**  
Antimicrobial activities of **Cit 1.1 (AMP-001)** and AMP analogs.

Minimal inhibitory concentration (MIC) $\mu\text{g/mL}$				
Peptide sequence	Peptide code	Sa <sup>a</sup>	Ec <sup>b</sup>	LogP <sup>c</sup>
GLFDVIKKVASVIGGL	AMP-001/ Cit 1.1	32	32	−3.60
SarLFDVIKKVASVIGGL	AMP-002	32	64	−3.17
AcGLFDVIKKVASVIGGL	AMP-003	$\geq 256$	$\geq 256$	−3.78
(CH <sub>3</sub> ) <sub>3</sub> GLFDVIKKVASVIGGL	AMP-004	$\geq 256$	$\geq 256$	−6.14
Hydrazine-LFDVIKKVASVIGGL	AMP-005	$\geq 256$	$\geq 256$	−2.50
GLFDVI(Orn)(Orn)VASVIGGL	AMP-006	> 32 <sup>d</sup>	32	−4.49
GLFDVI(Dab)(Dab)VASVIGGL	AMP-007	> 32	32	−5.52
GLFDVI(Dpr)(Dpr)VASVIGGL	AMP-008	> 32	64	−5.64
GLFDVI(Cit)KVASVIGGL	AMP-009	128	256	−4.56
(CH <sub>3</sub> ) <sub>3</sub> GLFDVIK(CH <sub>3</sub> ) <sub>3</sub> K (CH <sub>3</sub> ) <sub>3</sub> VASVIGGL	AMP-010	$\geq 256$	$\geq 256$	−13.64
GLFDVIK(CH <sub>3</sub> ) <sub>3</sub> K(CH <sub>3</sub> ) <sub>3</sub> VASVIGGL	AMP-011	$\geq 256$	$\geq 256$	−10.29
GLFDVIRRVASVIGGL	AMP-012	16	32	−5.16
GLFDVIRKVASVIGGL	AMP-013	16	> 32	−4.38
GLFDVIKKGVASVIGGL	AMP-014	$\geq 256$	64	−4.71
GLFEVIKKVASVIGGL	AMP-015	> 32 <sup>d</sup>	> 32	−3.31
GLWDVIKKVASVIGGL	AMP-016	8	16	−3.50
GLWRVIRKVASVIGGL	AMP-017	16	32	−4.55
PhenylGlyLWDVIRKVASVIGGL	AMP-018	16	> 32	−2.34
GL(Biphenylalanine)DVIKKVASVIGGL	AMP-019	8	32	−1.85
GL(1-Nap)DVIKKVASVIGGL	AMP-020	8	64	−2.61
SarLWDVIRKVASVIGGL	AMP-021	Ne	Ne	−3.85

<sup>a</sup> *Staphylococcus aureus* JE2 MRSA.

<sup>b</sup> *Escherichia coli* K12.

<sup>c</sup> Calculated from MarvinSketch Version 14.9.

<sup>d</sup> 64.

## 2. Results

### 2.1. Minimum inhibitory concentration (MIC assay)

**Cit 1.1** analogues were prepared using solid phase peptide synthesis (SPPS). **Table 1** shows the amino acid sequence of the synthesized peptides and the observed MIC values against *S. aureus* JE2 (MRSA) and *E. coli* K12 (see **Experimental S5** for detailed procedures). **Cit 1.1 (AMP-001)** displayed activity against MRSA (32  $\mu\text{g/mL}$ ) and *E. coli* (32  $\mu\text{g/mL}$ ) corroborating findings from previous studies (**Table 1**) [16,18,19]. **Cit 1.1**, however, did not demonstrate any activity against *Acinetobacter baumannii*, *Candida albicans* or *Cryptococcus neoformans* (**Table 2**). **AMP-002** with a methyl glycine (sarcosine, Sar1) substituent retained activity against *S. aureus* (32  $\mu\text{g/mL}$ ) but exhibited diminished activity against *E. coli* (64  $\mu\text{g/mL}$ ). The acetylation (**AMP-003**), the methylation to yield the quaternary ammonium analogue (**AMP-004**), or substitution by a hydrazine group (**AMP-005**) at the N-termini of **Cit 1.1** eliminated antibacterial activity (MIC  $\geq 256$   $\mu\text{g/mL}$ ).

Replacing the Lys residues (Lys7, Lys8) with ornithine (Orn), 2,4-diaminobutyric acid (Dab), or 2,3-diaminopropionic acid (Dpr) yielded analogues **AMP-006**, **AMP-007** and **AMP-008**, respectively. These changes diminished the potency against Gram-positive pathogen when compared to **Cit 1.1** (**Table 1**). The peptides displayed equal (**AMP-006** and **AMP-007**, 32  $\mu\text{g/mL}$ ) or reduced antibacterial action (**AMP-008**, > 32  $\mu\text{g/mL}$ ) against Gram-negative bacteria. On the **AMP-009** analogue Lys7 was replaced with citrulline, which substitution resulted in a lack of antibacterial activity. **AMP-010** was synthesized by methylating all of the available **Cit 1.1** amine groups, whereas **AMP-011** was generated by methylating the Lys amine moieties to produce analogues with a resident positive charge. Both **AMP-010** and **AMP-011** exhibited a complete lack of antibacterial activity. **AMP-012** was constructed by replacing Lys7 and Lys8 with arginine residues, while the **AMP-013** analogue was prepared by only substituting Lys7 for an arginine. The MICs for both **AMP-012** and **AMP-013** decreased 2-fold against the MRSA strains (16  $\mu\text{g/mL}$ ) while the activity against Gram-

**Table 2**  
Additional antimicrobial activities of Cit 1.1 (AMP-001) and selected AMP analogs.

Minimal inhibitory concentration (MIC) $\mu\text{g/mL}$								
Peptide sequence	Peptide code	Sa <sup>a</sup>	Ec <sup>b</sup>	Pa <sup>c</sup>	Kp <sup>d</sup>	Ab <sup>e</sup>	Ca <sup>f</sup>	Cn <sup>g</sup>
GLFDVIKKVASVIGGL	AMP-001/Cit 1.1	32	> 32	> 32	> 32	32	> 32	16
GLFDVI(Orn)(Orn)VASVIGGL	AMP-006	32	> 32	> 32	> 32	> 32	> 32	32
GLFDVIRRVASVIGGL	AMP-012	16	32	> 32	> 32	32	16	16
GLFDVIRKVASVIGGL	AMP-013	16	> 32	> 32	> 32	32	> 32	16
GLFEVIKKVASVIGGL	AMP-015	32	> 32	> 32	> 32	> 32	> 32	16
GLWDVIKKVASVIGGL	AMP-016	4	> 32	> 32	> 32	16	32	8
GLWRVIRKVASVIGGL	AMP-017	4	4	> 32	8	2	32	2
PhenylGlyLWDVIRKVASVIGGL	AMP-018	8	> 32	> 32	> 32	32	32	8
GL(Biphenylalanine)DVIRKVASVIGGL	AMP-019	4	32	> 32	> 32	16	32	> 32
GL(1-Nap)DVIRKVASVIGGL	AMP-020	4	32	> 32	> 32	16	32	> 32
SarLWDVIRKVASVIGGL	AMP-021	8	16	> 32	32	4	32	16

<sup>a</sup> *Staphylococcus aureus* ATCC 43300 MRSA.

<sup>b</sup> *Escherichia coli* ATCC 25922.

<sup>c</sup> *Pseudomonas aeruginosa* ATCC 27853.

<sup>d</sup> *Klebsiella pneumoniae* ATCC 700603.

<sup>e</sup> *Acinetobacter baumannii* ATCC 19606.

<sup>f</sup> *Candida albicans* ATCC 90028.

<sup>g</sup> *Cryptococcus neoformans* var. *grubii* H99 ATCC 20882.

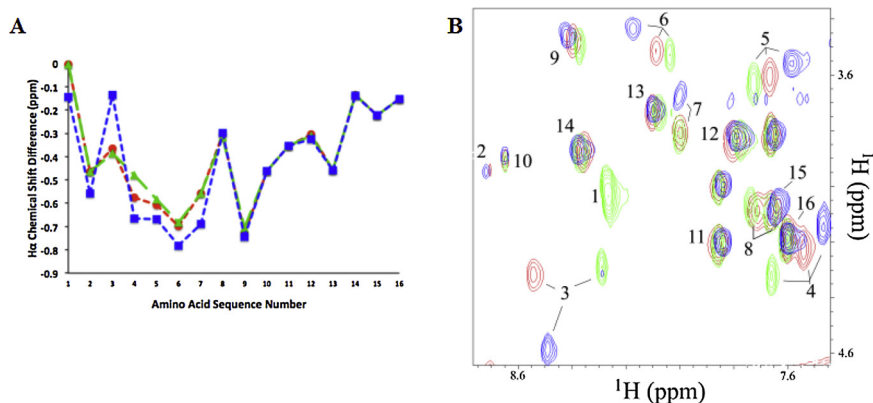


**Fig. 1.** (A) Plot showing the H $\alpha$  deviations (ppm) from statistical-coil chemical shifts. Amino acids are numbered according to their sequence in Cit 1.1 (red), AMP-003 (green), and AMP-016 (blue). (B) TOCSY H $\alpha$  region for Cit 1.1 (red), AMP-003 (green), and AMP-016 (blue). Peaks are labeled according to their respective amino acid position.

negative organisms was retained or diminished (MIC > 32  $\mu\text{g/mL}$ ) when compared to Cit 1.1 (Table 1 and 2). Interestingly, AMP-012 and AMP-013 exhibited antifungal activity with a MIC of 16  $\mu\text{g/mL}$  against *C. neoformans* while AMP-012 displayed MIC of 16  $\mu\text{g/mL}$  against *Candida albicans* (Table 2). A glycine residue was then inserted following Lys 8, in order to alter the relative position of potentially key  $\alpha$ -helical residues. AMP-014 was observed to be inactive against the tested bacterial strains. The AMP-015 analogue was designed with a modest substitution of Asp4 for Glu. Surprisingly, AMP-015 was inactive against all bacterial strains tested (MIC > 32  $\mu\text{g/mL}$ ) but inhibited the growth of *C. neoformans* with a MIC of 16  $\mu\text{g/mL}$ .

The AMP-016 analogue was constructed by replacing Phe3 with Trp, which yielded an AMP with improved antibacterial activity against MRSA with MIC values of 8  $\mu\text{g/mL}$  and 4  $\mu\text{g/mL}$  for *S aureus* JE2 and *S aureus* ATCC 43300, respectively. AMP-016 also exhibited a better antibacterial activity against *E. coli* K12 with an MIC value of 16  $\mu\text{g/mL}$ . AMP-016 did not demonstrate antibacterial activity against *K. pneumoniae* or *P. aeruginosa*, but it was active against *A. baumannii* (16  $\mu\text{g/mL}$ ), *C. albicans* (32  $\mu\text{g/mL}$ ) and *C. neoformans* (8  $\mu\text{g/mL}$ ). The Asp4 and Lys7 residues were changed to Arg in the AMP-017 analogue, producing the most potent analogue of the series which was effective against MRSA and *E. coli* (MIC 4  $\mu\text{g/mL}$ ), *K. pneumoniae* (MIC 8  $\mu\text{g/mL}$ ) *A. baumannii* (MIC 2  $\mu\text{g/mL}$ ). AMP-017 was also active against fungi with a MIC of 2  $\mu\text{g/mL}$  against *C. neoformans*. Replacement of Gly1 with PhenylGly (AMP-018), Phe3 with a biphenylalanine residue (AMP-019), or 1-Naphyl (AMP-020) resulted in AMPs with improved

antimicrobial activity against bacteria and fungi, when compared with the lead compound. For example, the MIC against MRSA was between 4–8  $\mu\text{g/mL}$ . AMP-019 and AMP-020 were also active against the dangerous *A. baumannii* with MIC = 16  $\mu\text{g/mL}$ . Gly1 was replaced with Sar to yield the AMP-021 analog, which presented promising MIC values against MRSA (8  $\mu\text{g/mL}$ ), *E. coli* (16  $\mu\text{g/mL}$ ), *A. baumannii* (4  $\mu\text{g/mL}$ ) and *C. neoformans* (16  $\mu\text{g/mL}$ ).

## 2.2. NMR spectroscopy

Negatively charged sodium dodecyl sulfate (SDS) micelles, which mimics the charge of Gram-positive bacterial membranes, were therefore chosen as a model for the structural elucidation of Cit 1.1, AMP-003, and AMP-016 peptides by NMR [20]. Standard two-dimensional (2D) TOCSY and NOESY datasets were collected for backbone and side-chain resonance assignments [21]. NMR assignments for Cit 1.1, AMP-003, and AMP-016 were nearly complete with 94% HN, 100% H $\alpha$ , 100% H $\beta$ , 88% H $\gamma$ , 90–100% H $\delta$ , 60–100% H $\epsilon$ , 0–33% H $\zeta$ , and 100% H $\eta$  of the assignments made (Table S7). Fig. 1A shows the H $\alpha$  chemical shift deviations from statistical-coil values for the three peptides bound to SDS micelles [22,23]. The three peptides showed negative chemical shift differences across the entirety of the sequence, which is strongly suggestive of an  $\alpha$ -helical conformation along the SDS micelle. Chemical shift differences between the Cit 1.1, AMP-003, and AMP-016 peptides were more apparent when HN chemical shifts were included. This is illustrated by an overlay of the H $\alpha$  region of the 2D TOCSY

spectra for the three peptides as shown in (Fig. 1B). Major chemical shifts changes were observed for residues 3 to 7, which are consistent with the H $\alpha$  chemical shift changes plotted in Fig. 1A. In order to reinforce this observation, we performed circular dichroism (CD) studies. It was found the AMPs, presented  $\alpha$ -helical character (with some random coils) in aqueous media (Fig. S6). The secondary structure of AMP-016 was also studied after 1 h incubation with *E. coli* and the data showed the conformation was retained upon interaction with the bacteria membrane (Fig. S7).

The NMR structures for the Cit 1.1, AMP-003, and AMP-016 peptides in SDS micelles were determined to further elucidate the role that structure plays in antimicrobial activity. The structural statistics for the three peptides (Table S8) indicates that the experimental data agrees well with the calculated structures. Backbone RMSDs for each of the peptides was 0.3 Å, 0.7 Å, and 0.4 Å for Cit 1.1, AMP-003, and AMP-016, respectively. The structures did not contain any NOE violations > 0.5 Å or dihedral angle violations > 5°. The high quality of the NMR structures is also evident by the PROCHECK z-scores of -0.3, -0.95, and -0.47 for Cit 1.1, AMP-003, and AMP-016, respectively [24]. Further, 92–94% of all residues are located in the most favored region of the Ramachandran plot. An overlay of the water refined 20 lowest energy NMR structures for the Cit 1.1, AMP-003, and AMP-016 peptides are shown in Fig. 2A–C.

The resulting NMR structures indicate that the Cit 1.1, AMP-003, and AMP-016 peptides adopt a head to tail helical dimer (Fig. 2D–F). The head to tail orientation of the peptides was confirmed by the presence of NOEs from Leu2 of strand A to Ile13/Leu16 of strand B. These long-range structural restraints are only possible for a head to tail dimer. Of particular note, a significant number of NOEs exist at the N-terminus (Fig. 2G, H), which is consistent with the presence of both an

$\alpha$ - and  $3_{10}$ -helix for the biologically active peptides (Cit 1.1 and AMP-016). It is possible that the peptides adopt both conformations (or are in equilibrium) when bound to a SDS micelle. In this case, the NMR structure would simply represent an overall average of the conformational exchange. Importantly, the inactive AMP-003 lacks a similar NOE pattern (and number of NOEs) at the N-terminus and, thus, it exclusively adopts an  $\alpha$ -helical structure (Fig. 2I). Since the only difference between Cit 1.1 and AMP-003 is the N-terminal acetylation, this clear difference in helix composition between the peptides is due to the acetylation.

Amide proton temperature titrations up to 70 °C were performed on the three peptides to characterize helical stability (Figs. S9–11). The titration data was binned according to the relative magnitude of the HN chemical shift changes ( $\Delta^{\text{HN}}$ ): minor (0 to -0.05, yellow), intermediate (-0.05 to -0.25, orange), and major (-0.25 to -0.45, red). The peptide ribbon diagrams in Fig. 2D–F are colored based on these HN chemical shift changes in order to qualitatively assess the thermal stability of the helices. Amino acid residues exhibiting major chemical shift changes upon heating are transitioning from a stable and structurally-ordered state to a disordered and unstructured state. Conversely, residues with relatively unchanged chemical shifts are likely already in a transiently disordered state at room temperature.

Next the peptides were titrated with gadolinium-diethylenetriamine pentaacetic acid (Gd-DTPA) and monitored by NMR to identify the solvent exposed residues while the peptide was bound to SDS micelles (Figs. S12–14). The addition of a paramagnetic species will reduce the NMR signal intensity for residues in contact with the solvent proportionally to the amount of the added paramagnetic species. Upon the addition of Gd-DTPA, the majority of the amino acids exhibited an approximate linear decrease in peak intensity regardless of location in

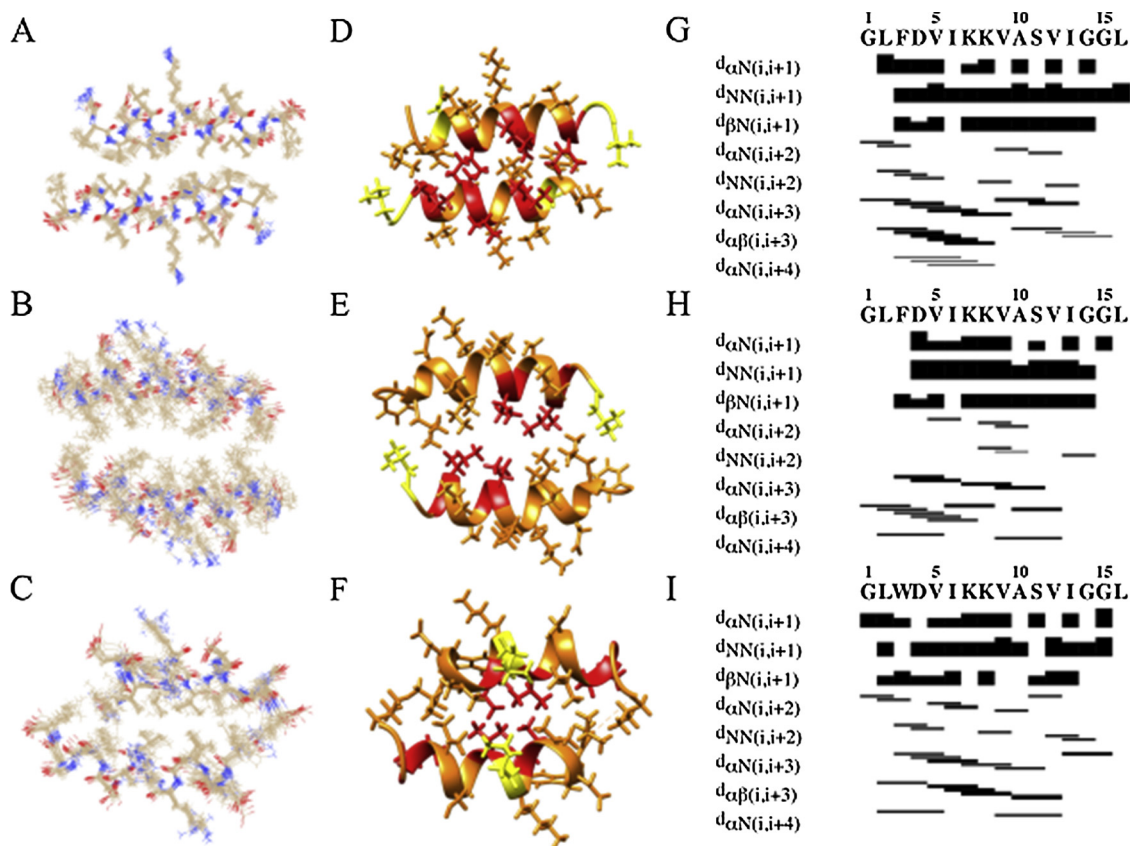


**Fig. 2.** The ensemble of the lowest energy, water refined structures of (A) Cit 1.1, (B) AMP-003, and (C) AMP-016. Peptide ribbon structures for (D) Cit 1.1, (E) AMP-003, and (F) AMP-016 are colored by the binned amide proton temperature titration data according to the  $\Delta\text{H}$  ranges 0 to -0.05 (minor chemical shift, yellow), -0.05 to -0.25 (intermediate chemical shift, orange), and -0.25 to -0.45 (major chemical shift, red). NOE connectivity plots for (G) Cit 1.1, (H) AMP-003, and (I) AMP-016. Weights of the connectivities are normalized to the NOE intensities.

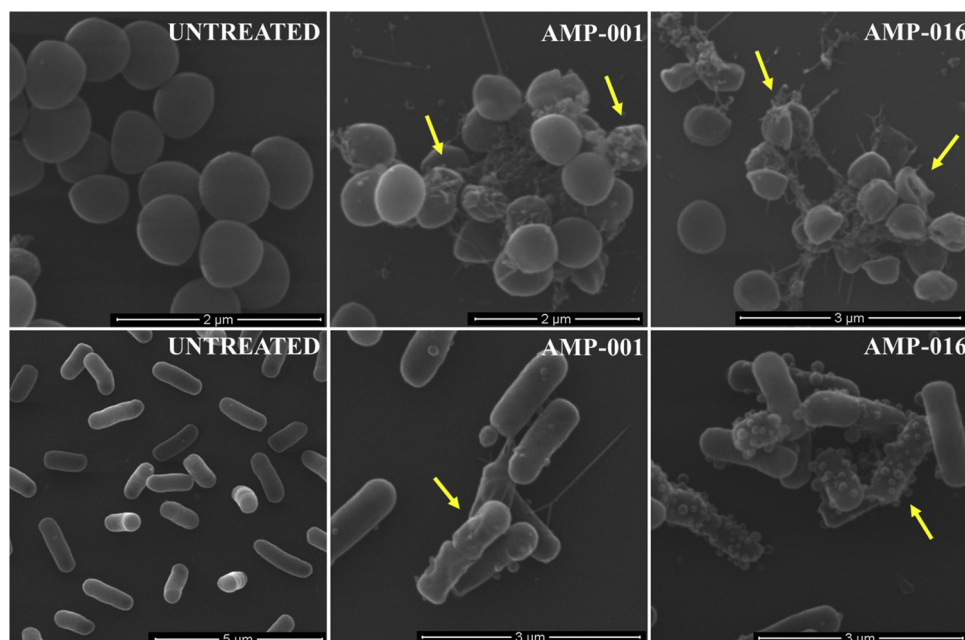


**Fig. 3.** SEM micrographs of *S. aureus* JE2 MRSA (top row) and *E. coli* K12 (bottom row) cells treated with either Cit 1.1 or AMP-016 at twice the MIC reported in Table 2.

the dimer structure. This is most likely due to multiple binding sites for Gd-DTPA on each peptide, an aggregation of the peptides along the surfaces of the micelles, and a dynamic association/dissociation of the dimer [25]. Leu2 in Cit 1.1 and AMP-016 was an exception to this general observation. The NMR peak intensity for Leu2 increased, at first, with the addition of Gd-DTPA. Of note, the peak intensity for Leu2 was relatively weak compared to the other residues (Fig. 1B), which is suggestive of a high exchange rate and/or a transiently disordered structure.

### 2.3. Scanning electron microscopy (SEM)

*S. aureus* JE2 and *E. coli* K12 cells were treated for 1 h with Cit 1.1 or AMP-016 at 2X MIC values. As clearly evident from the SEM images, AMP treatment led to membrane disruption accompanied by cytoplasmic leakage, deep holes and severe membrane deformations (Fig. 3). These morphological changes indicate that the AMPs kill bacteria by disrupting cell membranes, although the results do not exclude additional mechanisms of action. Please note the SEM micrographs present some differences between *S. aureus* and *E. coli*, which may suggest a different mechanism of action for AMP antimicrobial activity between Gram-positive and Gram-negative organisms. In the case of *S. aureus*, holes and cytoplasm release were observed. Conversely, membrane solubilization due to a mixed peptide/phospholipid vesicle formation (budding) with subsequent membrane thinning leading to only a small amount of cytoplasm release was observed for *E. coli*.

### 2.4. Propidium iodide (PI) uptake and flow cytometry

A PI uptake assay was performed to confirm the ability of AMPs to disrupt bacterial cell membranes. *S. aureus* JE2 and *E. coli* K12 cells were treated with Cit 1.1 or AMP-016 at 2X MIC values. The PI fluorescence intensity was measured relative to Polymyxin B (PMB) as a reference. Cit 1.1 and AMP-016 showed high PI uptake relative to controls (Fig. 4), further suggesting that bacterial cell death is associated with membrane damage, since PI can only cross damaged cell membranes. The cell membrane disruption of *S. aureus* JE2 and *E. coli* K12 was further evaluated with flow cytometry. Untreated (no AMPs)

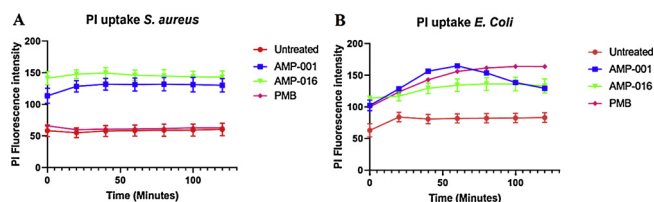


**Fig. 4.** PI uptake of AMPs. *S. aureus* JE 2 (A) and *E. coli* K12 (B) cells ( $1 \times 10^7$  CFU) were untreated, treated with AMPs (2xMIC) or treated with Polymyxin B (PMB, 16  $\mu$ g/mL) for 120 min. The PI fluorescence intensity was then measured at 20 min intervals for a total of 120 min. PMB is known to kill Gram-negative bacteria by disrupting cell membrane and was used as a positive control.

and treatment with 70% EtOH were used as negative and positive controls, respectively (Experimental S15 and Fig. S16). After 1 h treatment with either Cit 1.1 or AMP-016 at 2X MIC values, *S. aureus* cells showed an increased uptake, when compared to control, of 9.4% or 12.5%, respectively (Fig. S16). Similarly, *E. coli* cells treated with either Cit 1.1 or AMP-016 exhibited cell viability of 13.9% or 27.5%, respectively.

### 2.5. In vitro serum stability

Serum stability was assessed by incubating the peptides in human serum for over two hours followed by quantitation using LC-MS/MS. AMP-002 and -006 displayed the highest serum stability. Approximately 60%–80% of the peptides remained in the serum after 2 h. Cit 1.1, -012, -013, and -016 displayed similar stabilities with only 40–50% of the peptide remaining in the serum after 2 h (Fig. 5).

### 2.6. Cytotoxicity

The cytotoxicity of the active AMPs against human embryonic kidney cells (ATCC CRL-1573) was performed using a resazurin test and the  $IC_{50}$  values were determined from dose response curves. The hemolytic activity was determined against human red blood cells and the  $HC_{50}$  values (concentration at 50% hemolysis) were calculated by curve fitting of the inhibition values versus  $\log(\text{concentration})$ . The  $IC_{50}$  and  $HC_{50}$  values are summarized in Table 3. In general, the AMPs showed

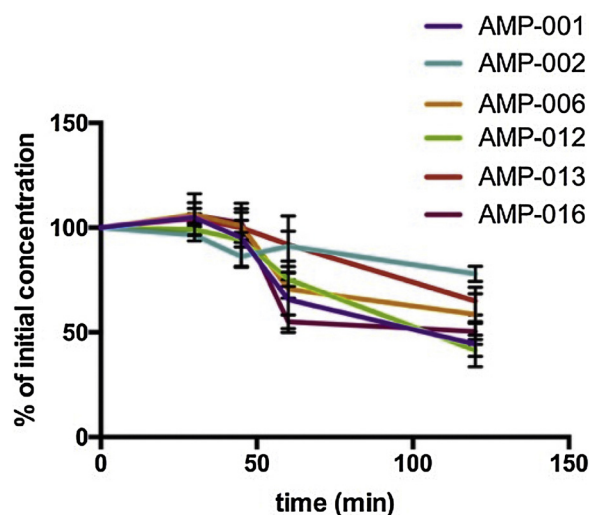


Fig. 5. Stability of Cit 1.1 and the AMP Analogues in Human Serum studied by LC-MS. AMP serum concentrations are normalized to initial concentrations (0 min, 100% AMP). The data is plotted as mean  $\pm$  SD from triplicate measurements.

Table 3  
AMP cytotoxicity and hemolytic activity.

Peptide sequence	Peptide code	IC <sub>50</sub> ( $\mu$ g/ mL) HEK- 293 <sup>a</sup>	HC <sub>50</sub> ( $\mu$ g/mL) Human red blood cells
GLFDVIKKVASVIGGL	AMP-001/ Cit 1.1	20.98	> 32
GLFDVI(Orn)(Orn)VASVIGGL	AMP-006	> 32	> 32
GLFDVIRRVASVIGGL	AMP-012	17.64	18.2
GLFDVIRKVASVIGGL	AMP-013	21.26	> 32
GLFEVIKKVASVIGGL	AMP-015	> 32	> 32
GLWDVIKKVASVIGGL	AMP-016	> 32	16.85
GLWRVIRKVASVIGGL	AMP-017	18.10	26.7
PhenylGlyLWDVIRKVASVIGGL	AMP-018	19.44	> 32
GL(Biphenylalanine)DVIKKVASVIGGL	AMP-019	17.04	> 32
GL(1-Nap)DVIKKVASVIGGL	AMP-020	16.85	> 32
SarLWDVIRKVASVIGGL	AMP-021	30.90	> 32

<sup>a</sup> Human embryonic kidney cells (ATCC CRL-1573). Assays were performed by The Community for Antimicrobial Drug Discovery (CO-ADD), Australia.

IC<sub>50</sub> values between 6.8 and 30.9  $\mu$ g/mL. AMP-012, AMP-016 and AMP-017 were exceptions and displayed IC<sub>50</sub> values higher than 32  $\mu$ g/mL. In addition, most of the AMPs exhibited low hemolytic activity with HC<sub>50</sub> values greater than 32  $\mu$ g/mL. AMP-006, AMP-015 and AMP-016 were exceptions and displayed lower HC<sub>50</sub> values corresponding to 18.2  $\mu$ g/mL, 16.8  $\mu$ g/mL and 26.7  $\mu$ g/mL, respectively.

### 3. Discussion

#### 3.1. Antimicrobial activity

We have rationally designed analogues of the AMP Cit 1.1 to understand the contribution of sequence and structure to its antibacterial activity. The N-terminus of AMPs tend to be polar or ionic, which is likely to play a key role in membrane interactions [11]. In the AMP-002 analogue Gly1 was replaced with a methyl glycine. This change should increase serum stability [26] and the lipophilicity at the N-terminus. The compound exhibited comparable activity to Cit 1.1 against *S. aureus* JE2, but was half as potent against *E. coli* K12, which suggests multiple H-bond donors may be needed at the N-terminus of AMPs for full activity. This is consistent with the results obtained with the AMP-003 analog, which is acetylated at the N-terminus. Acetylation of amines

alters the pK<sub>a</sub> (preventing protonation) and the isoelectric point while also reducing the net charge of the peptide [27].

To further investigate the importance of the primary amine on Cit 1.1 activity, the N-terminus was converted into a quaternary amine (AMP-004). This was based on the notion that resident positive charges aid antibacterial activity [28,29]. This modification was expected to have two distinct impacts on Cit 1.1 because: (1) a permanent positive charge is pH-independent, but cannot form a hydrogen bond; (2) the quaternary amine makes the AMP more resistant to proteolysis, which increases its bioavailability [30]. Unexpectedly, AMP-004 was observed to be inactive against *S. aureus* and *E. coli*, indicating that a positive charge on the N-terminal amine is not enough to interact with bacterial membrane. This suggests a role of H-bonding; either an interaction within the peptide (as suggested by others) or an association with the bacteria that is important for activity. Similarly, replacing Gly1 with a hydrazine group resulted in the loss of antibacterial activity for AMP-005. Hydrazines have a lower pK<sub>a</sub> (~8.3) than amines (~9.6), a value that should be further lowered by the neighboring electron-withdrawing group [31,32]. As a result, the hydrazine nitrogen may not be protonated (note that the alkylated nitrogen is the most likely site of protonation [33]) under the conditions of the MIC assay. Furthermore, it is possible that an internal hydrogen bond may form between the hydrogen on the hydrazine and the amide carbonyl. In addition to preventing a hydrogen bond with the bacterial membrane, this internal hydrogen bond may also affect the overall peptide structure and alter its biological activity. The inactive AMP-003, AMP-004 and AMP-005 analogues clearly emphasize the importance of the N-terminus in AMP activity and the potential critical role that hydrogen bond donors and acceptors play in the interaction with the bacterial membrane. It is important to note that although our NMR data clearly established different NOE patterns at the N-terminus between the active and inactive peptides, the presence of NOEs do not necessarily confirm the presence or absence of a hydrogen bond. Therefore, the speculation on intramolecular hydrogen bond formation in the AMPs and at the membrane interface is primarily based upon the chemical structures of the N-terminal modifications.

AMPs usually contain two or more cationic side chains such as Lys and Arg, allowing for a potential electrostatic interaction with the bacterial membrane. Accordingly, several modifications to Cit 1.1 were made to evaluate the role of these charged residues to antibacterial activity. Lys7 and Lys8 were replaced with progressively shorter amine bearing sidechains: Orn, Dab, and Dpr. This change was intended to diminish lipophilicity while instructing us of the role of charge projection within the  $\alpha$ -helix. Replacing with Orn (AMP-006) resulted in diminished activity against MRSA JE2 while the inclusion of Dab (AMP-007) and Dpr (AMP-008) abolished the antibacterial against most of the tested pathogens. These findings suggest the longer side chain of Lys is necessary for membrane interaction and the antibacterial activity of Cit 1.1. Another possibility is that there is an optimal hydrophobic index as a decrease in  $-\text{CH}_2$  units, results in lower hydrophobicity as seen by the LogP values (Table 1) of -4.49, -5.52, -5.64, and -3.60 for Orn, Dap, Dpr and Cit 1.1. Nevertheless, a direct correlation between LogP values and antibacterial activities was not observed across the series. Indicating antibacterial activities is dependent on a combination of multiple factors.

The Lys residues were methylated to explore the relative contribution of electrostatic interactions and hydrogen bonds to biological activity. Unexpectedly, and despite having a permanent +3 charge, both AMP-010 and AMP-011 were found to be inactive. This result implies a H-bond donor is key to the biological activity of Cit 1.1 and its analogs.

Arginine-rich peptides have also been shown to exhibit potent antibacterial activity [34,35]. In fact, a number of studies have indicated that an increase in arginine versus lysine content results in higher antimicrobial action [36,37]. To investigate this, a Cit 1.1 analogue (AMP-012) was constructed where Lys7 and Lys8 were replaced with an arginine. An AMP-013 analogue was also prepared that only

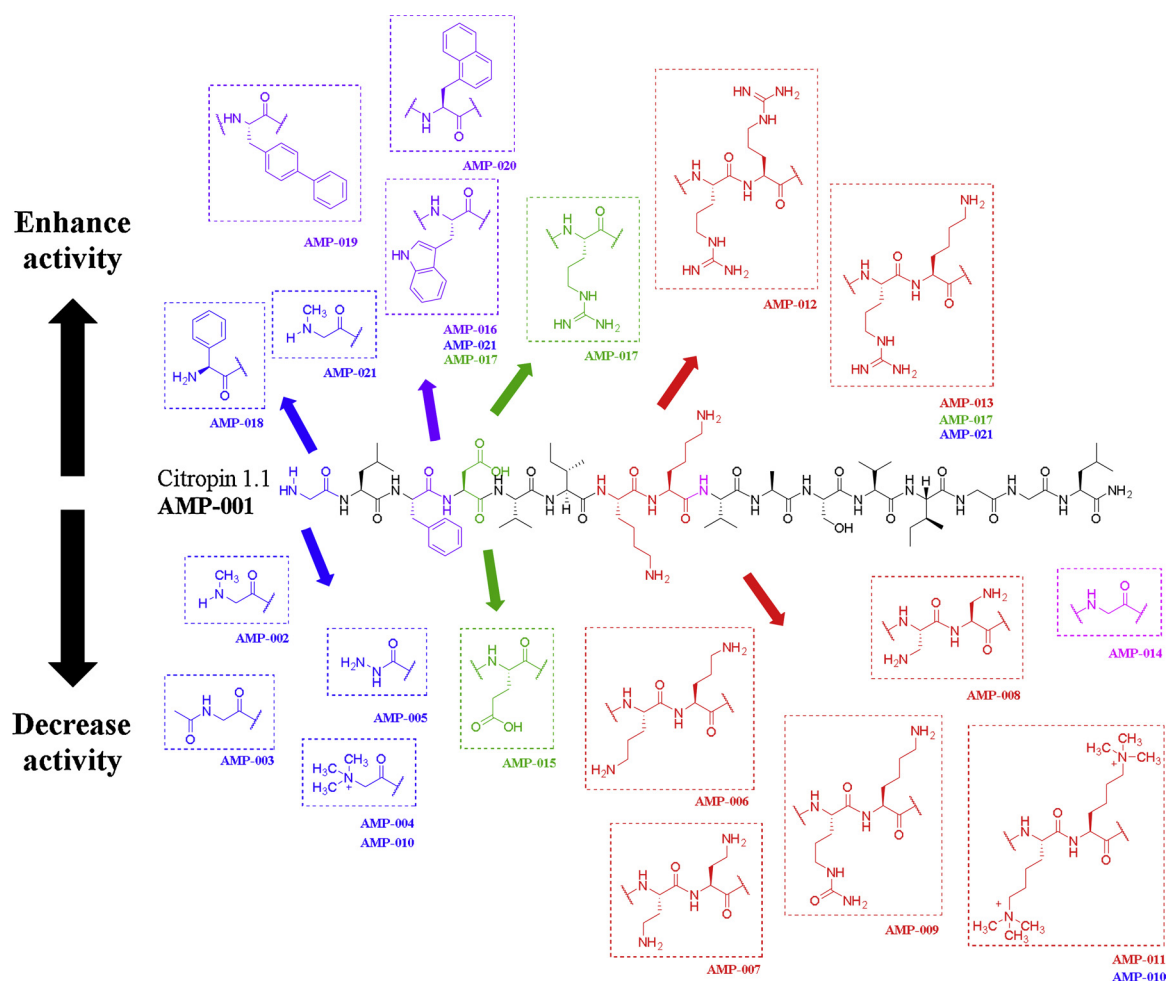


Fig. 6. Summary of the Cit 1.1 SAR.

replaced Lys7 with an arginine. The MICs for both **AMP-012** and **AMP-013** decreased 2-fold against *S. aureus* to 16  $\mu\text{g}/\text{mL}$ . The increase in antimicrobial activity may be explained by an enhanced translocation of peptides within the *S. aureus* cells [38,39]. However, the **AMP-012** and **AMP-013** displayed diminished activity against most of the Gram-negative organisms tested. Interestingly, **AMP-012** exhibited antifungal activity against both *C. albicans* and *C. neoformans* (16  $\mu\text{g}/\text{mL}$ ). To further explore the importance of cationic residues on activity, citrulline a structural mimic of arginine containing a urea functional group instead of the charged guanidium group was constructed (**AMP-009**). This substitution resulted in a complete lack of antibacterial activity, further establishing the importance of a charged H-bonding donor at position 7 (the citrulline urea group is capable of forming a hydrogen bond but its side chain is uncharged). The citrulline substitution reduces the net charge of **AMP-009**, which suggests the net charge of the peptide also contributes to the antimicrobial activity of AMPs.

Previous studies have shown that **Cit 1.1** adopts an  $\alpha$ -helical conformation, but there has also been some conflicting evidence about the exact details of the **Cit 1.1** structure [15]. Instead of a single  $\alpha$ -helical chain, two helices have been suggested for the **Cit 1.1** structure [15]. To address this possibility, a glycine residue was inserted into the **Cit 1.1** sequence following Lys8 to create the **AMP-014** analog. The insertion of Gly9 was expected to provide added flexibility to the peptide [40,41] and potentially enhance its activity if the two-helix model was correct. **AMP-014** was observed to be inactive against all the bacterial strains tested and suggests the two-helix model for **Cit 1.1** may be incorrect. If the **Cit 1.1** structure is comprised of two  $\alpha$ -helices separated by a flexible link, then the inserted Gly may allow enough mobility for

the correct surface of the  $\alpha$ -helices to interact with the membrane. Nevertheless, it is important to note the Gly insertion lengthens the peptide and shifts the sequence beyond Lys8 affecting the charge distribution at the **Cit 1.1** surface. Thus, the loss in activity may also be explained by a change in the position of the hydrophobic and charged residues.

The **AMP-015** analog, which contains a Glu for Asp4 substitution, was also inactive. Others have suggested a potential H-bond between the *N*-terminus and residue 4 [16]. This change may affect such interaction but no change in activity was observed. **AMP-016** was constructed by replacing Phe3 with Trp. Tryptophan-rich peptides have been shown to enhance the activity of AMPs presumable due to a larger hydrophobic area [34,42] and the insertion of Trp residues at the membrane-water interface [41]. The **AMP-016** analogue exhibited a 4-fold and 2-fold increase in activity against *S. aureus* and *E. coli*, respectively. In addition, **AMP-016** was active against *C. neoformans* (8  $\mu\text{g}/\text{mL}$ ). Thus, we think the indole ring in tryptophan is likely acting as a better anchor to the bacterial membranes than the smaller phenyl ring [42].

**AMP-017**, **AMP-018** and **AMP-21** were designed to maintain the increased antimicrobial activity resulting from the inclusion of Trp at position 3, while investigating the impact of other amino acid substitutions at different positions. **AMP-017** (Asp4 and Lys7 were replaced by Arg) showed an increase in activity against *E. coli*, *K. pneumoniae*, *A. baumannii* and *C. neoformans* when compared with **Cit 1.1** or **AMP-016**. However, replacing Gly1 with PhenylGly and Lys7 with Arg (**AMP-018**) dramatically decreased the activity of **AMP-017** against bacteria (still, this compound was better than **Cit 1.1**). **AMP-021**,

where Gly1 was replaced by Sar and Lys7 by Arg, showed a slight decrease in activity against Gram-negative strains that **AMP-017**. However, the molecule had better activity than **Cit 1.1** or **AMP-018**. This results indicate the key role of Trp3 or Arg4 on activity.

We also replaced Phe3 with other aromatic amino acids; biphenylalanine or naphthylalanine (**AMP-019** and **AMP-020**). These replacements maintained the activity observed with **AMP-016** against *S. aureus*, while reducing activity against Gram-negative bacteria and fungi. The analogue was slightly more potent than **Cit 1.1**. These finding may also be correlated to the increasing hydrophobicity (LogP -1.85, -2.61, and -3.60 for **AMP-019**, **AMP-020** and **Cit 1.1**, respectively) which may facilitate the peptide insertion into the bacteria membrane. **Fig. 6** summarizes the structure-activity relationship for the series of AMP analogs.

### 3.2. NMR spectroscopy

**Cit 1.1**, **AMP-003**, and **-016** were analyzed by NMR to elucidate the relationship between structure and antimicrobial activity. Interestingly, **Fig. 1A** indicates that the largest *Ha* chemical shift difference between the three peptides occurs at the *N*-terminus between residues Asp3 and Lys7. Although the dissimilarity between **AMP-016** and **Cit 1.1/AMP-003** can be attributed to the tryptophan substitution at position 3, the minor deviation of Asp4 is likely a result of the acetylation of the *N*-terminus. In the case of **AMP-016**, the steric and electronic effects from the indole side chain at position 3 may lead to a significant decrease in helicity. *N*-terminal acetylation does not induce any significant effect on the overall helicity of **AMP-003** except for a slight decrease at Asp4. The removal of the charged *N*-terminus changes the polarity or the hydrogen-bond network around Asp4, which contributes to a decrease in helicity. **Fig. 1B** shows the overlay of the *Ha* region of the 2D TOCSY for the three peptides. The significant chemical shift differences of the *N*-terminal residues highlight a changing local environment for residues 3 to 7 that is likely a result of minor alterations in the structure of the three peptides. Accordingly, these subtle changes in the peptide's structure may be directly related to differences in antimicrobial activity.

Our NMR derived structures for **Cit 1.1**, **AMP-003**, and **-016** differ from the previous results of Sikorska et al. that describe the presence of two helices within **Cit 1.1** structure [15]. Experimentally determined NOEs were found along the full length of each of the peptides (**Fig. 2G–I**) and between the helices in a dimer orientation. Although the **Cit 1.1**, **AMP-003**, and **AMP-016** dimers are not completely superimposable, there are no major structural differences between the three peptide structures that appear to explain the difference in activity. In all cases, the dimers pack together along a hydrophobic face, which then exposes charged residues to the solvent. Consequently, the peptides' NMR structures are consistent with the prior observation that the number and distribution of hydrophobic residues is crucial for antimicrobial activity [43]. Increasing peptide hydrophobicity increases antimicrobial activity, but only if the overall hydrophobicity remains below an optimal upper threshold. Peptide aggregation likely occurs if too many hydrophobic residues are inserted into the peptide sequence, which leads to a loss in activity. Therefore, the **Cit 1.1** peptide must maintain a hydrophobic surface to allow for a stable dimer in order to carpet a bacterial cell membrane, but must also avoid the formation of inactive aggregates. The tryptophan substitution in **AMP-016** and the corresponding increase in antimicrobial activity supports the above hypothesis. The hydrophobic and electrostatic properties of tryptophan [44] allows **AMP-016** to maintain a similar overall hydrophobicity to **Cit 1.1** while also promoting peptide aggregation at the membrane surface, and a positive electrostatic interaction with the negatively-charged membrane. This, however, does not explain the differences in activity between the active (**Cit 1.1/AMP-016**) and inactive (**AMP-003**) peptides since all of the peptides form a similar head-to-tail dimer. Instead, the primary difference between the active and inactive peptide

dimers is the *N*-terminal acetylation.

It has been previously observed that *N*-terminal acetylation increases the propensity of  $\alpha$ -helix formation in peptides regardless of the amino acid sequence [45]. *N*-terminal acetylation also increases the overall stability of an  $\alpha$ -helix. In the case of **Cit 1.1**, the apparent increase in helical stability due to acetylation resulted in a loss of activity. Consequently, antimicrobial activity may be correlated with a certain amount of structural disorder or mobility within the peptide. Of course, this result can also be linked to the loss of basicity as explained earlier. The NMR also leads to the theory that antimicrobial activity may depend on an equilibrium between a disordered monomer in solution and helical dimers coating the membrane surface. In the presence of bacteria, the equilibrium shifts from disordered monomer to the helical dimer. The dimer is then able to associate with other dimers on the membrane surface and promote antimicrobial activity through a proposed carpet mechanism. However, if the peptide is stabilized in solution then the equilibrium is shifted away from interacting with the bacterial membrane and the antimicrobial activity is abolished. We hypothesize that **Cit 1.1** exists as a disordered monomer in solution and dimerizes and aggregates along the anionic surface of the bacterial membrane. In the inactive form, the *N*-terminal acetylation stabilizes the transiently formed  $\alpha$ -helix in solution. Consequently, the aggregation on the membrane surface, which promotes antimicrobial activity, is greatly diminished. Again, the observation that the inactive **AMP-003** dimer is exclusively  $\alpha$ -helical and the **Cit 1.1/AMP-016** dimers are a mixture of  $\alpha$ - and  $3_{10}$ -helix is supportive of the proposal that helix stability affects antimicrobial activity. To further investigate the role of  $\alpha$ -helical stability in regard to antimicrobial activity, NMR was used to measure the thermal stability and solvent accessibility of the **Cit 1.1**, **AMP-003**, and **AMP-016** peptides.

The temperature-dependent chemical shift changes clearly define the dimer interface as the residues with the largest  $\Delta^{\text{HN}}$  values (**Figs. 2D–F**, S1–3). The residues in the dimer interface correspond to: Ile6, Val9, Ala10, Ile13, and Gly14. Importantly, the inactive **AMP-003** peptide exhibited the smallest HN chemical shift changes for these residues. This suggests the inactive **AMP-003** is relatively less stable as a dimer in the SDS micelle compared to the active peptides. Interestingly, there are additional **AMP-003** residues outside of the dimer interface that also exhibit a temperature-dependent chemical shift change. This was not observed for the **Cit 1.1** or **AMP-016** peptides. One possible explanation for this difference is that the **AMP-003** peptide still maintains an  $\alpha$ -helical structure as a monomer, which undergoes further temperature-dependent denaturation. This does not appear to occur for **Cit 1.1** or **AMP-016**. In fact, more residues in the **Cit 1.1** peptide compared to **AMP-003** are disordered based on the lack of a temperature-dependent chemical shift change. These results suggest that a certain amount of structural disorder or dynamics is necessary for antimicrobial activity.

The presence of a helical dimer is also suggested by the Gd-DTPA titration experiments. At low concentrations of Gd-DTPA, the amide peak intensity for Leu2 was found to increase, which indicates a reduction in the chemical exchange with the solvent. It is plausible that the coordination of Gd-DTPA by the active peptides stabilizes the dimer structure and reduces the amide chemical exchange of Leu2 causing an initial sharpening of the peak. Only at higher Gd-DTPA concentrations does the Leu2 NMR resonance broaden like the other amino acid residues. This effect is not seen in the inactive peptide (**AMP-003**), suggestive of a more stable  $\alpha$ -helix along the entirety of the peptide monomer (**Fig. S4–6**).

### 3.3. Mechanism of action in bacteria membrane

Bacterial membrane disruption can be described by the worm-hole, the barrel-stave, or the carpet models [46,47]. Previously reported data on the **Cit 1.1** interaction with negatively charged lipid vesicles hinted towards involvement of the carpet mechanism [12]. In the carpet-



model of membrane disruption, the AMPs bind parallel to the bacterial membrane covering its entire surface. This causes cell membrane permeation and eventually release of small vesicles from the membrane [46,47]. A separate study involving giant unilamellar vesicles (GUVs) further supported the carpet mechanism proposed earlier [40]. Conversely, an atomic force microscopy study by Henderson and colleagues indicates that **Cit 1.1** can promote the formation of worm-like micelles, which could be an outcome of many toroidal pore formations [48]. However, those prior studies relied on negatively charged phospholipid model membranes, which are structurally simple compared to bacterial membranes. These model membranes do not accurately represent the complexity of single or double-membraned Gram-negative organisms. Furthermore, those studies relied on indirect fluorometric observations instead of direct microscopic imaging [12,46]. Treatment of *S. aureus* and *E. coli* with **AMP-016** lead to membrane disruption accompanied by the formation of protruding blebs and holes as visualized by SEM (Figs. 3) and transmission electron microscopy (not shown). The carpet mechanism of membrane disruption is commonly associated with detergent-like antibacterials displaying indiscriminate cell lytic properties and AMPs acting by this mechanism may possess some basic structural requirements [8]. Herein, we have shown that AMPs that disrupt membranes in a detergent like fashion are sensitive to subtle structural modifications. Additionally, the membrane damage in MRSA JE2 and *E. coli* K12 was also confirmed by a PI uptake assay and by flow cytometry experiments, showing an increase in the fluorescent intensity of PI after treatment with **AMP-016**.

### 3.4. In vitro serum stability studies

AMPs have found limited use due to their susceptibility to metabolic enzymes in serum and the liver. Accordingly, some of the **Cit 1.1** analogues were tested for serum stability. **AMP-002** was the most serum-stable peptide of the tested AMPs with about 80% of the peptide remaining after 2 h. of incubation. This was expected because peptides can be degraded starting from the *N*-terminus by exopeptidases [49]. Thus, an alkylated *N*-terminus may be a successful strategy for enhancing AMP stability [30], which may explain the two-fold increase in serum half-life for **AMP-002** compared to **Cit 1.1**. **AMP-006** was also more stable in serum compared to **Cit 1.1**, with approximately 60% of the peptide remaining after a 2-hr. incubation in serum. **AMP-006** had Lys7 and Lys8 substituted by Orn residues. The presence of this unnatural amino acid may prevent recognition by LysC and LysN endopeptidases [50]. *N*-terminus modification and substitution with unnatural amino acids may enhance AMP plasma stability and bioavailability [51], but retaining bioactivity is still paramount. The data suggests alkylation of the *N*-terminus is an interesting strategy to enhance the stability of **Cit 1.1** analogues.

### 3.5. Cytotoxicity

For therapeutic use, AMPs should display good selectivity for bacterial cells over mammalian cells. The active peptides, **AMP-016** and **AMP-017** showed both  $IC_{50}$  and  $HC_{50}$  values higher than their MICs and displayed minimal hemolytic activity against human red blood cells. We theorized that AMPs should possess a greater affinity for negatively charged bacterial membranes compared to zwitterionic mammalian cell membranes. In fact, prior studies have suggested that AMPs exhibit a higher affinity to bacteria compared to mammalian cells because of their distinct membrane characteristics [7,47,52]. For example, the transmembrane potential is more negative in bacteria cells, which suggest an increase affinity or sensitivity of bacteria cells for cationic antimicrobial peptides [7].

## 4. Conclusion

We have shown that AMP-membrane interactions impact

antimicrobial activity. Rationally designed **Cit 1.1** analogues were used to develop SAR and to elucidate previously unknown interactions responsible for membrane disruption and antibacterial activity. Our insights regarding **Cit 1.1** structural features essential for activity are summarized in Fig. 6. Hydrogen bond donors with a basic pKa at the *N*-terminus were found to be indispensable for antibacterial activity. Ablation of either the hydrogen bond donors or the positive charge resulted in inactivity; suggesting a complementary effect between hydrogen bonding and electrostatic interactions in disrupting membranes. Also, sufficient projections of the side chain amine groups were shown to be essential for membrane disruption. **AMP-016** and **AMP-017** are highly potent **Cit 1.1** analogues with a 2- to 8-fold increase in antimicrobial activity against MRSA. Both analogues have a Trp residue that replaces the native Phe. Thus, the improved activity may be due to an increase in the bulk of the hydrophobic anchor and an improved electrostatic interaction with the negatively-charged membrane. The W3F modification also made **Cit 1.1** analogues active against fungi. NMR studies revealed the propensity of AMPs to form head-to-tail helical-dimers on the surface of anionic membranes and bacterial surfaces. NMR spectroscopy exposed a positive correlation between AMP helicity and antibacterial activity, where *N*-terminal acetylation increased the  $\alpha$ -helical structure of the peptides in the absence of a membrane and, correspondingly, lead to a decrease in antibacterial activity. These experiments provide further support for the carpet model of membrane disruption, which was subsequently confirmed by electron microscopy in both Gram-positive and Gram-negative bacteria. The results presented herein provide the critical foundation for further evolving **Cit 1.1** analogues into novel broad-spectrum antibiotics for the treatment of drug-resistant bacterial infections.

## 5. Experimental section

### 5.1. Peptide synthesis and purification

AMPs were synthesized using solid phase peptide synthesis (SPPS) on a Focus XC automated peptide synthesizer (AAPTec, Louisville, KY) on a 0.25 mmol scale. All peptides were synthesized using Fmoc-Rink Amide AM resin support (AAPTec, Louisville, KY). The resin was wetted in dichloromethane (DCM) for 30 min. to promote swelling. The Fmoc- group was then deprotected twice using 20% 4-methyl piperidine in dimethyl formamide (DMF) (10 mL). The resin was thoroughly washed twice for 10 min. using a 15 mL 1:1 mixture of DCM and DMF. The desired amino acids were then added to obtain a predetermined sequence in the peptide synthesizer. Molecular weight of the AMPs was confirmed by MALDI using a 4800 MALDI TOF/TOF analyzer (SCIEX, Ontario, Canada). The AMPs were purified using a preparative high-performance liquid chromatography (HPLC) using a water (0.1% trifluoroacetic acid (TFA)) and acetonitrile (0.1% TFA) gradient on an HPLC system (Agilent, Santa Clara, CA) with a reverse phase column (Kinetex5 u XB-C18 100 A, 150 × 30.0 mm column). Each AMP was confirmed to be > 95% pure. The relative hydrophobicity of the AMPs was determined by simultaneously measuring retention times with the analytical HPLC system described above.

Special peptide modifications were done on resin and described as follows:

**AMP-002** was synthesized by coupling a Sar instead of glycine following the procedure described above.

**AMP-003** was acetylated by shaking the complete peptide loaded resin in 1 mL acetic anhydride dissolved in 5 mL (DCM:DMF = 1:1) for 6 h at ambient temperature.

**AMP-004** was synthesized by methylating the Fmoc-deprotected *N*-terminus by adding 4 mL methyl iodide and 200  $\mu$ L triethylamine to the resin in 10 mL DCM and then gently heating at 45 °C for 5 days.

**AMP-005** was synthesized by substituting the glycine residue with bromoacetic acid using the same coupling procedure as described above. The bromine was then displaced with 10 mL hydrazine hydrate

by reacting it on the resin for 24 h.

**AMP-010** was synthesized by first making **GLFDVIK(Alloc)K(Alloc)VASVIGGL** on the resin. The *N*-terminus Fmoc was deprotected following the procedure described above. The side chain Alloc was deprotected on resin by treatment with 0.35 eq of Pd(PPh<sub>3</sub>)<sub>4</sub> and 20 eq of Phenyl silane in DCM for 45 min. Methylation of the free primary amines was achieved by adding 4 mL methyl iodide and 200 μL triethylamine to the resin in 10 mL DCM and then gently heating at 45 °C for 5 days.

**AMP-011** was synthesized by first making **Fmoc-GLFDVIK(Alloc)K(Alloc)VASVIGGL** on the resin. The side chain Alloc was deprotected on the resin by treatment with 0.35 eq Pd(PPh<sub>3</sub>)<sub>4</sub> and 20 eq Phenyl silane in 10 mL DCM for 45 min. Methylation of the free primary amines were achieved by adding 4 mL methyl iodide and 200 μL triethylamine to the resin in 10 mL DCM and then gently heating at 45 °C for 5 days. Finally, the Fmoc- group was deprotected following the procedure described above.

### 5.2. Minimum inhibitory concentration assay (MIC)

MICs for **Cit 1.1** and the **Cit 1.1** analogues were measured using the following bacterial strains: *S. aureus* JE2 and *E. coli* K12. The MICs was determined using the broth microdilution method as previously described [52]. A stock solution of each peptide was prepared in milliQ water and then serial 2-fold dilutions were made in Difco™ Muller Hinton Broth (MHB) (BD Diagnostics, Becton Drive, NJ) in Cellstar 96-well microtiter plates (Greiner Bio-One, Kremsmünster, Austria). Bacterial cultures were prepared using the direct colony suspension method to  $1.5 \times 10^8$  colony forming unit (CFU)/mL (0.5 McFarland) and diluted from 2 mL into 40 mL of MHB. Each well was inoculated with 10 μL of bacterial cultures. Plates were statically incubated at 37 °C for 24 h. MIC values correspond to the lowest AMP concentration that yielded no observable bacterial growth based on analysis with the unaided eye or a microplate reader. The optical density (O.D.) value at 600 nm was recorded using an AccuSkan, MultiSkan FC (Thermo Fisher, Waltham, MA). Vancomycin (Sigma, St. Louis, MO) and gentamicin (Alfa Aesar, Ward Hill, MA) were used as positive controls. Blank media was used as a negative control. All assays were performed in triplicates using three independent measurements. All assays were performed in triplicates using three independent measurements.

### 5.3. NMR structure determination

Unlabeled **Cit 1.1** and the **Cit 1.1** analogues samples were prepared similarly to previous studies [15]. Briefly, 2 mM of **Cit 1.1**, **AMP-003**, or **AMP-016** were dissolved in 90% H<sub>2</sub>O and 10% D<sub>2</sub>O with 120 mM of SDS-d<sub>25</sub> (Cambridge Isotope, Ewksbury, MA), 50 mM trimethylsilylpropanoic acid (TMSP), and PBS buffer at pH 7 (uncorrected). NMR experiments were collected at 25 °C on a 700 MHz Avance III spectrometer (Bruker, Billerica, MA) equipped with a 5 mm QCI-P probe with cryogenically cooled carbon and proton channels. <sup>1</sup>H chemical shift and NOE assignments were accomplished with TOCSY, DQF-COSY, and NOESY experiments with chemical shifts referenced to TMSP. NMR spectra were collected with 32 transients and 512 points in the indirect dimension. NOESY spectra were collected with mixing times of 100 ms and 200 ms. Inter-strand NOEs were identified using a 3D X-filtered experiment with a mixing time of 120 ms and a 50/50 mixture of unlabeled peptide and a peptide uniformly <sup>13</sup>C, <sup>15</sup>N labeled at Leu2 [53]. Initial models of the AMPs were generated from H $\alpha$  chemical shifts using the CS-Rosetta webserver at the BMRB [54]. Structural refinement was carried out with XPLOR-NIH with dimer symmetry enforced [55]. The three AMP dimer structures were determined with 536 to 622 intramolecular NOE restraints, and 16 intermolecular (peptide-peptide) NOE restraints. A total of 400 models were calculated per AMP and the lowest 20 energy structures were subsequently subjected to water refinement in XPLOR-NIH. Validation of the AMP ensembles was done

using the Protein Structure Validation Software (PSVS, <http://psvs-1.5-dev.nesg.org/>) suite from the Northeast Structural Genomics Consortium (NESG) [56].

### 5.4. One-dimensional NMR temperature titration

The unlabeled NMR **Cit 1.1**, **AMP-003**, or **AMP-016** samples used for structure determination were also subjected to a temperature titration to monitor structure stability. 1D <sup>1</sup>H NMR spectra were recorded at temperatures of 25, 30, 40, 50, 60, and 70 °C with 64 transients, 131k data points, and a spectral width of 12.87 ppm. Between each experiment, the samples were allowed to rest at the target temperature for 5 min before data collection. Following the titration, the 25 °C spectrum was recollected to ensure that the sample did not undergo irreversible degradation upon heating.

### 5.5. Paramagnetic relaxation enhancement titration

The unlabeled NMR **Cit 1.1**, **AMP-003**, or **AMP-016** samples used for structure determination were also used to observe the effects of a diethylenetriaminepentaacetic acid gadolinium (III) dihydrogen salt hydrate (Gd-DTPA) titration. Gd-DTPA was titrated into the samples to concentrations of 0, 2, 4, 8, 16, and 24 mM. 1D <sup>1</sup>H NMR spectra were recorded with 128 transients, 64k data points, and a spectral width of 12.87 ppm. Effects resulting from sample dilution were accounted for by normalizing peak intensities to TMSF.

### 5.6. Scanning electron microscopy (SEM)

*E. coli* K12 and *S. aureus* JE2 were cultured in MHB and incubated at 37 °C. The resultant mid-log phase cultures were diluted to a final concentration of  $1.5 \times 10^8$  CFU/ml (0.5 McFarland). The bacteria cells were treated with **Cit 1.1** or a **Cit 1.1** analogue at 2X the MIC value and incubated for 1 h at 37 °C. A control was prepared by adding only media. After AMP treatment, the cells were immediately washed thrice with HyClone™ Dulbecco's PBS solution (GE Healthcare Life Science, Marlborough, MA) and fixed with 2.0% (v/v) glutaraldehyde [57]. The bacterial suspension was then placed on 0.1% Poly-L Lysine coated glass slide and allowed to adhere for 30 min. The slides were washed thrice with PBS to remove excess fixative. Samples were post-fixed in a 1% solution of OsO<sub>4</sub> for 30 min. to facilitate conductivity. The samples were then dehydrated in a graded ethanol series (50, 70, 90, 95, and 100%). Ethanol was removed by washing the slides thrice with hexamethyldisilazane (HMDS). HMDS was allowed to evaporate overnight to dryness. The glass slides were attached to aluminum SEM stubs with double-sided carbon tape. Silver paste was applied to enhance conductivity, which was allowed to dry overnight. Samples were then coated with approximately 50 nm gold-palladium alloy in a Hummer VI Sputter Coater (Anatech, Battle Creek, MI) and imaged at 30 kV in a Quanta 200 SEM (FEI, Hillsboro, OR) operating in high vacuum mode.

### 5.7. Propidium iodide (PI) uptake

The PI uptake assay was performed according to Shireen et al [58]. *S. aureus* JE2 and *E. coli* K12 cells were grown in BHI broth to the mid logarithmic-phase and the bacterial cells were harvested by centrifugation at 5000 rpm for 5 min and washed once with PBS buffer. Cells were diluted to 10<sup>7</sup> cfu/ml using PBS buffer. AMPs were added to each well at twice the MIC. Similarly, 10 μg/mL of PI was also added to each well. Polymyxin B was used as a reference drug and cells with no AMP treatment were used as a control. PI fluorescence was measured at 37 °C and at 20 min intervals for a total duration of 120 min. The PI fluorescence was measured using a spectrofluorometer with excitation and emission wavelengths set at 544 nm and 620 nm, respectively.

### 5.8. *In vitro* human serum stability studies

**Cit 1.1** and **Cit 1.1** analogues were incubated in human serum for 2 h in a shaking water bath (90 rpm) at 37 °C. Peptide content in the reaction mixture was below 0.5% (v/v). At select time intervals of 0, 30, 45, 60 and 120 min, 100 µL of the serum-AMP mixture was extracted and quenched with 400 µL of methanol containing oxibendazole as an internal standard. Samples were mixed and centrifuged at 17,950 × g for 15 min. at 4 °C. 100 µL of the supernatant was removed for analysis. Stability results were expressed as a percentage of AMP remaining in the serum as a function of time. AMP stability was represented as the percentage of the AMP remaining relative to the first time-point (0 min; 100% AMP). All experiments were performed in triplicate.

A LabSolutions LCMS Ver.5.6 controlled UPLC and MS system consisting of a Shimadzu LC-MS/MS 8060 equipped with a DUIS source, two pumps (LC-30 AD), a column oven (CTO-30AS) and an auto-sampler (SIL-30AC) were used to quantitate AMPs in human serum. The MS/MS system was operated at unit resolution in the multiple reaction monitoring (MRM) mode using the precursor ion to product ion combinations of: (i) 538.92 to 86.20 *m/z*, (ii) 543.60–86.20 *m/z*, (iii) 557.60–86.25 *m/z*, (iv) 529.60–86.25 *m/z*, (v) 548.25 to 143.20 *m/z*, and (vi) 551.95 to 86.20 *m/z* for **Cit 1.1**, **AMP-002**, **AMP-006**, **AMP-012**, **AMP-013** and **AMP-016**, respectively. All of the AMPs were triply charged (*m* + 3). Mass detection occurred in the positive ionization mode with the following parameters: nebulizer gas: 2.0 L/min; heating gas: 10 L/min; drying gas: 10 L/min; interface temperature: 375 °C; desolvation line temperature: 250 °C; and heat block temperature: 400 °C.

Acceptable resolution and peak shape were achieved for the AMPs on a BEH C18 (1.7 µg/mL, 2.1 × 100 mm, Waters, Milford, MA) column protected with a C<sub>18</sub> guard column (Phenomenex, Torrance, CA). The mobile phase consisted of 0.1% formic acid in water (mobile phase A) and methanol (MeOH) (mobile phase B) at total flow rate of 0.25 mL/min. Chromatographic separation was achieved using an 8-minute gradient elution. The initial mobile phase composition was 35% B, which was increased linearly to 95% B over 6 min. The mobile phase was then held constant at 95% B for 1.0 min and returned to the initial condition in 0.5 min followed by a 1 min equilibration. The sample injection volume was 5 µL. Calibration curves were established for each analyte using the peak area ratio (analyte/IS) and known concentration. Each calibration curve consisted of a blank sample, a zero blank (blank and IS), and eight non-zero concentrations. All analytes were extracted from the respective matrix by simple protein precipitation extraction using methanol spiked with the IS. The method was linear over the range from 1 to 1000 ng/mL for all analytes. The acceptance criteria for each back calculated standard concentration was ± 15% standard deviation (SD) from the nominal value except at LLOQ, which was set at ± 20%.

### Declaration of Competing Interest

The authors declare no competing financial interest.

### Acknowledgements

This work was funded by UNMC-startup funds (MC-S), National Institute of Health-NIGMS, Nebraska Center for Molecular Target Discovery and Development (1P20GM121316-01A1, PI: Robert Lewis, Project Leader, MC-S), and by the USA Department of Defense-Peer Reviewed Medical Research Program 2017 (W81XWH-18-1-0113, MC-S). This work was supported by funding from the Redox Biology Center (P30 GM103335, NIGMS, RP) and the Nebraska Center for Integrated Biomolecular Communication (P20 GM113126, NIGMS, RP). The research was performed in facilities renovated with support from the N.I.H. (RR015468-01). Some antimicrobial tests (as detailed in the SI) were performed by The Community for Antimicrobial Drug Discovery

(CO-ADD), funded by the Wellcome Trust (UK) and The University of Queensland (Australia). The authors thank Dr. Andrew Dudley, Tom Bargar, and Nicholas Conoan (UNMC-Electron Microscopy Core Facility, EMCF) and Samantha Wall (UNMC-Flow Cytometry Research Facility, FCRF) for technical assistance. The EMCF and FCRF are supported by the Nebraska Research Initiative (NRI), the University of Nebraska Foundation, and the UNMC-Office of the Vice Chancellor for Research. FCRF is also supported by The Fred and Pamela Buffett Cancer Center's through the NCI.

### Appendix A. Supplementary data

Supplementary material related to this article can be found, in the online version, at doi:<https://doi.org/10.1016/j.peptides.2019.170119>.

### References

- [1] D.M. Livermore, Bacterial resistance: origins, epidemiology, and impact, *Clin. Infect. Dis.* 36 (Suppl. 1) (2003) S11–23.
- [2] J. O'Neil, Review on antimicrobial resistance, *Antimicrobial Resistance: Tackling a Crisis for the Health and Wealth of Nations* 2014, (2014).
- [3] C. Walsh, Molecular mechanisms that confer antibacterial drug resistance, *Nature* 406 (6797) (2000) 775–781.
- [4] F.C. Tenover, Mechanisms of antimicrobial resistance in bacteria, *Am. J. Infect. Control* 34 (5) (2006) S3–S10.
- [5] D.L. Paterson, Resistance in gram-negative bacteria: enterobacteriaceae, *Am. J. Med.* 119 (6) (2006) S20–S28.
- [6] J. Lin, K. Nishino, M.C. Roberts, M. Tolmashy, R.I. Aminov, L. Zhang, Mechanisms of antibiotic resistance, *Front. Microbiol.* 6 (2015).
- [7] M.R. Yeaman, N.Y. Yount, Mechanisms of antimicrobial peptide action and resistance, *Pharmacol. Rev.* 55 (1) (2003) 27–55.
- [8] Y. Shai, Mode of action of membrane active antimicrobial peptides, *Pept. Sci.* 66 (4) (2002) 236–248.
- [9] K.A. Brogden, Antimicrobial peptides: pore formers or metabolic inhibitors in bacteria? *Nat. Rev. Microbiol.* 3 (3) (2005) 238–250.
- [10] M.A. Sani, F. Separovic, How membrane-active peptides get into lipid membranes, *Acc. Chem. Res.* 49 (6) (2016) 1130–1138.
- [11] M. Zasloff, Antimicrobial peptides of multicellular organisms, *Nature* 415 (6870) (2002) 389.
- [12] M.P. Boland, F. Separovic, Membrane interactions of antimicrobial peptides from Australian tree frogs, *Biochim. Biophys. Acta Biomembr.* 1758 (9) (2006) 1178–1183.
- [13] M. Jaskiewicz, M. Orlowska, G. Olizarowicz, D. Migon, D. Grzywacz, W. Kamysz, Rapid screening of antimicrobial synthetic peptides, *Int. J. Pept. Res. Ther.* 22 (2) (2016) 155–161.
- [14] W. Kamysz, P. Nadolski, A. Kedzia, O. Cirioni, F. Barchiesi, A. Giacometti, G. Scalise, J. Lukasiak, M. Okroj, In vitro activity of synthetic antimicrobial peptides against *Candida*, *Pol. J. Microbiol.* 55 (4) (2006) 303–307.
- [15] E. Sikorska, K. Greber, S. Rodziejewicz-Motowidlo, L. Szultka, J. Lukasiak, W. Kamysz, Synthesis and antimicrobial activity of truncated fragments and analogs of citropin 1.1: the solution structure of the SDS micelle-bound citropin-like peptides, *J. Struct. Biol.* 168 (2) (2009) 250–258.
- [16] J. Doyle, C.S. Brinkworth, K.L. Wegener, J.A. Carver, L.E. Llewellyn, I.N. Olver, J.H. Bowie, P.A. Wabnitz, M.J. Tyler, nNOS inhibition, antimicrobial and anticancer activity of the amphibian skin peptide, citropin 1.1 and synthetic modifications, *Eur. J. Biochem.* 270 (6) (2003) 1141–1153.
- [17] A.N. Calabrese, K. Markulic, I.F. Musgrave, H. Guo, L. Zhang, J.H. Bowie, Structural and activity changes in three bioactive anuran peptides when Asp is replaced by isoAsp, *Peptides* 38 (2) (2012) 427–436.
- [18] A. Giacometti, O. Cirioni, W. Kamysz, C. Silvestri, M.S. Del Prete, A. Licci, G. D'Amato, J. Lukasiak, G. Scalise, In vitro activity and killing effect of citropin 1.1 against gram-positive pathogens causing skin and soft tissue infections, *Antimicrob. Agents Chemother.* 49 (6) (2005) 2507–2509.
- [19] B. Chia, Y. Gong, J.H. Bowie, J. Zuegg, M.A. Cooper, Membrane binding and perturbation studies of the antimicrobial peptides caerin, citropin, and maculatin, *Biopolymers* 96 (2) (2011) 147–157.
- [20] E. Strandberg, A.S. Ulrich, NMR methods for studying membrane-active antimicrobial peptides, concepts, *Magn. Reson. Part A* 23A (2) (2004) 89–120.
- [21] A. Bax, Two-dimensional NMR and protein structure, *Annu. Rev. Biochem.* 58 (1) (1989) 223–256.
- [22] D.S. Wishart, C.G. Bigam, A. Holm, R.S. Hodges, B.D. Sykes, 1H, 13C and 15N random coil NMR chemical shifts of the common amino acids. I. Investigations of nearest-neighbor effects, *J. Biomol. NMR* 5 (1995) 67–81.
- [23] S. Schwarzingler, G.J.A. Kroon, T.R. Foss, J. Chung, P.E. Wright, H.J. Dyson, Sequence-dependent correction of random coil NMR chemical shifts, *J. Am. Chem. Soc.* 123 (2001) 2970–2978.
- [24] R.A. Laskowski, M.W. MacArthur, D.S. Moss, J.M. Thornton, PROCHECK: a program to check the stereochemical quality of protein structures, *J. Appl. Cryst.* 26 (2) (1993) 283–291.

- [25] G.M. Clore, J. Iwahara, Theory, practice, and applications of paramagnetic relaxation enhancement for the characterization of transient low-population states of biological macromolecules and their complexes, *Chem. Rev.* 109 (2009) 4108–4139.
- [26] L. Di, Strategic approaches to optimizing peptide ADME properties, *AAPS J.* 17 (1) (2014) 134–143.
- [27] E.M. Spencer, Isoelectric heterogeneity of bovine plasma albumin, *J. Biol. Chem.* 246 (1) (1971) 201–208.
- [28] C.Z. Chen, N.C. Beck-Tan, P. Dhurjati, T.K. van Dyk, R.A. LaRossa, S.L. Cooper, Quaternary ammonium functionalized poly (propylene imine) dendrimers as effective antimicrobials: structure-activity studies, *Biomacromolecules* 1 (3) (2000) 473–480.
- [29] T. Thorsteinsson, M. Másson, K.G. Kristinsson, M.A. Hjálmsdóttir, H. Hilmarsson, T. Loftsson, Soft antimicrobial agents: synthesis and activity of labile environmentally friendly long chain quaternary ammonium compounds, *J. Med. Chem.* 46 (19) (2003) 4173–4181.
- [30] L. Gentilucci, R. De Marco, L. Cerisoli, Chemical modifications designed to improve peptide stability: incorporation of non-natural amino acids, pseudo-peptide bonds, and cyclization, *Curr. Pharm. Des.* 16 (28) (2010) 3185–3203.
- [31] E. McCleskey, W. Almers, The Ca channel in skeletal muscle is a large pore, *Proc. Natl. Acad. Sci.* 82 (20) (1985) 7149–7153.
- [32] D.L. Nelson, A.L. Lehninger, M.M. Cox, *Lehninger Principles of Biochemistry*, Macmillan, 2008.
- [33] A. Bagno, E. Menna, E. Mezzina, G. Scorrano, D. Spinelli, Site of protonation of alkyl- and arylhydrazines probed by <sup>14</sup>N, <sup>15</sup>N, and <sup>13</sup>C NMR relaxation and quantum chemical calculations, *J. Phys. Chem. A* 102 (17) (1998) 2888–2892.
- [34] D.I. Chan, E.J. Prenner, H.J. Vogel, Tryptophan-and arginine-rich antimicrobial peptides: structures and mechanisms of action, *Biochim. Biophys. Acta* 1758 (9) (2006) 1184–1202.
- [35] L. Jin, X. Bai, N. Luan, H. Yao, Z. Zhang, W. Liu, Y. Chen, X. Yan, M. Rong, R. Lai, A designed tryptophan-and Lysine/Arginine-Rich antimicrobial peptide with therapeutic potential for clinical antibiotic-resistant *Candida albicans* vaginitis, *J. Med. Chem.* 59 (5) (2016) 1791–1799.
- [36] J. Svenson, R. Karstad, G.E. Flaten, B.-O. Brandsdal, M. Brandl, J.S. Svendsen, Altered activity and physicochemical properties of short cationic antimicrobial peptides by incorporation of arginine analogues, *Mol. Pharm.* 6 (3) (2009) 996–1005.
- [37] K.E.S. Locock, T.D. Michl, J.D.P. Valentin, K. Vasilev, J.D. Hayball, Y. Qu, A. Traven, H.J. Griesser, L. Meagher, M. Haeussler, Guanylated polymethacrylates: a class of potent antimicrobial polymers with low hemolytic activity, *Biomacromolecules* 14 (11) (2013) 4021–4031.
- [38] D.J. Mitchell, L. Steinman, D.T. Kim, C.G. Fathman, J.B. Rothbard, Polyarginine enters cells more efficiently than other polycationic homopolymers, *J. Pept. Res.* 56 (5) (2000) 318–325.
- [39] I. Nakase, S. Okumura, S. Katayama, H. Hirose, S. Pujals, H. Yamaguchi, S. Arakawa, S. Shimizu, S. Futaki, Transformation of an antimicrobial peptide into a plasma membrane-permeable, mitochondria-targeted peptide via the substitution of lysine with arginine, *Chem. Commun.* 48 (90) (2012) 11097–11099.
- [40] E.E. Ambroggio, F. Separovic, J.H. Bowie, G.D. Fidelio, L.A. Bagatolli, Direct visualization of membrane leakage induced by the antibiotic peptides: maculatin, citropin, and aurein, *Biophys. J.* 89 (3) (2005) 1874–1881.
- [41] M.R.R. de Planque, B.B. Bonev, J.A.A. Demmers, D.V. Greathouse, R.E. Koeppe, F. Separovic, A. Watts, J.A. Killian, Interfacial anchor properties of tryptophan residues in transmembrane peptides can dominate over hydrophobic matching effects in peptide–lipid interactions, *Biochemistry* 42 (18) (2003) 5341–5348.
- [42] B.E. Haug, J.S. Svendsen, The role of tryptophan in the antibacterial activity of a 15-residue bovine lactoferricin peptide, *J. Pept. Sci.* 7 (4) (2001) 190–196.
- [43] Y. Chen, M.T. Guarnieri, A.I. Vasil, M.L. Vasil, C.T. Mant, R.S. Hodges, Role of peptide hydrophobicity in the mechanism of action of alpha-helical antimicrobial peptides, *Antimicrob. Agents Chemother.* 51 (4) (2007) 1398–1406.
- [44] W.-M. Yau, W.C. Wimley, K. Gawrisch, S.H. White, The preference of tryptophan for membrane interfaces, *Biochemistry* 37 (42) (1998) 14713–14718.
- [45] A. Chakrabarty, A.J. Doig, R.L. Baldwin, Helix capping propensities in peptides parallel those in proteins, *PNAS* 90 (1993) 11332–11336.
- [46] T. Salditt, C. Li, A. Spaar, Structure of antimicrobial peptides and lipid membranes probed by interface-sensitive X-ray scattering, *Biochim. Biophys. Acta* 1758 (9) (2006) 1483–1498.
- [47] A. Giuliani, G. Pirri, A. Bozzi, A. Di Giulio, M. Aschi, A. Rinaldi, Antimicrobial peptides: natural templates for synthetic membrane-active compounds, *Cell. Mol. Life Sci.* 65 (16) (2008) 2450–2460.
- [48] J.M. Henderson, A.J. Waring, F. Separovic, K.Y.C. Lee, Antimicrobial peptides share a common interaction driven by membrane line tension reduction, *Biophys. J.* 111 (10) (2016) 2176–2189.
- [49] C.F. Deacon, M.A. Nauck, M. Toft-Nielsen, L. Pridal, B. Willms, J.J. Holst, Both subcutaneously and intravenously administered glucagon-like peptide I are rapidly degraded from the NH<sub>2</sub>-terminus in type II diabetic patients and in healthy subjects, *Diabetes* 44 (9) (1995) 1126–1131.
- [50] S. Kawabata, E. Davie, A microsomal endopeptidase from liver with substrate specificity for processing proproteins such as the vitamin K-dependent proteins of plasma, *J. Biol. Chem.* 267 (15) (1992) 10331–10336.
- [51] A.K. Marr, W.J. Gooderham, R.E. Hancock, Antibacterial peptides for therapeutic use: obstacles and realistic outlook, *Curr. Opin. Pharmacol.* 6 (5) (2006) 468–472.
- [52] A.L. Leber, *Clinical Microbiology Procedures Handbook*, (2004).
- [53] A.L. Breeze, Isotope-filtered NMR methods for the study of biomolecular structure and interactions, *Prog. Nucl. Magn. Reson. Spectrosc.* 36 (1999) 323–372.
- [54] Y. Shen, O. Lange, F. Delaglio, P. Rossi, J.M. Aramini, G. Liu, A. Eletsky, Y. Wu, K.K. Singarapu, A. Lemak, A. Ignatchenko, C.H. Arrowsmith, T. Szyperski, G.T. Montelione, D. Baker, A. Bax, Consistent blind protein structure generation from NMR chemical shift data, *PNAS* 105 (12) (2008) 4685–4690.
- [55] C.D. Schwieters, J.J. Kuszewski, G.M. Clore, Using Xplor-NIH for NMR molecular structure determination, *J. Magn. Reson.* 48 (2006) 47–62.
- [56] A. Bhattacharya, R. Tejero, G.T. Montelione, Evaluating protein structures determined by structural genomics consortia tools for structure quality evaluation, *Proteins* 66 (2007) 778–795.
- [57] M. Hartmann, M. Berditsch, J. Hawecker, M.F. Ardakani, D. Gerthsen, A.S. Ulrich, Damage of the bacterial cell envelope by antimicrobial peptides gramicidin S and PGLa as revealed by transmission and scanning electron microscopy, *Antimicrob. Agents Chemother.* 54 (8) (2010) 3132–3142.
- [58] T. Shireen, S. Venugopal, D. Ghosh, R. Gadepalli, B. Dhawan, K. Mukhopadhyay, In vitro antimicrobial activity of alpha-melanocyte stimulating hormone against major human pathogen *Staphylococcus aureus*, *Peptides* 30 (9) (2009) 1627–1635.

**Dr. Martin Conda-Sheridan**

[martin.condasheridan@unmc.edu](mailto:martin.condasheridan@unmc.edu)

Assistant Professor

Department of Pharmaceutical Sciences

University of Nebraska-Medical Center

<https://www.condasheridanlab.com/>

PDD 3016

986125 UNMC

Omaha, NE, 68198-5830

402-559-9361 (office)

---

## Education

2007–2012 Ph.D. Medicinal Chemistry Purdue University, West Lafayette, IN

2005–2007 M.S. Chemistry, University of Utah, Salt Lake City, UT

2002–2005 B.S. Chemistry, Brigham Young University, Provo, UT

## Professional Experience

2015–present Assistant Professor, University of Nebraska Medical Center, Omaha, NE

2012–2015 Postdoctoral Fellow, Northwestern University. Advisor, Prof. Samuel I. Stupp

2007–2012 Graduate Researcher, Purdue University. Advisor, Prof. Mark Cushman

2005–2007 Graduate Researcher, University of Utah. Advisor, Prof. Janis Louie

2004–2005 Undergraduate Researcher, Brigham Young University. Advisor, Prof. Morris J. Robins

2003–2005 Undergraduate Researcher, Brigham Young University. Advisor, Prof. John D. Lamb

## Honors

2021 Young Observer for 2021 General Assembly; International Union of Pure and Applied Chemistry (IUPAC)

2020 CAREER award, National Science Foundation

2019 Best Work, XXI Argentinean Congress of Physical Chemistry and Inorganic Chemistry; Physical Chemistry of Materials

2019 Guest Editor, Medicinal Research Reviews. Special issue honoring Professor Mark Cushman

2018 Early Career Reviewer, National Institute of Health

2018 Milstein Fellowship, Ministry of Science and Technology, Argentina

2016 New Investigator Award, University of Nebraska Medical Center

2011 Cancer Prevention Fellowship, NCI, R25CA128770, Purdue University

2005 Undergraduate Research Award, Brigham Young University

2004 Summer Undergraduate Research Fellowship, University of Texas – SWMC

2004, 2005 Office of Research (ORCA) Award, Brigham Young University

## External Support

### Current

- Design and Understanding of Complex Biomaterials. Award# 1941731. Direct Costs: \$372,09. National Science Foundation-CAREER (Conda-Sheridan, PI). 03/01/2020-02/28/2025

- Role of the Clp Protease Systems in the Growth and Pathogenesis of Chlamydia. 1R56AI146062-01A1, Direct Costs: \$250,000 (Conda-Sheridan group ~\$35,000), NIH-NIAID (Ouellette, PI). 10/01/2020-09/31/2021

## Completed

- Modifying Heterocycles to Treat Gram + and Gram – Bacteria. PRMRP#PR172445, Direct Costs: \$200,000, Department of Defense. (Conda-Sheridan, PI). 05/01/2018-10/31/2020
- Nebraska Center for Molecular Target Discovery and Development. P20-GM121316, Direct Costs: \$510,980, NIH-NIGMS. (Lewis, PI; Conda-Sheridan, Co-I). 03/01/2018-08/31/2020
- Nebraska Bankers Association, Equipment grant, Direct Costs: \$15,000 (Conda-Sheridan, PI). 01/01/2018-04/30/2018
- The Evolution of Self-Assembled Organic Materials. PRF# 57434-DNI7, Direct Costs: \$110,000, American Chemical Society (Conda-Sheridan, PI). 09/01/2017-08/31/2019
- Developing Sugar Amphiphiles, Novel Bioinspired Nanodrugs. DHHS#2018-17, Direct Costs: \$ 50,000, Nebraska Department of Human Health (Conda-Sheridan, PI). 07/01/2017-06/30/2018
- Towards an Effective Prostate Cancer Targeting Biomaterial. 1R03EB022141-01, Direct Costs: \$100,000, NIH-NCI (Conda-Sheridan, PI). 04/01/2016-03/31/2018

## Internal Support

### Current

- UNMC Diversity Award. \$100,000 (Conda-Sheridan, PI). 06/01/2019-05/31/2021

### Completed

- UNMC Diversity Award. \$100,000 (Conda-Sheridan, PI). 06/01/2015-05/31-2017
- Developing Supramolecular Antibacterials. P20-GM103480, \$ 125,000, NIH-NIGMS. (Bronich, PI; Conda-Sheridan, Co-I). 07/01/2015-06/30/2017
- Enhancing PDGF-B activity to prevent chronic HIV infections. CHAIN – NIH P30 MH062261, \$ 50,000, NIH-NIMH. (Buch and Fox, PIs; Conda-Sheridan, Co-I). 11/01/2018-04/30/2019

## Publications (\* denotes equal contribution)

### Independent career

1. Xing, H.; Chin, S. M.; Udumula, V.; Krishnaiah, M.; Rodrigues de Almeida, N.; Huck-Iriart, C.; Picco, A. S.; Zaldivar, G.; Jackson, K. A.; Tagliazucchi, M.; Stupp, S. I.; Conda-Sheridan, M. Self-Assembly Control of Peptide Amphiphile Supramolecular Nanostructures by Bioisosteric Replacement. *To be Submitted*.
2. Zaldivar, G.; **Conda-Sheridan, M.**; Tagliazucchi, M. Molecular Basis for the Morphological Transitions of Surfactant Wormlike Micelles Triggered by Encapsulated Non-Polar Molecules. *Langmuir ASAP*
3. Wood, N.; Blocker, A.; Seleem, M.; **Conda-Sheridan, M.**; Fisher, D.; Ouellette, S. The AAA+ ATPase ClpX Is Critical for Growth and Development of *Chlamydia Trachomatis*. *mBio*02016-20 *ASAP*
4. Seleem, M.; Rodrigues de Almeida, N.; Chhonker, Y. S.; Murry, D. J.; Guterres, Z.; Blocker, A. M.; Kuwabara, S.; Fisher, D. J.; Leal, E. S.; Martinefski, M. R.; Bollini, M.; Monge, M. E.; Ouellette, S.; **Conda-Sheridan, M.** Synthesis and Antichlamydial Activity of Potential Activators of Cylindrical Proteases. *J. Med. Chem.* **2020**, *63*, 4370-4387
5. Zaldivar, G.; **Conda-Sheridan, M.\***; Tagliazucchi, M. Twisting of Charged Nanoribbons to Helicoids Driven by Electrostatics. *J. Phys. Chem. B* **2020**, *124*, 3221-3227
6. Sang, M.; Wang, H.; Shen, Y.; Rodriguez de Almeida, N.; **Conda-Sheridan, M.**, Li, Y.; Du, L. Identification of an Anti-MRSA Cyclic Lipodepsipeptide, WBP-29479A1, by Genome Mining of *Lysobacter antibioticus*. *Org. Lett.* **2019**, *21*, 6432-6436

7. Rodriguez de Almeida, N.; Catazaro, J.; Chhonker, Y.; Murry, D.; Powers, R.; **Conda-Sheridan, M.** Understanding Interactions of Citropin 1.1 Analogues with Model Membranes and Their Influence on Biological Activity. *Peptides* **2019**, 170119
8. Zaldivar, G.; Vemulapalli, S.; Udumula, V.; **Conda-Sheridan, M.**;\* Tagliacruzchi, M.\* Self-Assembled Nanostructures of Peptide-Amphiphiles: Charge Regulation by Size Regulation. *J. Phys. Chem. C* **2019**, *123*, 17606-17615
9. Rodrigues de Almeida, N.; Han, Y.; Perez, J.; Kirkpatrick, S.; Wang, Y.; **Conda-Sheridan, M.** Design, Synthesis, and Nanostructure-Dependent Antibacterial Activity of Cationic Peptide Amphiphiles. *ACS Appl. Mater. Interfaces*. **2019**, *11*, 2790-2801
10. Wood, N.; Chung, K.; Blocker, A.; Rodriguez de Almeida, N.; **Conda-Sheridan, M.**; Fisher, D.; Ouellette, S. Initial Characterization of the Two ClpP Paralogs of Chlamydia trachomatis Suggests Unique Functionality for Each. *J. Bacteriol.* **2018**, JB.00635-18
11. Zaldivar, G.; Samad, M.; **Conda-Sheridan, M.**; Tagliacruzchi, M. Self-Assembly of Model Short Triblock Amphiphiles in Dilute Solution. *Soft Matter* **2018**, *14*, 3171-3181
12. Samad, M.; Krishnaiah, M.; Rodriguez de Almeida, N.; **Conda-Sheridan, M.** Facile Protocol for the Synthesis of Self-Assembling Polyamine-based Peptide Amphiphiles (PPAs) and Related Biomaterials. *JoVE*. **2018**, *25*.
13. Krishnaiah, M.; Rodrigues de Almeida, N.; Udumula, V.; Song, Z.; Chhonker, Y. S.; Abdelmoaty, M. M.; Aragao do Nascimento, V.; Murry, D. J.; **Conda-Sheridan, M.** Synthesis, biological evaluation, and metabolic stability of new antibacterial phenazines. *Eur. J. Med. Chem.* **2018**, *143*, 936-947
14. Dias de Oliveira, P.; Rodrigues de Almeida, N.; **Conda-Sheridan, M.**; do Prado Aparecido, R.; Michelettia, A. C.; Pereira Carvalhoc, N. C.; dos Anjos dos Santos, E.; Marques, M. R.; de Arrudae, E. J.; Braz Alcantara, G.; Silva de Oliveira, L. C.; Pires de Lima, D.; Beatriz, A. Ozonolysis of neem oil: Preparation and characterization of potent antibacterial agents against multidrug resistant bacterial strains. *RSC Adv.* **2017**, *7*, 34356-34365
15. Samad, M. B.; Chhonker, Y. S.; Contreras, J. I.; McCarthy, A.; McClanahan, M., Murry, D. J., **Conda-Sheridan, M.** Developing Polyamine-based Peptide Amphiphiles with Tunable Morphology and Physicochemical Properties. *Macromol. Biosci.* **2017** *17*, 1700096
16. Basiri, A.; Xiao, M.; Mc Carthy, A.; Dutta, D. Byrereddy, S. N.; **Conda-Sheridan, M.** Design and synthesis of new piperidone grafted acetylcholinesterase inhibitors. *Bioorg. Med. Chem. Lett.* **2017**, *27*, 228– 231
17. Udumula, V\*.; Endres, J. L. ; Harper, C. N.; Jaramillo, L.; Zhong, H.; Bayles, K. W. ; **Conda-Sheridan, M\***. A Simple Synthesis of Endophenazine G and Its Analogues and Their Biological Evaluation as anti-methicillin-resistant Staphylococcus aureus agents. *Eur. J. Med. Chem.* **2016**, *128*, 710– 721

### **Before independent career**

18. **Conda-Sheridan, M.\***; Lee, S. S.\*; Preslar, A. T.; Stupp, S. I. Esterase-Activated Release of Naproxen from Supramolecular Nanofibres. *Chem. Comm.* **2014**, *50*, 13757– 13760
19. **Conda-Sheridan, M.\***; Park, E. J.\*; Beck, D. E.; Reddy, P. V. N.; Nguyen. T. X.; Hu, B.; Chen, L.; White J. J.; van Breemen, R. B.; Pezzuto, J. M.; Cushman, M. Design, Synthesis, and Biological Evaluation of Indenoisoquinoline Rexinoids with Chemopreventive Potential. *J. Med. Chem.*, **2013**, *56*, 2561–2605
20. **Conda-Sheridan, M.\***; Reddy, P. V. N.\*; Morrell, A.; Chen, L.; van Breemen, R. B.; Park, E. J.; Kondratyuk, T. P.; Pezzuto, J. M.; Cushman, M. Synthesis and Biological Evaluation of Indenoisoquinolines That Inhibit Both Tyrosyl-DNA Phosphodiesterase I (Tdp1) and Topoisomerase I (Top1). *J. Med. Chem.*, **2013**, *56*, 182– 200
21. **Conda-Sheridan, M.\***; Chen, L.\*; Reddy, P. V. N.; Morrell, A.; van Breemen, R. B.; Park, E. J.; Kondratyuk, T. P.; Pezzuto, J. M.; Cushman, M. Identification, Synthesis, and Biological Evaluation of the Metabolites of 3-Amino-6-(3'-aminopropyl)-5H-indeno[1,2-c]isoquinoline-5,11-(6H)dione (AM6–36), a Promising Rexinoid Lead Compound for the Development of Cancer Chemotherapeutic and Chemopreventive Agents. *J. Med. Chem.*, **2012**, *55*, 5965–5981
22. Nguyen, T. X.; Morrell, A.; **Conda-Sheridan, M.**; Marchand, C.; Agama, K.; Bermingham, A.; Stephen, A. G.; Chergui, A.; Naumova, A.; Fisher, R.; O'Keefe, B. R.; Pommier, Y.; Cushman, M. Synthesis and

- Biological Evaluation of the First Dual Tyrosyl-DNA Phosphodiesterase I (Tdp1)–Topoisomerase I (Top1) Inhibitors. *J. Med. Chem.*, **2012**, *55*, 4457–4478
23. Park, E. J.; Kiselev, E.; **Conda-Sheridan, M.**; Cushman, M.; Pezzuto, J. M. Induction of Apoptosis by 3-Amino-6-(3-aminopropyl)-5,6-dihydro-5,11-dioxo-11*H*-indeno[1,2-*c*]isoquinoline via Modulation of MAPKs (p38 and Jun *N*-terminal Kinase) and *c*-Myc in HL-60 Human Leukemia Cells. *J. Nat. Prod.*, **2012**, *75*, 378–384
  24. Zhang, K. **Conda-Sheridan, M.**; Cooke, S. R.; Louie, J. *N*-Heterocyclic Carbenes Bound to Nickel(I) Complexes and Their Role in Catalysis. *Organometallics*, **2011**, *30*, 2546–2552
  25. Park, E.; J.; Kondratyuk, T.P.; Morrell, A.; Kiselev, E.; **Conda-Sheridan, M.**; Cushman, M.; Ahn, S.; Choi, Y.; White, J.J.; van Breemen, R. B.; Pezzuto, J. M. . Induction of Retinoid X Receptor Activity and Consequent Up-regulation of p21<sup>WAF1/CIP1</sup> by Indenoisoquinolines in MCF7 Cells. *Can. Prev. Res.* **2011**, *4*, 592–607
  26. Marler, L.; **Conda-Sheridan, M.**; Cinelli, M.A.; Morrell, A.E.; Cushman, M.; Chen, L.; Huang, K.; Van Breemen, R.; and Pezzuto, J. M. Cancer Chemopreventive Potential of Aromathecins and Phenazines, Novel Natural Product Derivatives. *Anticancer Res.* **2010**, *30*, 4873–4882
  27. **Conda-Sheridan, M.**; Marler, L.; Park, E. J.; Kondratyuk, T. P.; Jermihov, K.; Mesecar, A. D.; Pezzuto, J. M.; Asolkar, R. N.; Fenical, W.; Cushman, M. Potential Chemopreventive Agents Based on the Structure of the Lead Compound 2-Bromo-1-hydroxyphenazine, Isolated from *Streptomyces* Species, Strain CNS284. *J. Med. Chem.* **2010**, *53*, 8678–8689
  28. Wang, S. C.; Troast, D. M.; **Conda-Sheridan, M.**; Zuo, G.; LaGarde, D.; Louie, J.; Tantillo, D. J. Mechanism of the Ni(0)-Catalyzed Vinylcyclopropane–Cyclopentene Rearrangement. *J. Org. Chem.* **2009**, *74*, 7822–7833
  29. Gardner, J. S.; **Conda-Sheridan, M.**; Smith, D. N.; Harrison, R. G.; Lamb, J. D. Anion Binding by a Tetradipicolylamine-Substituted Resorcinarene Cavitand. *Inorg. Chem.* **2005**, *44*, 4295-4300
  30. Nowak, I.; **Conda-Sheridan, M.**; Robins, M. J. Nucleic Acid Related Compounds. 127. Selective *N*-Deacylation of *N,O*-Peracylated Nucleosides in Superheated Methanol *J. Org. Chem.* **2005**, *70*, 7455-7458

## Reviews

1. Rodriguez de Almeida, N.; **Conda-Sheridan, M.** A Review of the Molecular Design and Biological Activities of RXR Agonists. *Med. Res. Rev.* **2019**, *39*, 1372-1397

## Patents

1. Cushman, M.; Nguyen, T. X.; **Conda-Sheridan, M.** Synthesis and use of dual tyrosyl-DNA phosphodiesterase I (tdp1)- topoisomerase I (top1) inhibitors. US 2013-13834652. Dec 26, **2013**

## Book Chapters

1. **Conda-Sheridan, M.**; Krishnaiah, M. Protecting Groups in Organic Synthesis. Peptide Synthesis - Methods and Protocols. 1<sup>st</sup> ed. Waleed Hussein, Mariusz Skwarczynski, Istvan Toth Eds.; Springer, **2020**, Ch 7; pp 111-128
2. **Conda-Sheridan, M.** Self-assembling biomaterials as nanocarriers for the targeted delivery of drugs for cancer. Self-assembling Biomaterials: Molecular Design, Characterization and Application in Biology and Medicine. 1<sup>st</sup> ed. Helena S. Azevedo, Ricardo M. P. da Silva Eds.; Woodhead Publishing, **2018**, Ch 23; pp 495-532

## Editorials

1. **Conda-Sheridan, M.** Editorial page, special issue honoring Professor Mark Cushman. *Med. Res. Rev.* **2019**, *39*, 1233-1234

## Scientific Service

### Grant Reviewer



1. NSF, General Review panel. Jan 2021
2. NSF, SBIR/STTR - Therapeutic Molecules. Dec 2020
3. NIH, ZAI1 JHM-X (J2) Study Section. Dec 2020
4. NIH, ZAI1-CB-W-S2 Study Section. Aug 2020
5. Targeted Support Grants for Technology Development, Michigan State University. Jul 2020
6. NSF, Division of Materials Research (DMR), BMAT panel. Apr 2020 (mail)
7. Johnson Cancer research Center, Kansas State University. Apr 2020
8. AAAS, Research Competitiveness Program. Mar 2019
9. NIH, ZGM1 RCB-6 Study Section. Nov 2018
10. NIH, DMP Study Section. Jun 2018
11. AAAS, Research Competitiveness Program. Feb 2018
12. AAAS, Research Competitiveness Program. May 2018
13. NSF, Division of Materials Research (DMR), BMAT panel, Oct 2016 (mail)
14. ACS, Petroleum Research Found (PRF), Committee 10. Feb 2016
15. NSF, Division of Materials Research (DMR), BMAT panel, Oct 2015 (mail)

#### Journal Reviewer

1. ACS Applied Materials and Interfaces; ACS Infectious Diseases; ACS Omega; Advances in Pharmacology; AIMS Biophysics; Angewandte Chemie International Edition; Anti-Cancer Agents in Medicinal Chemistry; Bioorganic Chemistry; Bioorganic and Medicinal Chemistry; ChemMedChem; European Journal of Medicinal Chemistry; Heliyon; Journal of Agricultural and Food Chemistry; Journal of Medicinal Chemistry; Journal of the Chemical Society of Pakistan; Letters in Drug Design and Discovery; Nanomedicine: Nanotechnology, Biology, and Medicine; Peptide Science, Small, Sustainable Chemistry and Pharmacy.

#### Other Service

1. Young Observer for 2021 General Assembly; International Union of Pure and Applied Chemistry (IUPAC)
2. Guest Editor, Medicinal Research Reviews 2019; special issue honoring Professor Mark Cushman
3. Judge, Midwest Student Biomedical Research Forum. March, 2016
4. Member Faculty Development Section, AACP, 2016
5. At the college level: Admission and Recruiting for the Pharm.D. program, and Academic Performance Committees. At the university level: NMR, Imaging, and Microscopy Cores Advisory Committees

#### **Invited Lectures/Courses**

1. Soft Matter, December 10 (2 hr), University of Buenos Aires, Buenos Aires, Argentina
2. Synthesis of Heterocycles, November 10-19, 2020 (10 hr, 5 lectures), Federal University of Itajuba, Minas Gerais, Brazil
3. Heterocyclic Chemistry: Synthesis and Biological Applications. July 30- August 3, 2018 (20 hr, complete course). Centro de Investigaciones en Bionanociencias (CIBION), Buenos Aires, Argentina

#### **Invited Seminars**

1. Heterocycles to treat Infectious Diseases: Old Chemistry, Old Infections, New Treatments. Federal University of Grande Dourados, Brazil, November 30, 2020 (Zoom). Host: Roberto Gomez/Vitor Rodrigues de Souza
2. Química, Ingeniería, y Ciencia de los Materiales; Intersección en la Nanotecnología (Seminar in Spanish). National University of General Sarmiento, Buenos Aires, Argentina, November 18, 2020 (Zoom). Host: Carlos Belmar Orellana
3. Peptide Amphiphiles; Structural Characteristics and Microbiology of a Promising Class of Biomaterials. University of Nebraska at Omaha, November 16, 2020 (Zoom). Host: Nathalia Rodrigues de Almeida
4. Peptide Amphiphiles; Structural Characteristics and Microbiology of a Promising Class of Biomaterials. INIFTA, University of La Plata, Buenos Aires, Argentina, July 20, 2020 (Zoom). Host: Agustin Picco

5. Peptide Amphiphiles, Microbiology and Structural Characteristics of a Promising Class of Biomaterials. Federal Fluminense University, Rio de Janeiro, Brazil, October 25, 2019. Host: Fabio Alves
6. Design and Synthesis of Heterocycles as New Antibacterial Agents. Federal University of Itajuba, Minas Gerais, Brazil, October 22, 2019. Host: Mauricio Santos
7. Peptide Amphiphiles, Microbiology and Structural Characteristics of a Promising Class of Biomaterials. Kansas State University, October 15, 2019. Host: Jeffrey Comer
8. Nanostructures as Antibacterial Agents. Role of Supramolecular Morphology in Biological Action. Georgia State University, April 23, 2019. Host: Binghe Wang
9. Nanostructures as Antibacterial Agents. Role of Supramolecular Morphology in Biological Action. University of Illinois at Chicago, April 3, 2019. Host: Richard Gemeinhart
10. Design, Synthesis, and Evaluation of Amphiphilic Peptides as New Antimicrobial Agents. Wichita State University, October 3, 2018. Host: Dennis Bruns
11. The Development of Small Molecule Antibacterials. DePaul University, September 14, 2018. Host: Charles Rubert Perez
12. Synthesis, Biological Evaluation, and Metabolic Studies of Phenazines, 2018 ACS-National Meeting, August 20, 2018. Host: Kyung Myung
13. Development of Self-Assembling Biomaterials with Biomedical Applications. Center of Investigations in Biosciences (CIBION), Argentina, August 1, 2018. Host: Leonardo Lizarraga
14. Design and Development of Self-Assembling Biomaterials. University of Buenos Aires-INQUIMAE, Argentina, July 30, 2018. Host: Mario Tagliazucchi
15. Design and Development of Self-Assembling Biomaterials. University of San Martin, Argentina, July 27, 2018. Host: Fernanda Cardinal
16. Development of Self-Assembling Biomaterials with Biomedical Applications. University of Chile, Chile, July 4, 2018. Host: Dante Miranda
17. Design and Development of Self-Assembling Biomaterials. University of Sao Paulo-Ribeirao Preto, Brazil, June 23, 2018. Host: Flavio Da Silva Emery
18. Antimicrobial Activity of Amphiphilic Peptides-Composition and Structure. Federal University of Grande Dourados, Brazil, June 20, 2018. Host: Eduardo Arruda
19. Antimicrobial Activity of Amphiphilic Peptides. Federal University of Mato Grosso do Sul, Brazil, June 19, 2018. Host: Adilson Beatriz
20. Small Molecules, Peptides, and Nanostructures; Where Can We find the Next Antibacterial? University of Nebraska at Lincoln, April 10, 2017. Host: LiangCheng Du
21. Synthesis and Development of Novel Self-assembling Biomaterials. University of Nebraska at Omaha, October 5, 2015. Host: Andy Zhong

## Transition Plan Questionnaire

**Directions:** Please answer all questions that apply for each product under development. Please fill out one document per product. *This is not an application for funding; however, answers will help us understand the outcomes and products from your award.*

1. After the award closes, would you be willing to periodically provide voluntary information (via email) regarding the project status (i.e. where the research is headed)? **Yes** or **No**

*These responses will help CDMRP demonstrate the return on its investments and will help demonstrate that the CDMRP is a responsible and successful steward of federal research funding.*

2. What **conclusion(s)** does your final data support?

3. Will you/have you applied for/obtained follow-on-funding for this project? **If yes**, please list (a) funding organization, (b) total budget requested/obtained, and (c) title of the funded proposal. *This information will be recorded as an outcome to this award.*

4. What will be **the next step(s)** for this project?

5. How would you classify your **lead candidate product**? *Please choose the best option or add explanation for multiple selections.*

(a) Therapeutic (Small Molecule, Biologic, Cell/Gene Therapy):

(b) Diagnostic

(c) Device

(d) Research Tool to Address a Research Bottleneck

(e) Knowledge Product (Non-material product such as a compound library, database, something that improves clinical practice, education, etc.)

(f) Other - Please Specify:

6. How does your candidate product aid the Warfighter, Veteran, Beneficiary, and/or General Population?

## **7. Therapy / Product Development, Transition Strategies, and Intellectual Property**

Describe the steps and relevant strategies required to move the candidate product (knowledge or tangible) to the next phase of development and/or commercialization. Please address any issues with intellectual property.

*PIs are encouraged to explore the technical requirements and the current regulatory strategies involved in product development as well as to work with their organization's Technology Transfer Office (or equivalent regulatory/legal office), federal/international regulatory experts, to develop the transition plan and to explore developing relationships with industry, DoD advanced developers (e.g. USAMMDA), and/or other funding agencies to facilitate moving the product into the next phase.*